International
Progress Report

IPR-04-37

Äspö Hard Rock Laboratory

Äspö Task Force

Modeling transfers in a single fracture system : from site characterization to performance assessment models

Contribution to Task 6A and 6B from the Äspö modeling Task Force exercise

Christophe Grenier

CEA – CE/SACLAY

February 2003

Svensk Kärnbränslehantering AB
Swedish Nuclear Fuel
and Waste Management Co
Box 5864
SE-102 40 Stockholm Sweden
Tel 08-459 84 00
+46 8 459 84 00
Fax 08-661 57 19
+46 8 661 57 19

Äspö Hard Rock
Laboratory

Report no.
IPR-04-37
No.
F65K
Author
Christophe Grenier
Date
Feb. 2003
Checked by
Date

Approved
Christer Svemar
Date
2004-11-19

Äspö Hard Rock Laboratory

Äspö Task Force

Modeling transfers in a single fracture system : from site characterization to performance assessment models

Contribution to Task 6A and 6B from the Äspö modeling Task Force exercise

Christophe Grenier

CEA – CE/SACLAY

February 2003

Keywords: Transfers, Single fracture, Matrix diffusion, Heterogeneity, Stochastic, Identification, Calibration, Monte Carlo, PA model, Prediction, Radial flow

Modeling transfers in a single fracture system : from site characterization to performance assessment models. Contribution to Task6A and 6B from the Äspö modeling Task Force exercise.

Christophe Grenier

Abstract

The objective of Task 6 from the Äspö modeling Task Force exercise is to build a bridge between site characterization (SC) models and performance assessment (PA) models on the basis of the Äspö underground laboratory (Sweden). The first type of models are typically complex, incorporating detailed physical and geochemical properties and calibrated against short term and small scale in situ experiments. Performance assessment models are simpler, restrained to the main physical features, generally used to study a variety of possible configurations and apply to long time scales as well as larger spatial scales.

We present here the main results for Task 6A and 6B modeling work. The focus is put for these sub tasks on a single fracture case, namely feature A, part of TRUE-1 (Tracer Retention Understanding Experiment). We study the transfer several tracers within this unit in different flow conditions: forced flow in pumping conditions and natural flow corresponding to post closure conditions.

Even at the level of a single fracture, the uncertainties relative to the main flow and transport features remain large. Moreover, the complexity of the geometry of the system as well as the diversity of the materials constituting the fracture make it a difficult task to build a representative model of the transport behavior. Several items are of interest like the structure of the flow (one or multi-channeled) and its consequences on transport features, assessment of the influence of the uncertainties, and role played by the different diffusion zones in the retention of the plume.

We focus here mainly on the influence of heterogeneity of matrix zones and the role they play at different regimes. We therefore generally limit the flow features to a single channel. This is nevertheless the situation expected for the cases involving tracer tests under pumping conditions (radial flow).

We introduce several models, from simple to more complex geometries of matrix zones. These models are first calibrated against the experimental breakthrough curves for a series of none sorbing to moderately sorbing tracers. Then, we study the regimes of these systems for slow velocity cases (typical of PA time scale for radial and uniform flow conditions) stressing the major features that have to be retained in building the prediction for PA time scale. A procedure for moving from SC to PA models is proposed. Sensitivity of the predictions to uncertainties is examined and major parameter requirements are identified as well as the level of information provided by tracer tests.

Sammanfattning

Syftet med Task6 i Äspö Task Force är brygga över gapet mellan platsundersökningsmodeller (Site Characterisation Models, SC) och de modeller som används vid funktions- och säkerhetsanalyser (Performance Assessment Models, PA). The första typen av modeller karakteriseras av att de är komplexa och inkluderar detaljerade beskrivningar av fysikaliska och kemiska egenskaper samt att de kalibreras mot småskaliga fältförsök med kort varaktighet. Säkerhetsanalysmodeller är enklare och begränsade till att beskriva de huvudsakliga fysikaliska företeelserna. De används allmänt för att studera ett flertal möjliga konfigurationer och är tillämpliga på långsiktigare förlopp såväl som på mer storskaliga system.

Här presenteras huvudresultaten av modelleringsarbetet i Task 6A och 6B. I dessa deluppgifter ligger fokus på en enskild spricka som i TRUE-1 (Tracer Retention Understanding Experiment) benämns Feature A. Vi har studerat transporten av flera spårämnen i denna spricka under olika flödesbetingelser: påtvingat flöde under pumpade förhållanden respektive naturligt flöde motsvarande förhållandena under slutförvarsskedet.

De osäkerheter som hänger samman med beskrivningen av de väsentligaste flödes- och transportegenskaperna förblir stora även på nivån enskild spricka. Därtill kommer att komplexiteten av systemets geometri och den mångfald material som bygger upp sprickan försvårar uppgiften att bygga en representativ modell av transportprocesserna. Flera frågeställningar är av intresse såsom flödesstrukturen (en eller flera kanaler) och dess konsekvenser på transportegenskaperna, utvärdering av påverkan från osäkerheterna, och den roll som olika diffusionszoner spelar för fördröjningen av plymen.

Här koncentrerar vi oss huvudsakligen på påverkan från matriszonernas heterogenitet och den roll dessa spelar under olika förhållanden. Vi har därför i allmänhet begränsat flödet till en enskild kanal. Detta är i vilket fall som helst den förväntade situationen under pumpade förhållanden (radiellt flöde).

Vi introducerar flera modeller som spänner från enkla till mera komplexa geometrier för matriszonen. Dessa modeller kalibreras först mot genombrottskurvor för icke sorberande till svagt sorberande spårämnen. Därefter studerar vi hur dessa system fungerar för fall med små flödeshastigheter (typiska för de tidsskalor som är aktuella för säkerhetsanalyser och radiella och likformiga flödesbetingelser) med betoning på sådana företeelser som behöver inkluderas när man bygger förutsägelser för tidsskalor som är aktuella i säkerhetsanalyser. En procedur föreslås för att extrapolera från platsundersökningar till säkerhetsanalyser. Förutsägelsernas känslighet för osäkerheter undersöks och de viktigaste parameterkraven identifieras liksom den nivå av information som kan fås från spårämnesförsök.

Executive summary

We provide here contributions to the questions addressed within Task 6A&B. The aim of the present task is to provide a bridge between detailed modeling scale called site characterization scale (SC type) corresponding to experimental time scale to performance assessment time scales (PA type) involving simplified models adapted to the post closure conditions. This is done here considering transfers in a single fracture system, Feature A, at Äspö site.

The system is indeed heterogeneous, potentially involving different levels of fracturation and alteration of the rock due to several geological, geochemical and transport events. It is in addition only partially characterized. As such it is important to (i) capture the main features of the system for the spatial and temporal scales considered for the modeling work, and (ii) take benefit of all available information (direct measurement or indirect information provided e.g. by series of hydraulic and tracer tests) and additionally specify other types of data requirements if sufficient level of information is missing.

We do not integrate in this study the whole (potential) complexity of the system. We consider Feature A as a 2D plane, accounting for heterogeneity in the fracture plane by means of a dispersion tensor. We more focused our study on studying the effects of matrix diffusion (and sorption in the bulk of the matrix) as a retention factor. Fractions of the plume are indeed removed from the mobile flow zones (fractures) by diffusion processes (and/or sorption) and later given back to the flow zones if concentration decreases in those units. This phenomenon causes retardation of the plume. The effect is from corrective to dominating when moving from short term transfers (more typical of tracer tests in pumping conditions) to long term transfers (more typical of post closure situations).

We focus our study on the influence of heterogeneity of the matrix, the behavior of the different types of matrix zones for the different regimes considered, the impact of their heterogeneity on retention properties, their identifiability from tracer tests, the parameter requirements for the different regimes ... The flow path is here considered simple leading to modeling a single channel or an homogeneous fracture plane. The actual validity of this approach as compared with others involving larger levels of heterogeneity is discussed in the body of the document. We consider it justified to a large extent according to the present knowledge of feature A and the requirements of present Task6 A & B. For later stages of this task (Task6 D & E), other levels of heterogeneity will have to be taken into account.

The impact of matrix diffusion heterogeneity on the retention processes is studied considering different deterministic models to represent the actual geometry (as expected from in situ characterization), associated to sensibility analysis on the one hand, and stochastic modeling on the other hand. The corresponding models are labeled Model 1, 2 and 3 and represented on figure 1 as well as the conceptual representation of feature A according to [*Winberg et al. 98*]. Model 1 is a simple homogeneous matrix model considered as a

simple first step approach and serves as a PA model as well. Model 2 considers deterministic lateral heterogeneity (different matrix zones in the depth of the block, Type 1 fault zone according to [*Winberg et al. 02*]). Model 3 is treated within a stochastic approach considering heterogeneous matrix diffusion fields along the fracture as well as in the depth of the block (with a profile decreasing with the depth).

Our results are briefly summed up below along the following major lines : role played by the different matrix zones present in feature A, construction of a simplified PA model, estimation/calibration of the different parameters required, sensitivity of the model to identify the most important parameter requirements and the estimate the quality of the predictions :

- *Role played by different matrix diffusion zones.* We consider different matrix zones: gouge material, fracture coating, cataclasite/mylonite, altered diorite, non altered diorite (see [*Winberg et al. 02*]). These zones are listed here from higher diffusion coefficient values to lower, the same is true for porosity. The first correspond to zones in the vicinity of the fracture, the latter more in the depth of the matrix blocks. Three flow regimes are considered in the present document, corresponding to experimental time scales (Task6A) to PA time scales (1000 times slower for Task6B1 and similar to post closure situation for Task6B2).
  - *Short term tracer tests* explore matrix zones in the close vicinity of the fracture due to limited contact times of the plume with matrix zones. In addition, only the higher diffusion and porosity zones play a significant role in retention processes. In the present case, gouge is the most important unit to be considered as well as fracture coating as well as (partly) Cataclasite / Mylonite units. In contrast, deeper rock units as well as less diffusive zones are not explored by short term tracer tests.
  - *For slower flows (post closure regimes)*, all zones considered are accessed by the plume (penetration depth of several decimeters). A distinction should nevertheless be made as for their behavior. Two major transport regimes indeed appear for higher and lower diffusion zones. The most diffusive zones behave as buffers almost immediately (as compared with the advective time) in equilibrium with the fracture. In an equivalent approach their role is efficiently modeled by a linear sorption term or by an increased total porosity coefficient affected to the mobile zone. The less diffusive zones in the depth of the rock behave as classical diffusion zones providing slight skip in the arrival time and level and long tailing.
- *Construction of a simplified model for post closure conditions (PA type model).* Explicit modeling of all types of zones for large time scale applications (Task6B) shows that the behavior of the different matrix zones falls in two main categories: those following the fracture behavior (equivalently modeled by surface sorption) and those classically transitorily storing mass. The first are then gathered and modeled by means of a single equivalent retention coefficient. The second have to be explicitly modeled as diffusion zones, possibly homogenized into a single equivalent matrix zone. The resulting PA like model that we propose is then very simple and similar to Model 1 (refer to figure 1): one fracture (equivalent mobile zone) and one diffusion

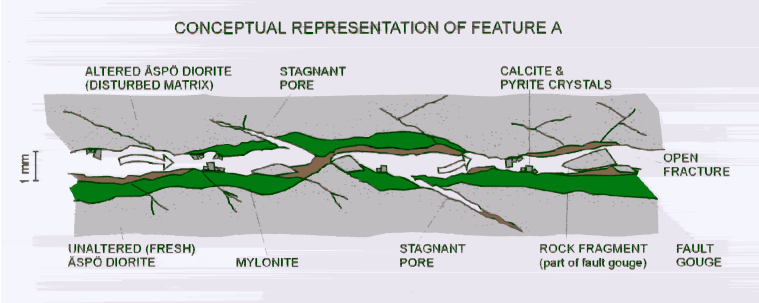

(a) Conceptual representation for Feature A

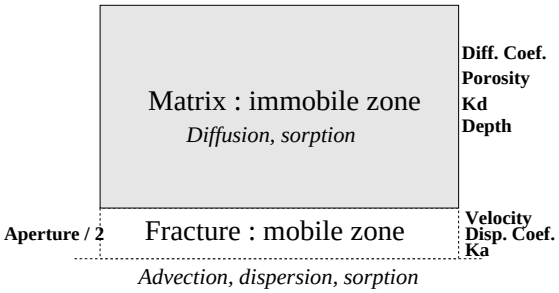

(b) First model

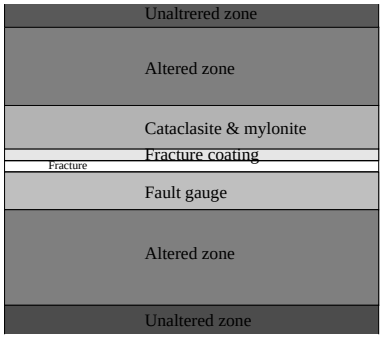

(c) Second model

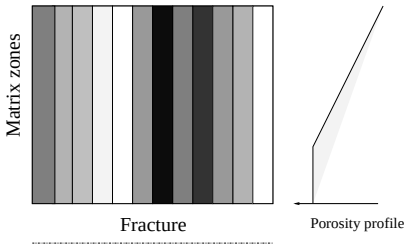

(d) Third model

Figure 1: Conceptual representation for Feature A (according to [*Winberg et al. 98*]) and 3 models considered in the present study addressing the impact of the matrix diffusion zones on the retention properties of the system.

zone (equivalent immobile zone), both associated with equivalent parameters that homogenize the different zones modeled for the regime considered.

- *Calibration, inverse problem.* The previous considerations are based on the information available for Feature A but all the rock volume explored by the plume is not covered. Uncertainties remain concerning the structure of the heterogeneity of the system as well as the quantitative parameter values for the different useful coefficients (porosity, diffusion coefficient, Kd ...). As a consequence, it is necessary to incorporate as much information in the system as possible to constrain the results. Direct measurements can be easily incorporated but remain scarce. Tracer test conducted in situ are another source of (indirect) information about the characteristics of the system. We discuss here the level of information provided by such tracer tests in the considered conditions :

  - First we can recall here that more in depth matrix zones as well as less diffusive zones are not accessed by the plume for tracer test flow conditions. These can not be identified by such a mean.
  - Second, it is important to say that even for the matrix zones explored by the plume in such conditions, the parameters identified from tracer tests conducted at experimental time scale in fact differ from the parameters required for models run at post closure time scale. For instance, considering Model 1 geometry, the system is governed for quick flow regimes by a first parameter group involving matrix diffusion, porosity, retention, fracture aperture ... for slow flow conditions, the system is governed by a second parameter group different from the first, involving, matrix depth, porosity, retention coefficient. So, strictly speaking, and for the conditions considered here, the information obtained from tracer tests in pumping conditions is of no use to characterize post closure transfer regimes.
  - This is of course no more true if independent information can be introduced into the problem. We study this situation by considering a given relation (built from available measurements) between matrix diffusion coefficient, porosity and a given fracture aperture and spatial characteristics for the different matrix units. In such a situation, the matrix diffusion field indeed controls both regimes alone. This is done with Model 3 approach, where we study the issue of identification a matrix diffusion field from tracer test results (breakthrough curve). We work here within a stochastic framework by means of Monte-Carlo simulations. Results show that such a test provides an averaged information on the matrix diffusion zones 'seen' by the plume with a larger discrimination effect for zones in the vicinity of the injection hole due to the radial structure of the flow for such pumping conditions. Nevertheless, the level of information introduced remains limited (low reduction of variance for the process at stake).

  As a conclusion, tracer tests do not provide major insights into the actual structure and quantitative features of the system for PA time scale purposes. On should rely as much as possible on direct measurements of the most relevant parameters, possibly obtained on geologic analogues of the system.

- *Sensitivity.* The most important features to be characterized as well as parameter

requirements are identified by means of sensitivity analysis. For post closure time scales, predictions are most sensitive to the most diffusive matrix zones in the vicinity of the fracture via a parameter group involving matrix zone depth, porosity and retention coefficient. Characteristics of more in depth zones are in the present case (Task6B1&2) of second order for the estimation of the peak arrival level and time. As a consequence, we ask for the best level of characterization possible for fractured zones in the vicinity of the mobile zones (fractures), possibly conducted on geological analogous rock block.

However, these results depend to a large extent on the actual fracture parameter values as well as the flow regimes considered and should not be considered as general results whatever the site and post closure regimes considered. Moreover, further steps of the task will provide better insight into the issue.

Further results are to be found in the body of the report. Performance measures as expected from the task requirements are provided in chapter 7 for the Model2 geometry considered. The Task6 questionnaire is provided as well in appendix A.

Contents

List of Figures

List of Tables

Chapter 1

Introduction

We present here a contribution within the framework of the Task Force organized by SKB with the Äspö database (see e.g. [1]). The present stage of the task, called Task 6 is devoted to providing a bridge between detailed modeling scale (short time transport over several meter to decameter scale, corresponding to experimental scale) to the PA (Performance Assessment) scale (slower flow velocity conditions corresponding to natural or post closure conditions, longer spatial scale). The present report provides the first part of the TASK6 modeling work, namely Task 6A and 6B corresponding to a single feature problem based on the rich experimental data set obtained from feature A at TRUE-1 site.

The main phases of the work are outlined here (see [*Selroos et Elert 01*]) :

- The experimental situation corresponds to a formerly identified single fracture at the Äspö site, called feature A. A large variety of hydraulic and tracer tests were conducted in this feature. A selection of these were made corresponding to radial flow regime (pumping at KXTT3-R2 location) and tracer tests along a 5 m flow path (called STT-1b test for an injection location at KXTT1-R2 and a pumping location at KXTT3-R2). These tests serve as common input for the modelers.
- The first phase of the work (Task 6A) consists of building models of feature A taking into account the current knowledge of the fracture as well as honoring the breakthrough curves measured. Several tracers are considered (sorbing and non sorbing).
- In the second phase (Task 6B1), predictions are proposed for the same radial flow conditions and travel path but for slower flow conditions (1000 times slower). 5 tracers are considered ranging from non sorbing, to intermediate sorbing tracers.
- In a third phase (Task 6B2), uniform flow conditions are considered. This phase is supposed to approach the post closure situation : natural flow within the structure and collection of flux at the outlet of the fracture. The same group of 5 tracers is considered here.

A common concern throughout the work is to identify the main flow and transport features as well as parameter required for the system considered. This is in fact a challenging task because of the expected complexity of the system as well as the restricted

level of direct information available. The feature A natural system is indeed known as providing a complex heterogeneity of the fracture aperture as well as matrix blocks properties. Moreover, at the present stage, these properties are (i) measured locally from 5 boreholes intersecting the unit, (ii) inferred from direct measurements conducted in similar geological units elsewhere at Äspö, (iii) can be indirectly inferred from several hydraulic as well as tracer tests. Due to the scarcity of the measurements as well as uncertainties in the estimations, the level of information available remains limited.

So, building a good level of confidence in the proposed predictions addresses several questions which are included in the Task6 objectives :

- Identify the main flow and transport features for the experimental test regime.
- For this regime, characterize the requirements in terms of parameter measurements, estimate the level of information provided by the different tests and direct local measurements provided, characterize the level of uncertainties in the calibration phase, identify the sensitivity of the system to the different units ...
- Provide a bridge toward larger time scales : mechanisms that are at stake for post closure conditions, characterize the mobile and immobile zones as well as the units concerned for this regime, identify related parameter requirements and the way to obtain them, for instance what kind of level of information is provided by tracer tests ? It should be stressed that this time scale is not accessible by experimental means.
- Build simplified models to be used for large time scales for sensitivity analysis within performance assessment procedures. Reduce the complexity of the system to the most important mechanisms, homogenize the heterogeneity and equations, ...

In our study, we address all the preceding questions. We nevertheless don't address all the levels of complexity of the system. We indeed mainly focus on the role played by the heterogeneous matrix zones along one flow path. This study is a contribution to characterizing one of the main retention processes relevant in fractured media (see e.g. [2]).

These questions are in line with other former studies related with transfers in fractured medial (e.g. [*Grenier et al. 99*], [*Grenier et al. 98*]) and follow previous participations in Task Force : Task 4 ([*Mouche et Treille 98*], [*Mouche et Treille 98*]) and Task 5 [*Grenier et Benet 02*].

In the following, we first present the transport model in radial flow conditions considered as well as its implementation within Cast3M code (chapter 3). Then we propose different models as a representation of the heterogeneity of the immobile zones. The models differ in complexity and as deterministic or stochastic approaches. These systems are calibrated and general analysis of the role played by different matrix zones is analysed (see chapter 4). We then move on to the predictions for the radial flow case (Task6B1, see chapter 5) and the uniform flow case (Task6B2, see chapter 6). We conclude with a discussion.

Chapter 2

Modeling tasks

2.1 Task 6A

This task consists in studying the flow and transport problem at the experimental temporal scale. We build here a refined model for the time scale considered : the flow reduces to a flow tube in radial flow conditions and different representations of the immobile zones are considered and calibrated against the experimental breakthrough curves provided for Iodine, Strontium and Cobalt. We consider 3 models differing by the complexity of the heterogeneity of the matrix zones.

2.2 Task 6B1

This sub task aims at providing predictions for performance assessment time scale for the same system (radial flow conditions for 1000 times slower flow conditions). This implies proposing a way to build a bridge between short time scale and long time scale. We consider here as well 3 models of the fracture implying levels of heterogeneity. Performance measures are produced on the second model case.

2.3 Task 6B2

This subtask is comparable to the former although the single fracture system is here considered for natural flow conditions (uniform flow across the system). We only consider here the second model involving the deterministic matrix zone heterogeneity calibrated previously.

Chapter 3

Radial flow model

We present here the flow and transport model considered for radial flow conditions. We indeed rely upon this model for Task 6A and B1. For Task6B2, a uniform flow model is considered and similarly implemented in our code (Cast3M).

In contrast to former modeling efforts during Task4 (involving uniform flow in the fracture), we prefer here a transport model based on radial flow conditions. This model was developed by [*Moench 89*] and is used here to validate our Cast3M code for these flow conditions. We nevertheless prefer here a numerical approach to the semi analytical solution by Moench due to the versatility of the numerical approach : include non 1D diffusion, heterogeneity in the matrix parameters ...

3.1 Basic model for radial flow conditions by Moench

The model by [*Moench 89*] corresponds to radial flow conditions and transport by advection and dispersion. No matrix diffusion is considered there but special care is devoted to the choice of the boundary conditions. Dispersivity is constant and the dispersion coefficient considered is expressed as the dispersivity multiplied by the local velocity. The velocity varies inversely proportional to the distance to the pumping well.

This model was used in our study for its semi analytical solutions. They were used to validate our code against them for these flow conditions. This point is worth mentioning since the velocity field varies strongly over the distance to the pumping location (velocity inversely proportional to the radius) and could potentially lead to discretization difficulties. In the numerical approach we don't treat the system in radial coordinates but rather consider a Cartesian slice of the system (typically relating the injection well to the origin, the pumping well). This is further developed below.

We compare the features of this radial flow model to those of a uniform flow model. A classical result is that, transport problem for a uniform flow model is equivalent to radial flow conditions provided the velocity at mid distance is considered for this model. This is nevertheless only true as far as the breakthrough curve is concerned. The above

mentioned equivalence is provided by [*Maloszewski et Zuber 85*] and demonstrated within a stochastic framework by [*Maugis et al. 02*].

This is nevertheless not true for all boundary conditions, in particular for total mass flux boundary conditions. This is examined by [*Wang et Crampon 95*] where this point is treated. The differences are globally most important for low Peclet and practically negligible for Peclets larger than 10. They provide as well approached formulas to simulate radial flow transport behavior based on uniform flow transport analytical solutions.
[*Chen et al. 96*] provides another insight into the solutions by [*Moench 89*] by comparing the former solutions with a similar problem involving another boundary condition at the inlet of the system : they derive solutions of the same system but including input well conditions allowing for back dispersion of the injected plume. The differences between radial model an uniform model are significative for low Peclets. These differences disappear for Peclets larger than 10 (corresponding to high velocities).

Another development of the model by [*Moench 89*] is provided by [*Chen et al. 99*] : they consider a 2D system including transverse dispersion (not limited to a 1D flow tube as previously). It appears that transverse dispersion has no influence on the breakthrough curve due to the radial nature of the problem. As a consequence transverse dispersion can't be measured by a classical test as the one conducted here. [*Chen et al. 99*] suggest measuring the concentration with a small representative volume in one location (suggested along the flow line between the injection and the pumping well).

In the following, we add further features to this system, in particular heterogeneous matrix diffusion. Solutions to such systems can't be obtained through analytical solutions. We proceed in the following by numerical simulations among the cast3M code.

3.2 Presentation of the model, its properties and parameter dependencies

The model considered here is based on the model by [*Moench 89*] including matrix diffusion in one homogeneous zone. This model is later refined to account for heterogeneity within the matrix zone.

The flow is governed by a classical Darcy law.

The equation transport equation, it is expressed in Cartesian coordinates, the zone modeled is therefore a non rectangular slice to account for the shape of the flow tube in radial conditions.

$$\frac{\omega R \partial C}{\partial t} = \nabla(\overline{D}\nabla C - \vec{U}C). \tag{3.1}$$

The parameters considered vary in space (take different values for fracture and matrix zones).

fracture :
- $\omega = 1$ fracture porosity,
- $R = R_a$ surface retention coefficient,
- $\vec{U}$ Darcy velocity,
- $\overline{D} = \begin{bmatrix} \alpha_L U + \omega D_{mol} & 0 & 0 \\ 0 & \alpha_T U + \omega D_{mol} & 0 \\ 0 & 0 & \alpha_T U + \omega D_{mol} \end{bmatrix}$.

matrix :
- $\omega = \omega_m$ porosity,
- $R = R_d$ bulk retention coefficient,
- $\vec{U} = \vec{0}$,
- $\overline{D} = \omega D_p$, diffusion coefficient.

As can be seen, this system depends on a large number of parameters. Nevertheless, only a limited number of parameter groups remain. This is here further developed considering a classical analytical solution to a very similar system with the difference that matrix diffusion is 1D orthogonal and the flow uniform (solutions by [*Tang et al. 81*] and [*Maloszewski et Zuber 85*]). The system considered is provided below. It is obtained by averaging the concentration in the fracture over the depth of the aperture. For x along the fracture and z across : *fracture equation:*

$$R_a \frac{\partial C_{fr}}{\partial t} = D_L \triangle C_{fr} - \vec{U}\vec{\nabla} C_{fr} + a_w \omega D_p \frac{\partial C_m}{\partial z}, \tag{3.2}$$

Matrix equation :

$$R_d \frac{\partial C_m}{\partial t} = D_p \triangle C_m. \tag{3.3}$$

for :

$\vec{U}$	Darcy velocity m/s	
C_{fr}	Concentration in fracture, mol/m^3	
C_m	Concentration in matrix, mol/m^3	
D_p	Diffusion coefficient (matrix), m^2/s	
R_a	Surface retention coefficient	$R_a = 1 + a_w K_a$
K_a	Surface sorption coefficient, m	
a_w	Specific surface, m^{-1}	$a_w = 2/b$, b aperture
R_d	Bulk matrix retention coefficient	$R_d = 1 + \frac{1-\omega}{\omega}\rho_S K_d$
K_d	Sorption Coefficient (matrix), m^3/kg	
ρ_S	Volumetric mass of solid (matrix), kg/m^3	

The homogeneous matrix case is based on four parameters as can be expected by comparison with the uniform flow situation. One may refer for instance to [*Maloszewski et Zuber 85*], where an analytical solution to the 1D fracture with uniform advection, dispersion and 1D orthogonal matrix diffusion. This system is represented by four groups of parameters :

- t_0, advective time (or flow velocity)
- P_e, Peclet (or dispersion coefficient)

- a, coefficient representing matrix diffusion term
- δ, coefficient representing the effect of limited diffusion (penetration depth)

These coefficients follow, for x the observation location and according to [*Maloszewski et Zuber 85*] ($R_a = 1$, no surface retention) :

$P_e = Ux/D$, Peclet
$t_0 = x/U$, advective arrival time
$a = \omega\sqrt{R_d D_p}/2b$
$\delta = (L/2 - b)\sqrt{R_d}/\sqrt{D_p}$

L corresponds to the depth of the matrix and U to Darcy velocity.

This system boils down to a 3 parameter system for unlimited matrix diffusion (or if the plume doesn't penetrate deeply into the matrix and doesn't see the limit as is the case for short term tracer tests). It can be further reduced to the classical two parameter system by [*Neretnieks 80*] by suppressing dispersion within the fracture.

As a four parameter system, this model is already complex for calibration based on a single breakthrough curve. On the whole three tests are provided in the present study but the last two include sorption, adding retention parameters. General remarks are that penetration depth can't be identified if the plume does not penetrate deep enough into the rock. Dispersion within the fracture as well as matrix diffusion both lead to a spread in the breakthrough curves. They are in practice hard to discriminate. Moreover, the matrix diffusion effect is potentially reduced in case of limited matrix diffusion (low matrix depth).

Some other theoretical considerations are interesting. One may for instance report to [*Ostensen 98*] where the author identifies (in agreement with [*Neretnieks 80*]) three transport regimes. For two extreme regimes, the system doesn't behave as a dual porosity system but rather as a single porosity system. The system is as such reduced to a simpler one and is then described differently : for very short times, the matrix zones don't play their retention role, for very long time scale, the matrix is filled up with concentration and the system is reduced to a single porosity system where the velocity of the plume correspond to the total porosity of the system fracture and matrix. These extreme systems are described by two parameters : dispersion and real velocity (corresponding to a fracture porosity in the first short time case and to the total porosity for the long time scale). This point as well as the consequences in terms of providing a bridge to PA model scale is discussed below in relation with the feature A situation (see 4.2).

3.3 implementation within the Cast3M code

As mentioned before, the former equation is simulated in Cast3M code, considering a slice like geometry to mimic the shape of the flow tube. The parameters vary depending on their belonging to the fracture or matrix zones. We consider there is no flow in the matrix (immobile zone). Heterogeneity of matrix parameters is naturally considered in this framework. We first validated the numerical approach without matrix diffusion against Moench solutions ([*Moench 89*]). We found that although the velocity profile

varies strongly along the fracture to the pumping well, Eulerian approach based on a constant time step was providing excellent results. For a low number of meshes along the well axis (50 elements) we considered a constant time step corresponding to a Courant number of 0.5 for the velocity at mid distance. These conditions were kept for the rest of the study involving matrix diffusion zones. For matrix diffusion, the discretization of the matrix was conducted to account for Fourier numbers around 1 in the vicinity of the fracture to larger values in the depth of the matrix (to optimize the number of meshes). The same approach was considered for heterogeneity in the matrix zones. The basic case involves constant unit concentration at the inlet. Further modeling correspond to a unit mass in the mesh corresponding to the well location. For this latter case, the system had to be extended upstream the well to take upstream dispersion into account. Convolution with the injected signal was considered for the calibration phase based on the precedent concentration step solution.

Chapter 4

Calibration (Task6A)

The calibration phase is based on the radial flow conditions transport model presented previously. The system is therewith reduced to a one flow channel system. The channel corresponds to the main flow tube existing in feature A between KXTT1 and KXTT3. This assumption is realistic considering the knowledge of feature A and the fact that the system should, for quick velocity conditions, exhibit the behavior of a main channel (see discussions in [*Selroos et Elert 01*]). The calibration efforts done show indeed that a consistent approach of feature A is possible for the test considered based on a single channel approach.

We consider different levels of solutions where the main focus of the study is the influence of the matrix zones on tracer transport behavior. One basic point is that only one flow channel is represented here as expected from the flow features during the experiment : the larger part in transport features is played by one dominant flow channel connecting the injection well to the pumping well (see [*Selroos et Elert 01*]). We consider for calibration three fracture models represented schematically on figures 4.1 and 4.7 and described below :

1. *An equivalent unique matrix zone approach.* This approach was the first considered as a sufficient SC model due to the low level of information formerly available. We address the question of identifiability of parameters and conduct sensitivity analysis to different parameters in the prediction phase. In the sequel, we nevertheless show the limits of such a simple approach.

2. *A more complex deterministic matrix geometry* based on the information recently provided (involving different matrix zones materials : gouge, fracture coating, cataclasite and mylonite and altered and unaltered diorite). This variability is present orthogonally to the fracture direction. This model, incorporating more information than the former is chosen for predictions and final performance measures.

3. *An approach involving the same kind of zones but within a stochastical framework and considering different 1D like zones distributed along the fracture.* This approach was limited to assessing the influence of the heterogeneity in the case of Iodine. The level of uncertainty of the predictions for a large number of solutions to the calibration issue is studied.

4.1 First model : equivalent 1 matrix zone

The model considered is represented on figure 4.1. It consists of a mobile zone (named fracture) in contact with an immobile zone (named matrix). The flow is radial (practically achieved with Cast3M with Cartesian coordinates by working on a slice of the axisymetric system). Transport in the fracture is by advection, dispersion, diffusion with linear sorption for reactive tracers. Matrix is accessed by diffusion only, sorption in the rock is considered as well for reactive tracers.

The immobile zone is named here equivalent medium since it does not represent an identified medium but rather acts equivalently. We confirm in the following that this equivalent medium presents average properties as compared with the different immobile zones provided for feature A (gouge material, fracture coating, mylonite ...). We consider here limited matrix diffusion (including a sensitivity analysis to the matrix depth) and 2D diffusion in the matrix (3D in a thin slice to be more accurate). This should not make a great difference with classical 1D diffusion processes currently modeled due to the high velocity considered for the calibration problem (fracture kinetic impose the speed of the front).

The calibration is conducted manually. In this, each of the 7 parameter of the system has to be specified for the simulations (fracture aperture, dispersivity, sorption coefficient, matrix penetration depth, porosity, diffusion and sorption coefficient). Some of these parameters were previously estimated based on measurements in [*Selroos et Elert 01*]. Three experimental breakthrough curves are considered for the fit. They correspond to a non sorbing tracer (Iodine) and two sorbing tracers (Strontium and Cobalt). We provide below a single 'best fit' for all 3 tracers that is later used for predictions purposes.

The quality of the fit is measured by means of a distance from the calibration curve to the experimental : mean relative error, expressed in % on the figures :

$$relative\,error = \sqrt{\frac{1}{N_{exp}} \sum_{k=1}^{k=N_{exp}} (C_{sim}(t_k) - C_{exp}(t_k))^2} \tag{4.1}$$

Where N_{exp} is the number of times for which the experimental concentration C_{exp} was measured. C_{sim} represents the simulated concentration curve.

In this framework, calibration of the system should be done taken into account what was presented in former section. Indeed, calibrating the system first appears as providing a parameter vector of dimension 7 as mentioned just before. Nevertheless, practical calibration efforts show parameter dependencies like for instance dependence of porosity and diffusion coefficient : a similar fit is obtained by increasing porosity and decreasing diffusion coefficient while the product of these quantities remains roughly constant. Independent parameter groups have to be considered for the calibration. These could result from dimensional considerations from the system of equations of better from analytical

solutions. Unfortunately, the system considered though fairly simple does not have analytical solutions. But it is similar to the model by [*Maloszewski et Zuber 85*] presented in the previous section, only differing through the type of flow (uniform against radial). [*Maloszewski et Zuber 85*] shows that the system behaves as a 4 parameter system. One is related with the advection arrival time, the other with the Peclet (dispersion in the fracture), one characterizes the impact of matrix diffusion, the last one stands for limited matrix depth. In relation with matrix diffusion influence, the parameter of interest writes:

$$a = \omega\sqrt{RD_p}/e \tag{4.2}$$

Where ω stands for porosity of the matrix, R, the retention coefficient for the matrix, D_p, the matrix diffusion coefficient, e the fracture aperture. This means that the best way to proceed is not by considering each parameter separately but by working with the relevant parameter groups. Nevertheless, the present system is not identical with the system by [*Maloszewski et Zuber 85*] : flow is radial, matrix diffusion is not 1D. But simple considerations on the equation set shows that the number of unknowns should be comparable though the exact expression of the parameters groups is not available.

In addition to this, another level of uncertainty originates from the fact that calibration is done on a system including convolution with the injection curve introducing another unknown, the injection rate, roughly estimated from the curves of concentration in the injection loop.

So, (i) there is probably not a unique solution to the problem as expressed in term of well chosen parameter groups (for instance matrix diffusion and dispersion are similarly responsible for spreading of the curves and might not be separated due to the shape of the injection signal providing bad observation of the tailing of the curves), (ii) several combinations of these parameters might lead to the same solution (dimension 7). As mentioned, a similar fit as the one provided below for Iodine can be obtained by considering lower diffusion coefficient but larger porosity (choose $\omega = 0.2$ and $D_p = 5.10^{-11} m/s$). This is clearly understandable considering the expression of parameter a introduced formerly.

It should be noted that the more complicated the system the larger the number of unknowns we get. We generally assume here that, based on the knowledge of the fracture, some of the features are sufficiently known or well estimated so that the inverse procedure or calibration exercise can be limited to some other features. In a second step, sensitivity analysis are conducted or we proceed within a stochastic framework.

Anyway, as we will see below, for the higher diffusion zones with low penetration depths, only the total volume of the zone is of interest for the PA time scale. A special focus should as such be put on the estimation of the range of variation for the porosity as well as the depth of the zone (the porosity is corrected by the retention coefficient for sorbing tracers). Diffusion coefficient values are no more relevant for this slower flow regime.

General comments for the fits follow (see figures 4.2 and related data set on table above) : the fit is globally acceptable showing that the simple one-channel model with one a single matrix diffusion zone is fair. It does not seem necessary here to consider models with radically more complex geometrical features. Iodine and Strontium are fitted within 15% and 7.5% respectively. The shape for the first arrival times is not completely

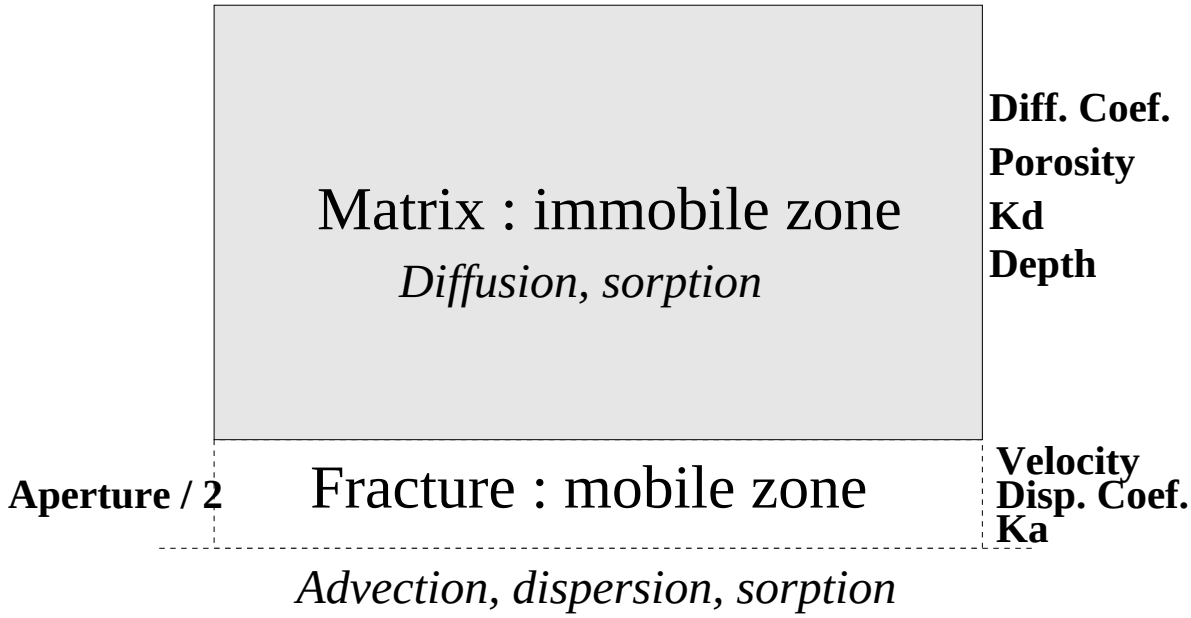

Figure 4.1: Feature A : first conceptual model

Calibrated data set	**model 1**
Fracture aperture	$2mm$
Matrix penetr. depth	$1.5cm$
Porosity (fracture)	1.
Porosity (matrix)	10%
Diffusion coefficient (fracture)	$10^{-9}m^2/s$
Diffusion coefficient (matrix)	$2.10^{-10}m^2/s$
Dispersivity (longitudinal)	$25cm$
Dispersivity (transverse)	$2.5cm$
Strontium	$R_a = 1.5,\ K_a = 5.10^{-4}m$
Strontium	$R_d = 15,\ K_d = 5.810^{-4}m^3/kg$
Cobalt	$R_a = 1,\ K_a = 0.$
Cobalt	$R_d = 8500,\ K_d = 3.510^{-1}m^3/kg$

Table 4.1: Calibrated parameter set for the first model considered (1 equivalent immobile zone)

captured for Iodine suggesting that some further features should be added in the system. The fit for Strontium is considered excellent taking all the uncertainties of the system into account. The fit for Cobalt is poor and can't be significantly improved based on the model and parameter set considered. Directions for improvement should more probably imply sorption the sorption model. Cobalt is probably not under instantaneous equilibrium conditions for the sorption phenomena. As a consequence, we put a very limited level of confidence in the calibrated parameters. These will not be used for prediction in the rest of our work : we prefer values from lab measurements and will consider among them the sorption values corresponding to the largest contact time. For Iodine and Strontium, the

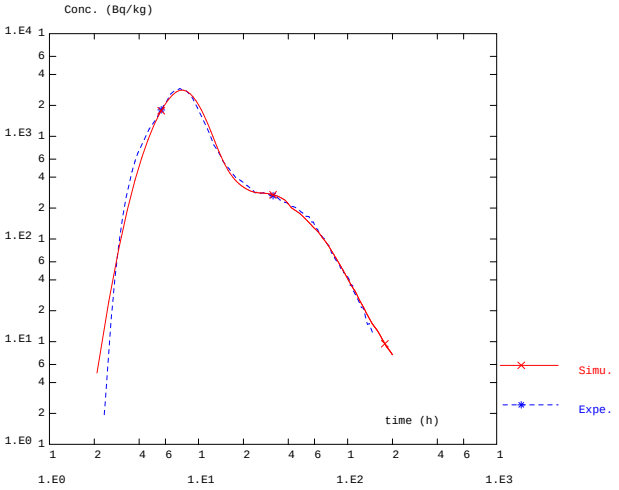

(a) Iodine, relative error by 15.%

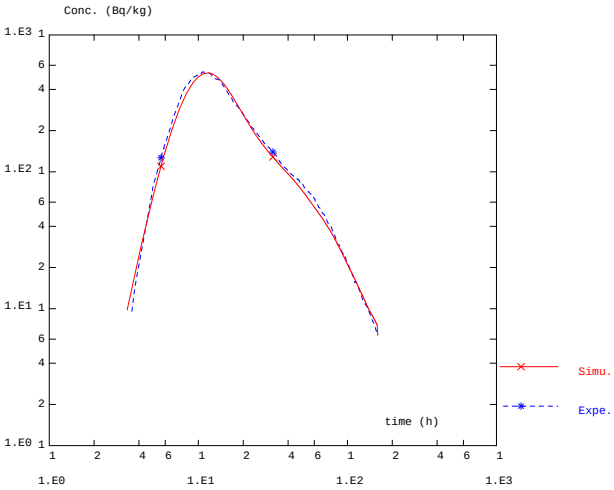

(b) Strontium, relative error by 7.5%

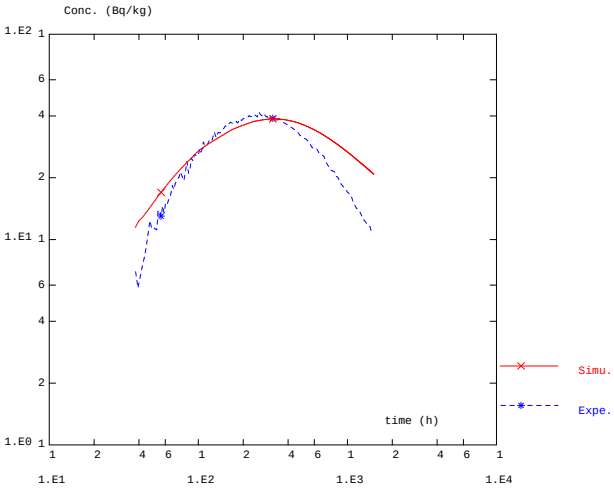

(c) Cobalt, relative error by 20%

Figure 4.2: Calibration of the first model : simple 1 matrix zone system

fitted parameters fall into the range proposed. So these values will be considered for the prediction phase.

A sensitivity analysis to the penetration depth was conducted : depth by $5mm$, $1cm$, $1.5cm$ and $2cm$ were considered. This is in agreement with the spatial dimensions of the different zones (see Tab. 4.2 below). Only minor changes were observed for Strontium and Cobalt for this range of values. The influence on Iodine was sensitive for depths ranging from $5mm$ to $1.5cm$ meaning that above $1.5cm$ the matrix behaved as an infinite medium for Iodine under current transport conditions (the mass doesn't travel to this depth). The best fit was obtained for $1.5cm$. This value was retained in the following. It is finally acceptable considering the fact that the depth of the most diffusive zones (apart from thin fracture coating) range from $5mm$ for gouge to $2cm$ for mylonite and cataclasite (see Tab. 4.2).

4.2 Role played by different immobile zones for quick and slow flow regimes

Different zones correspond to immobile zones playing a retention role for the plume (i.e. temporally removing fractions of the plume from the mobile zones by diffusion processes). The geometry of these zones is rather complex as can be seen from the sketched proposed on figure **??**. In addition, the accurate localization of the different zones was not measured. These points are developed for instance in [*Winberg et al. 02*], where simplified models of the different zones as well as a tentative quantitative parameter data set is provided. Two types of fracture zones are presented : type 1 typical for a fault zone and type 2 typical of a non fault fracture zone. Feature A corresponds to a reactivated mylonite zone [*Winberg et al. 98*], close to the Type 1 feature provided. In terms of matrix zones, it consists of stagnant water pore zones or porous media adjacent to the open fracture like fault gouge, fracture coating, cataclasite and mylonite, altered diorite, unaltered zone (report to [*Winberg et al. 02*]). Typically, fault gouge, fracture coating and partly cataclasite and mylonite are dominantly in the vicinity of the open fracture, whereas altered and non altered diorite are mostly to be found in the depth of the matrix. The former show larger diffusion and porosity parameter values than the latter.

We conduct here a theoretical study with the idea of preparing the way to answer the following questions :

- Characterize the role played by the different matrix zones mentioned above for the different flow regimes considered in the task (A and B1).
- Propose an equivalent model to account for the presence of these different zones.

For this we visualize the impact of these different zones by considering successively and alone each of the matrix zones mentioned in contact with the fracture as in the model 1 geometry (see figure 4.1). We show there the impact of each individual zone for the two transport regimes considered (experimental time scale and 1000 times slower for same flow patterns). This study is provided for Iodine (non sorbing tracer) and encloses for sake

of comparison the calibrated equivalent medium (see below). We call this a theoretical study, since, in reality all of these zones are present along the fracture and in the depth of the rock block. A complementary study is conducted further below in section 6 for the uniform flow conditions of Task6 B2 and involves the presence of all of these matrix zones in a single model corresponding to the Type 1 geometry from [*Winberg et al. 02*]. In this complementary study, we show the evolution of tracer masses in the different matrix zones. This leads to similar results as the ones provided below with the very simple homogeneous matrix diffusion model.

We consider the same geometrical features are previously : a single channel ($5.03m$ length), connecting input and output wells. We work here on the breakthrough curves corresponding to a Dirac input (more accurately, derivative of the curves obtained for constant imposed concentration input). We previously fitted the experimental breakthrough curve by means of a similar one channel, one homogeneous diffusion zone model. This lead to the following parameters : fracture aperture by $2mm$, matrix properties by $\omega = 0.1$, $D_p = 2.10^{-10} m^2/s$. Since diffusion in matrix zone plays a minor role, this fracture aperture provides the arrival time of the peak for an advective dispersive model without matrix diffusion. We keep here the same fracture opening. Nevertheless the actual matrix zone depths have to be considered for the slow velocity case because the results are very sensitive to this dimension. We present on figures 4.3 below breakthrough curves obtained for the same advective dispersive transport patterns in the fracture but different matrix zones. The first step corresponds to experimental conditions (quick flow) and a penetration depth by $1cm$ of all materials. The second step corresponds to a 1000 slower flow and penetration depth as provided by [*Winberg et al. 02*] (different for each material). Refer to figure 4.3. The parameter values are summed up on table 4.2.

Immobile zones	Extent (cm)	Porosity	Diffusion Coef. Dp (m2/s)
Fault gouge	0.5	20%	5.10^{-10}
Fracture coating	0.05	5%	2.10^{-10}
Cataclasite and mylonite	2.	1%	10^{-10}
Altered zone	20.	0.6%	8.10^{-11}
Unaltered zone	–	0.3%	5.10^{-11}
Calibration	1.	10%	2.10^{-10}

Table 4.2: Immobile zone parameters (length, porosity and pore diffusion coefficient). According to [*Winberg et al. 02*]

We first comment the breakthrough curves obtained in terms of transport regime :

- Matrix diffusion globally plays a limited role for the quicker flow regime (report to figure 4.3-a). This can be seen by comparing the breakthrough curves obtained for the different materials against the case involving no matrix diffusion. More detailed analysis shows that, for the quick flow considered (tracer test conditions), matrix diffusion plays no significant role for altered and non altered zones and for cataclasite/mylonite. It plays a limited role for fracture coating. Gouge material has the major role in retention process in this case : slight retardation of the peak arrival time and tailing effect.

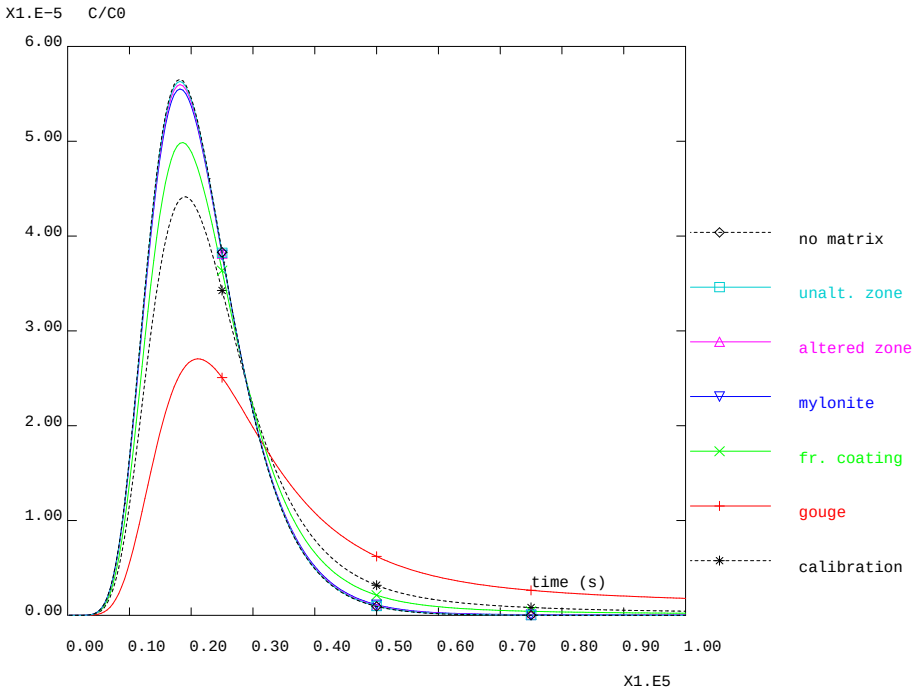

(a) Experimental conditions

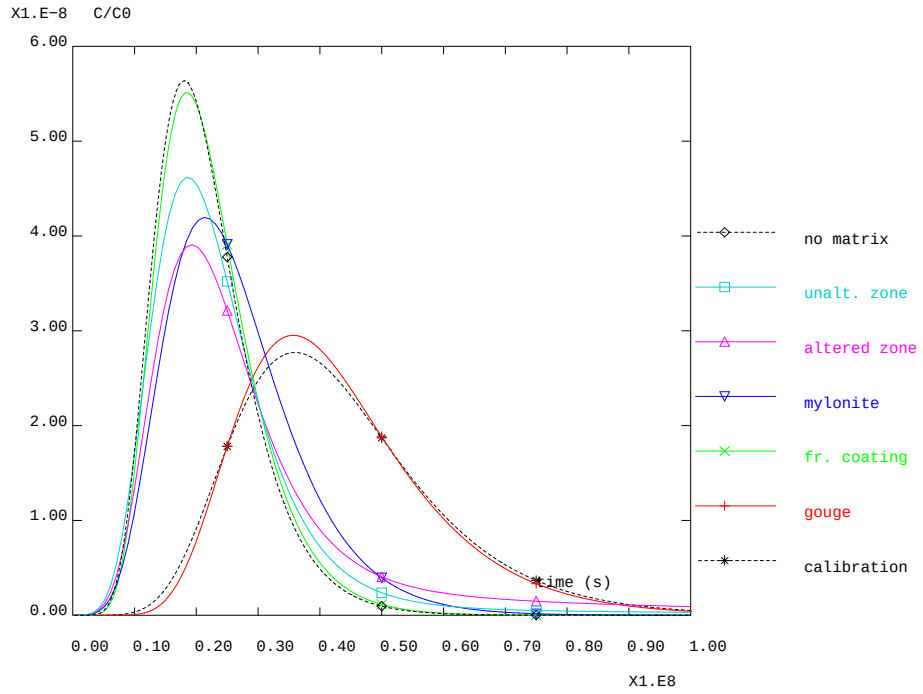

(b) PA time scale : 1000 times slower flow conditions

Figure 4.3: Influence of different matrix zones on the transport regimes for (a) the experimental flow conditions and (b) 1000 times slower flow

- For the slower flow regime, (1000 times slower, see figure 4.3-b), matrix diffusion plays a larger role as can be seen from the breakthrough curves as compared with the no matrix diffusion case. This is a classical result : the contact time of the plume with the matrix diffusion zones is larger leading to increased impact of this phenomenon. The impact for each of the matrix zones considered depends on the several parameters : diffusion coefficient, porosity, depth of the zone. The larger these parameters, the larger the impact of matrix diffusion. This is in agreement with the results. One can stress that the most efficient zone in retarding the arrival time and decreasing the peak level is the gouge material. It leads to similar results as the equivalent matrix calibrated previously. This is indeed due to the fact that although this equivalent zone has lower diffusion coefficient and porosity than the gouge, diffusion occurs over a larger depth. In order of importance appear next, the altered and the cataclasite/mylonite zones. The difference in the relative shape of the curves is explained below (more or less tailing effect). Non altered zones and the very thin fracture coating play minor roles.

As a conclusion, only the more diffusive zones are expected to play a significative role for the quicker flow regime. These are gouge and fracture coating. Moreover these zones are filled up by the plume over a limited depth. For the slower flow regime, the diffusion parameters as well as the depth of the zone should be taken into account to explain the behaviors : fracture coating plays a very limited role due to its very limited volume, gouge, cataclasite/mylonite, altered rock are potentially important.

In a second step, we look here for potentially equivalent models for the slower flow regime as required in the task objectives. A classical interesting result is the following (see [*Ostensen 98*] or [*Carrera et al. 98*] for instance). Consider one of the above systems (type model 1 as on figure 4.1, fracture with adjacent homogeneous matrix zone). (i) For a very quick flow regime, the characteristic advective time is very short, so is the contact time of the plume with the diffusion zone and as a consequence, matrix diffusion plays no significant role in the transport regime. (ii) For larger times, matrix diffusion plays a larger role as transitory storage zone for the transported mass. The type of breakthrough curve observed shows lower arrival peak level as well as a tailing effect (slow matrix mass release). (iii) For very large contact times, the whole of the matrix volume is invaded, and the result is that the peak arrival time is strongly delayed for associated very low level. But for such an extreme regime, one may observe that the breakthrough curve is no more asymmetrical in the was observed in the second regime described previously (showing tailing effect). This is what is observed here on figure 4.3-b for gouge material and mylonite/cataclasite for instance, this being in contrast to altered rock or non altered rock situation.
This third transport regime can be easily explained for the cases presented on figure 4.3-b : the gouge material is completely invaded by the plume. This occurs for time scales smaller than the advection time scale so that the whole matrix zone is locally filled up and equalizes its concentration with the fracture. As a consequence the progression of the plume along the fracture happens over the fracture aperture in addition to the depth of the gouge unit : as a wider front. This is qualitatively equivalent to enlarging the transport aperture to the gouge unit or more accurately to considering a larger total porosity.

This is illustrated on the following figures 4.4 and 4.5 where the breakthrough curves for

the initial system are compared with those obtained with the equivalent single continuum medium. As stated above this equivalent approach is valid in the third transport regime presented above. This is visually the case (see figure 4.3-b) for gouge, fracture coating and cataclasite/mylonite. This is not the case for altered and non altered diorite for which no simpler model can be proposed. As mentioned previously, for slow flow velocity, as compared with diffusion time scale in the matrix zone, the matrix zone is fully invaded so that the actual transport porosity should be increased to enclose matrix total porosity. Practically speaking, the equivalent model corresponds to the following equivalent depth $d_{eq} = e + d$ and porosity ω_{eq} :

$$\omega_{eq} = (1e + d\,\omega)/d_{eq} \tag{4.3}$$

for d, depth of the matrix unit and ω, associated porosity. e is the half fracture aperture.

An alternative and equivalent approach consists in considering this as the former porosity corrected by a term formally equivalent to a retention coefficient (R_eq) :

$$R_{eq} = (1 + d\,\omega)/e \tag{4.4}$$

Or expressed in terms of K_a, surface sorption coefficient :

$$K_a^{eq} = d\,\omega \tag{4.5}$$

The extension to sorbing tracers (sorption into the matrix zone) is straightforward and leads to :

$$K_a^{eq} = d\,(\omega\ +\ (1-\omega)\,K_d\,\rho) = d\,\omega\,R \tag{4.6}$$

Where the parameters are all relative to the matrix zone : d is for its depth (m), ω, its porosity, K_d, its sorption coefficient for a given tracer (m^3/kg), ρ, its density (kg/m^3), R matrix retention coefficient.

We observe on figures 4.4 that the fit is indeed excellent for the matrix materials concerned : gouge, fracture coating, mylonite/cataclasite. This is still true as seen on figures 4.5 for all 3 with the following geometry : on the one side of the fracture ($2e$ aperture), gouge, on the other side fracture coating and further in the depth, cataclasite/mylonite. As expected as well, the equivalence does not hold for the altered and non altered diorite.

So, for the objective of building a simplified PA model, we suggest characterizing the role played by the different zones identified by means of direct modeling of the system involving all these zones. The different zones can be organized into two groups : (i) those following the same kinetic as the fracture (fully invaded for characteristic times lower than a characteristic advection time, here gouge, fracture coating, cataclasite/mylonite) should be gathered with the fracture in an equivalent fracture where the total porosity associated is modified (or alternatively a K_a is associated); (ii) those providing transitory storage of the mass and posterior delayed release of it (altered and non altered zones) have to be modeled explicitly as matrix diffusion zones.
If these zones matrix diffusion zones are further homogenized into a single equivalent matrix zone (this was not done here), the final system is very simple and corresponds to the geometry of the first model presented previously : equivalent fracture and equivalent homogeneous matrix zone.

This approach is further applied in the rest of the present document. One may in particular refer to the section related to the uniform flow conditions (Task6B2, see chapter

6) where the selection of the zones is done based on the evolution of the total masses in each unit of the system : some follow the same evolution as for the fracture, others show independent behavior, providing large delays in the arrival times. It should be nevertheless stressed that the role played by the different zones depends upon :

1. The flow conditions (quick or slow velocity)
2. The tracer considered (non sorbing or more or less sorbing)

We will see in the sequel that for the cases considered, the situation does not change significantly whatever the tracer and flow regime considered : gouge, fracture coating and mylonite/cataclasite zones should be counted to the first group and the diorite zones to the second. Nevertheless, the flow velocity considered in Task6B2 is slower than for Task6B1. It leads to an increase in the role played by the second group of matrix zones. For stronger sorbing tracers (Americium and Technecium), cataclasite/mylonite zone does not strictly behave as a first group zone but shows some slight transitory behavior for the Task6B1 case. For the Task6B2 case, it always belongs to the first group.

How the parameters for these matrix zones can be estimated as well as the level of information provided by a tracer test (Task6A) is shortly discussed here and further developed below (see the discussion when comparing results from model 1 and 2).

A first remark is that a minimum level of information about the different matrix zones is required : their geometrical features, parameter values, ... These can be obtained from direct measurements on analogous features elsewhere at the studied site. How one can deal with deterministic or stochastically estimated heterogeneity of such systems is shown below with models 2 and 3. But another source of information can be obtained from in situ tests : pumping tests to estimate the hydraulic parameters, and tracer tests for transport features. It is clear from the preceding analysis that only high diffusion zones play a role in short time tracer tests. As such the other zones can't be characterized by means of tracer tests. Simple considerations on the system show that tracer tests provide an averaged estimation of matrix diffusion parameters as an integral of all the characteristics of the zones viewed by the plume. The longer the test, the larger the volume of the zone investigated. Nevertheless, a further particularity of tracer tests as a source of information is stressed by [*Ostensen 98*], it is a stronger limit to parameter estimation. As seen previously, the high diffusion zones playing a dominant role (like gouge, fracture coating, cataclasite/mylonite) are estimated in the second regime identified (matrix diffusion is efficient and plays a dynamic role). From the analogy with simple systems ([*Maloszewski et Zuber 85*]) it appears that a tracer test provides access to a parameter group (involving among others diffusion coefficient, porosity, fracture aperture ...) which characterizes matrix diffusion behavior. The same zones for slower flow velocities as considered in Task6B at PA time scale show features of the third regime where the zones are fully invaded by the plume. Here the parameter group required involves the total porosity as well as the depth of the zone (K_d as well for sorbing tracers). This means that the parameter group estimated from tests conducted in experimental regime is different from the one required for the prediction regime ! Without further independent parameter measurements, estimation of parameter group from a tracer test in one regimes brings no information for predictions in the other regime.

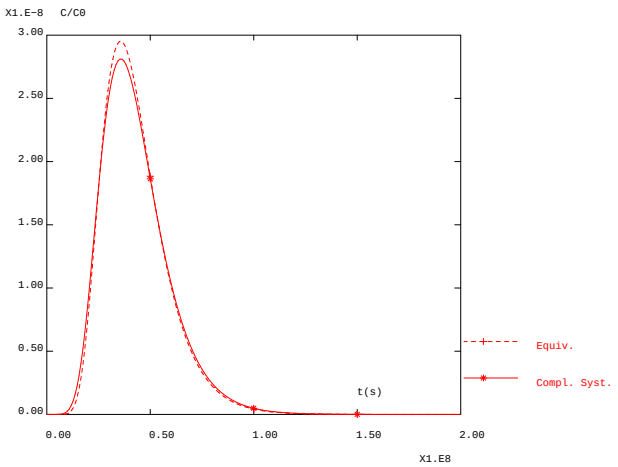

(a) Gouge

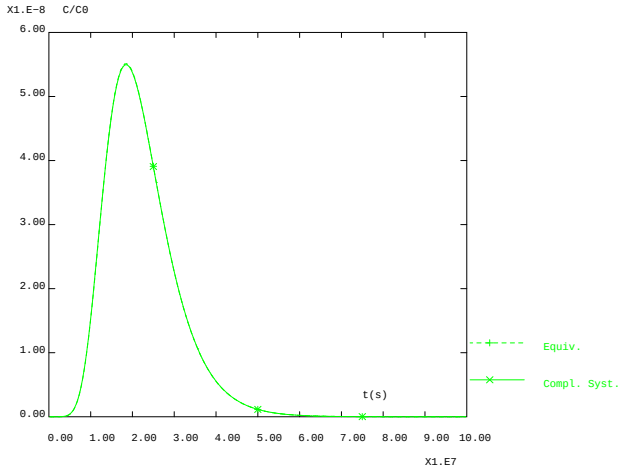

(b) Fracture coating

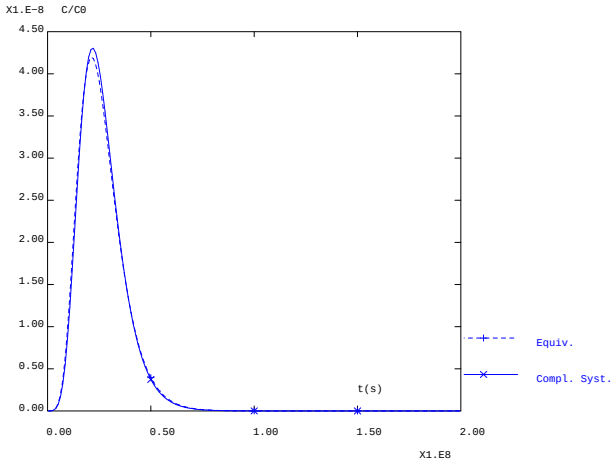

(c) Cataclasite and Mylonite

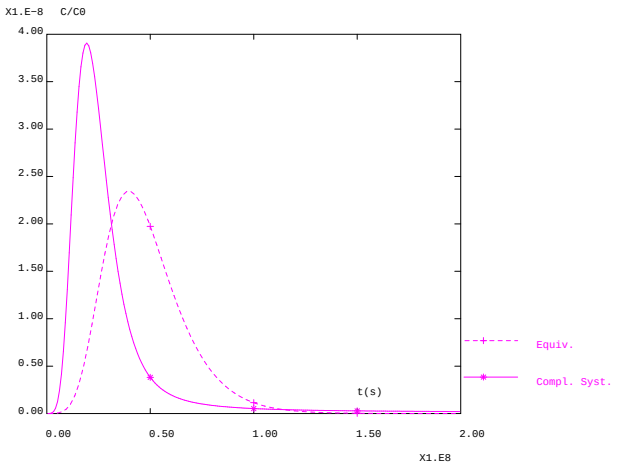

(d) Altered Diorite

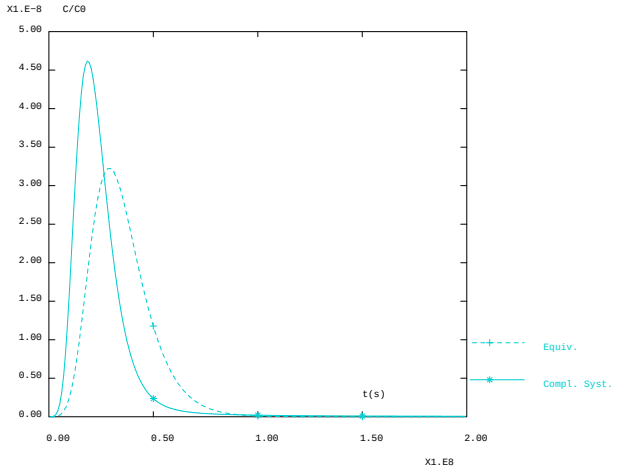

(e) Unaltered Diorite

Figure 4.4: Relevance of equivalent fracture only models for the PA time scale. The depth for all zones are as provided in tabular 4.2, the depth for the unaltered zone is here chosen as $20cm$, the same as for the altered zone

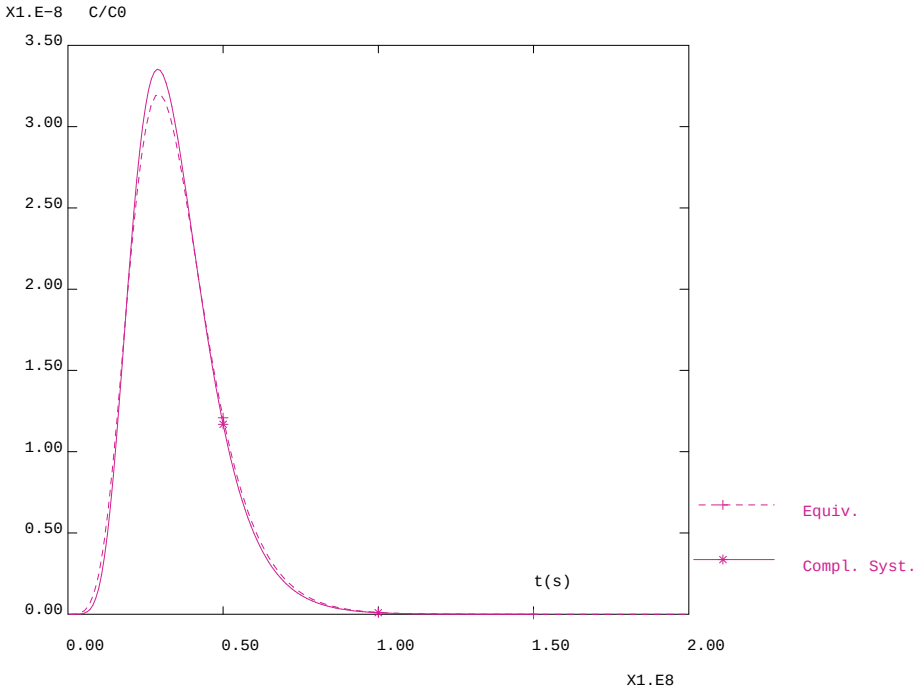

Figure 4.5: Relevance of equivalent fracture only models for the PA time scale. We consider here the 3 most diffusive zones (gouge, fracture coating, cataclasite/mylonite). The depth for all zones are as provided in tabular 4.2

We sum up here some of the major results obtained (these are to a certain extent related with the flow regimes considered as well as the feature A parameter set) :

- Experiments conducted at the month scale allow for identification of the most diffusive zones in the vicinity of the fracture. This allows for identification of a parameter group involving the diffusion coefficient of the zones as well as the porosity, fracture aperture ...
- For PA scale modeling, these zones do not play a dynamic role since they are instantaneously (as compared with advection characteristic time) fully invaded by the plume. Knowledge of another parameter group (involving total porosity and depth of the unit) is required for the prediction. This is not the quantity measured by a test conducted at experimental scale : it should be measured independently. The more dynamic role for inter-zone mass exchange is played by other matrix zones located more deeply into the rock. Short term tests do not provide physical access to these zones since the plume doesn't travel sufficiently deep to the corresponding depths : they can't be characterized by short term tracer tests.

In the sequel, we work with two other models of feature A :

- Model 2 takes into account all the direct measurements that were recently provided (see [*Winberg et al. 02*]) in contrast to what was attempted with model 1. The different in the predictions capacities of both models, one poor in information and the other that benefits from more direct information will be discussed. Performance measures are proposed based on this deterministic Model 2.
- Model 3 was introduced to characterize the type of detailed information that is provided by the tracer test. We consider here longitudinal as well as transverse heterogeneity within a stochastic framework. The analysis is limited to the Iodine case.

4.3 Further calibration steps including matrix heterogeneity

We present here further steps in the calibration efforts for the tests provided in feature A. We nevertheless keep some features of the previous model : the flow is still radial and the model is limited to a flow line connecting the input well with the output well. This is justified by the fact that for the time scale considered, the major transport path is expected along the quickest path and the transverse diffusion transfers play a minor role.

The feature A system as contemplated in [*Selroos et Elert 01*] is represented on figure 4.6. We try in the following to achieve a more realistic description of the system in terms of matrix zone heterogeneity.

We consider in the following two lines of improvement. We enclose heterogeneity of the matrix block corresponding to the different zones observed along the fracture at TRUE

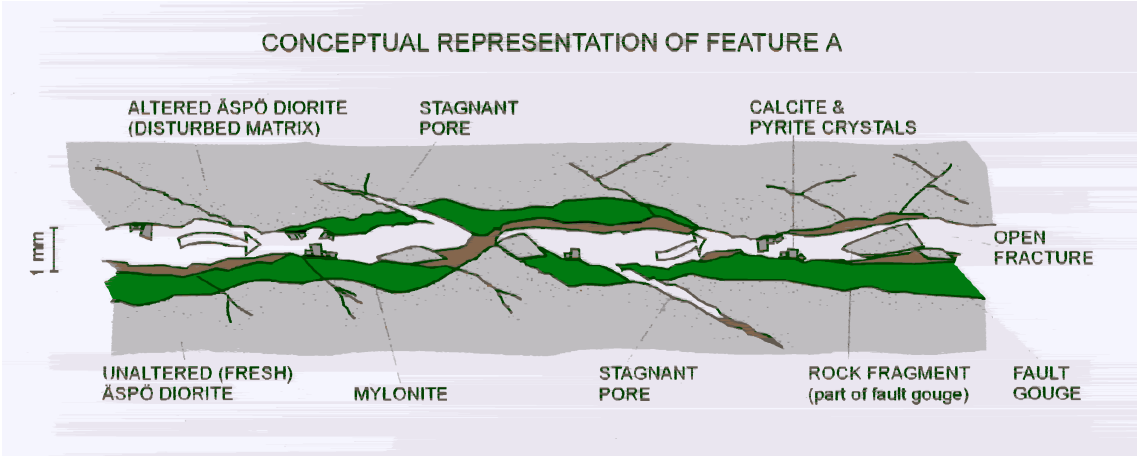

Figure 4.6: Sketch of Feature A, from [*Selroos et Elert 01*]

location (see [*Selroos et Elert 01*], [*Winberg et al. 02*]). The immobile zones are indeed : gouge material contained in the fracture, fracture coating, mylonite and cataclasite, altered and unaltered diorite. Most of the parameters corresponding to the properties of these zones are provided in the recent [*Winberg et al. 02*] as well as an idealized image of the fracture (type 1 fracture zone). Nevertheless, the actual position of these zones along the fracture plane remain largely unknown.

A remark can be made at this level : the calibrated matrix parameters for the simple one immobile zone model are in agreement with the diffusion and porosity parameters available for the different zones. Indeed, the calibrated parameters should come out as an averaged values of the immobile zones parameters in contact with the fracture (one centimeter scale). The plume should furthermore mainly see the first millimeters, this means that the averaging should be done on the first material types met from the fracture wall. The current values obtained in the calibration are indeed in good agreement in terms of porosity or diffusion coefficient with the values provided for the different zones.

Nevertheless, due to the present level of knowledge on the feature A situation, the above equivalent matrix approach is not sufficient. We study in the following the influence of the heterogeneity of the immobile zones properties. This is done in two ways :

1. First approach : the geometry of the matrix zones provided in [*Winberg et al. 02*] is considered according to the Type 1 case expected for feature A. The situation is sketched on figure 4.7-a. We therefore consider transverse heterogeneity within the immobile zone but work on an longitudinally homogenized medium.

2. Second approach : the heterogeneity of the matrix zones is approached as successive slices of different properties along the fracture. The reduction of porosity and diffusion coefficient with the depth of the rock is accounted for by superimposing a profile to the selected values : constant on the first 1 cm zone and decreasing with the depth to the values characteristic for altered and unaltered rock properties. The parameter values affected to the slices in the vicinity of the fracture are characteristic of the first zones expected (gouge, fracture coating, cataclasite and mylonite).

This approach is as far comparable with a multi rate approach. It nevertheless includes a transverse profile as well as 3D diffusion features (a low diffusion zone can be invaded from the fracture as well a from a parallel higher diffusion zone contrary to classical 1D diffusion models). In this second approach we furthermore introduce a concept of stochastic modeling : different diffusion coefficient and porosity fields are considered following a normal low and an exponential correlation structure. The best solutions are selected by trial and error approach (reject the bad solutions considering a measurement of distance to the experimental curve). The final results related to PA scale predictions will be obtained running the selected realizations on the slow velocity case. As a consequence, the whole procedure strictly corresponds to a Monte Carlo approach with trial and error selection to account for the measured features.

With the first approach we mainly study the influence of different successive deterministically located zones in the depth of the matrix. These zones are chosen realistically according to the Type 1 feature [*Winberg et al. 02*].

In the second approach we study the influence of heterogeneity longitudinal to the fracture. A profile is superimposed on this to account for a reduction of transport properties in the depth of the matrix.

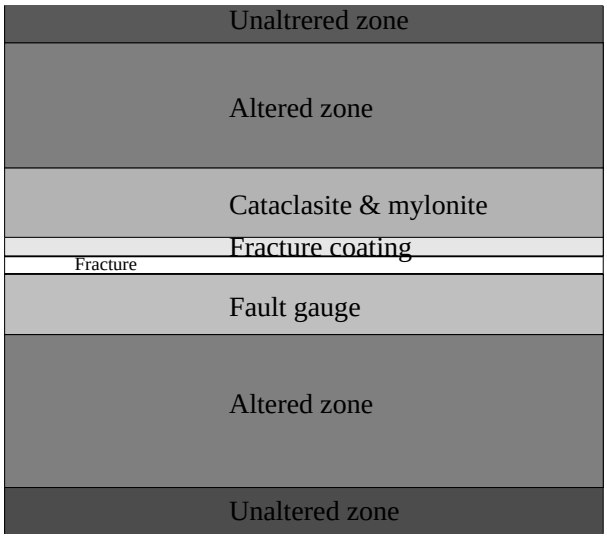

(a) Second model

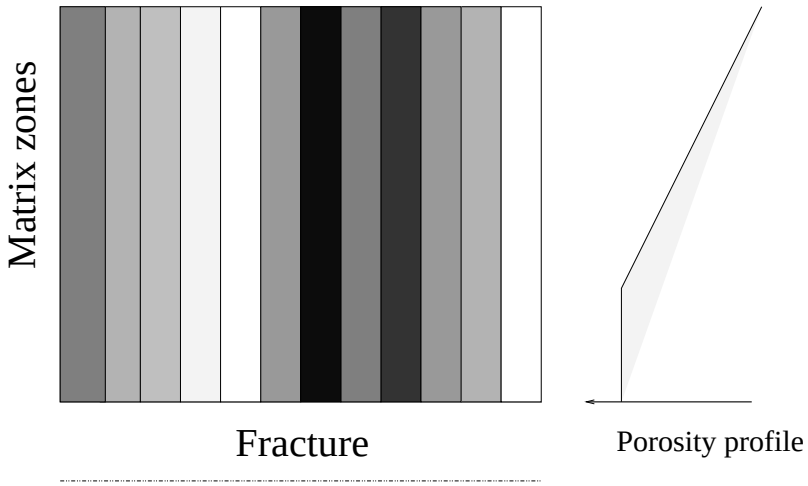

(b) Third model

Figure 4.7: Sketch of the geometries considered to address heterogeneity of the matrix immobile zones : second and third models.

4.3.1 Second model, integrating provided deterministic heterogeneity

We attempt here a calibration based on the geometry provided in [*Winberg et al. 02*] for the Type 1 fracture model. This geometry is provided on figure 4.7, as so called second model. This includes the 3 most diffusive zones : gouge, fracture coating, mylonite-cataclasite (altered and non altered zones do not influence the results due to the low penetration depth of the tracer). Direct simulation with the parameter values provided by SKB doesn't exactly lead to a satisfactory fit with experimental curves (although the orders of magnitude are fair). The best fit is obtained decreasing the porosity from 20% to 15% and the diffusion coefficient from 5.10^{-10} to 3.10^{-10}. The spatial discretization as well as a concentration field at 10 hours are provided on figure 4.8 fits are provided on figure 4.9.

Calibr. data set	Fracture	Gouge	Fracture Coating	Mylonite
Length	$2mm$	$5mm$	$0.5mm$	$2cm$
Porosity	1	15%	5%	1%
Diffusion coefficient	$10^{-9}m^2/s$	$3.10^{-10}m^2/s$	$2.10^{-10}m^2/s$	$10^{-10}m^2/s$
Strontium	$K_a = 5.10^{-4}m$	$K_d = 7.110^{-4}m^3/kg$	$K_d = 2.310^{-4}m^3/kg$	$K_d = 6.710^{-5}m^3/kg$
Strontium	$R_a = 1.5$	$Rd = 11.8$	$Rd = 12.8$	$Rd = 180$
Cobalt	$K_a = 0$	$K_d = 0.32m^3/kg$	idem	idem
Cobalt	$R_a = 1$	$Rd = 5000$	idem	idem
Dispersivity (longit.)	$25cm$			
Dispersivity (transv.)	$2.5cm$			

Table 4.3: Calibrated parameter set for the second model considered (fracture and the 3 most diffusive zones : gouge, fracture coating, mylonite and cataclasite). The parameters are the ones provided in [*Winberg et al. 02*] and [*Selroos et Elert 01*] except for the gouge material where the original data set considered a porosity by 20% and a diffusion coefficient by $5.10^{-10}m^2/s$

For this same dataset, we computed breakthrough curves corresponding to a unit mass Dirac input as well as continuous injection ($1Mbq/y$). These results can be found in chapter 7 gathering performance measures, including as well arrival times and values for peak maximum in the format required.

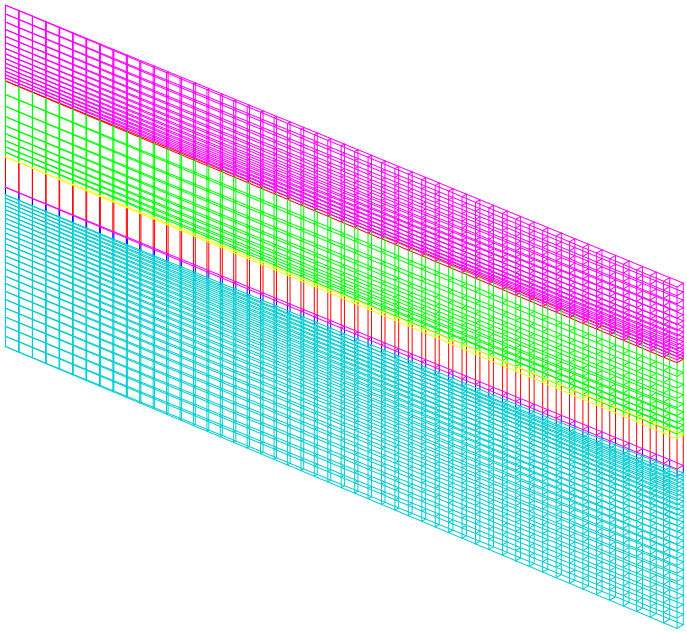

(a) Spatial discretization

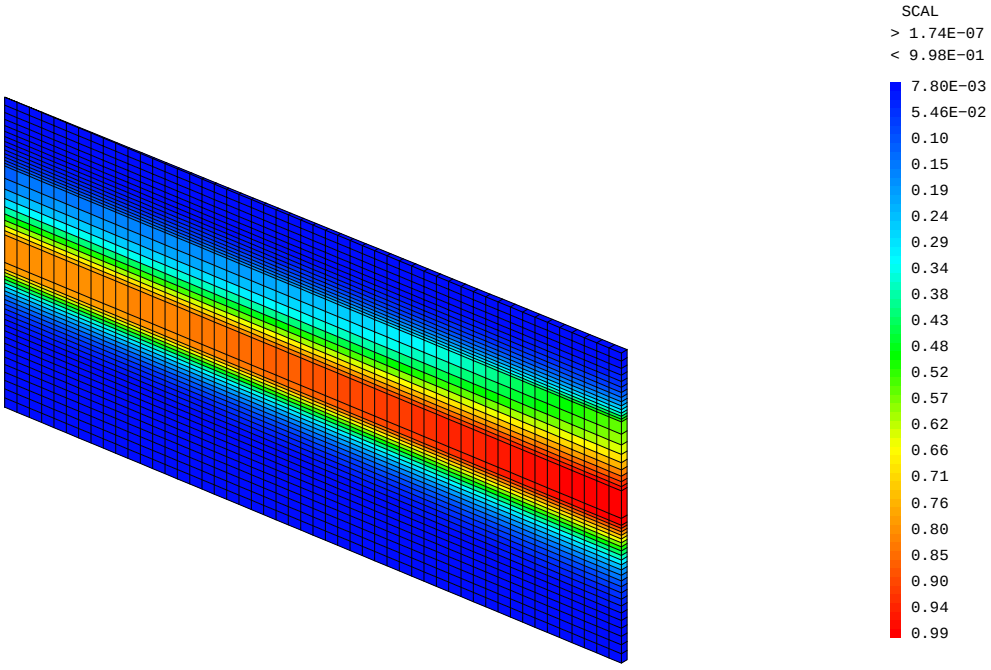

(b) Concentration field (10 h), unity concentration imposed at the fracture inlet to the right

Figure 4.8: Mesh and concentration field for the second model considered (from below to top) : Mylonite, fracture coating, fracture and gouge (on top in addition, altered zone by $5mm$ was added for sensitivity analysis to the presence of this zone)

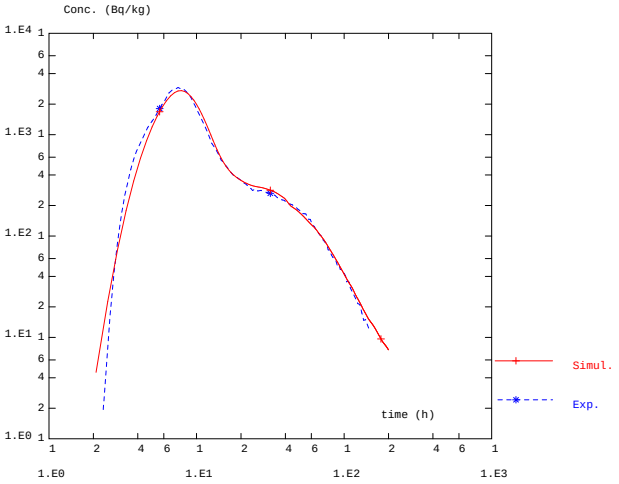

(a) Iodine, relative error by 15%

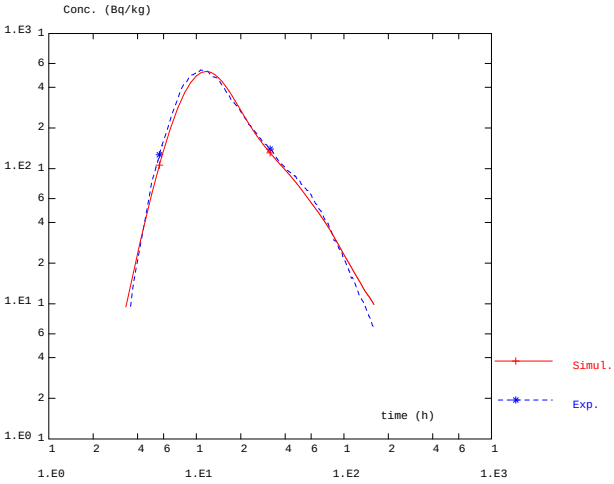

(b) Strontium, relative error by 10%

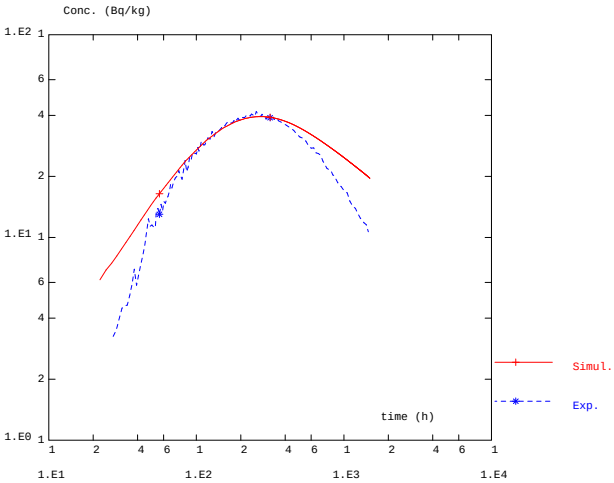

(c) Cobalt, relative error by 20%

Figure 4.9: Calibration of the second model : gouge, fracture coating and mylonite zones

4.3.2 Third model : Stochastic Monte Carlo modeling approach including longitudinal and transverse variability of matrix properties

Presentation

This next step is motivated by realistic considerations about the structure of the heterogeneity for the immobile zones. The structure as contemplated by [*Selroos et Elert 01*] includes a porosity and diffusion profiles in the depth of the immobile zones as treated previously but as well some heterogeneity along the fracture : presence or absence of gouge material, zones for which mylonite is in direct contact with the fractures and others for which presence of fracture coating is dominant ... see figure 4.6. In order to account for this heterogeneity, we consider here 2D diffusion coefficient heterogeneity (as well as correlated porosity and K_d variability). One may report to figure 4.7-b where the geometry is sketched out : heterogeneity along the fracture is achieved by realizations of a 1D stochastic process of gaussian structure; the heterogeneity in the depth of the matrix is achieved by superimposing a profile to the former values leading to a realistic decrease of these properties along the depth. One may report to figure 4.10 where the explanations are given.

As mentioned above, the purpose of this section is to take further levels of heterogeneity into account. This is done in agreement with the qualitative expected geologic picture of the feature. Nevertheless, this increases the complexity of the system. The question is then whether the quantitative parameters associated can be specified based on direct measurements or identification through tracer tests. Here, direct measurements for the geometrical matrix heterogeneity are not provided. One should therefore try to infer information from another source : the tracer test. We study here the inverse problem based on the results from the tracer test. As mentioned previously for simple homogeneous matrix system, such a test provides indeed information on a parameter group involving porosity of the matrix zone, diffusion coefficient, retention coefficient, fracture aperture. We introduce here a deterministic relation between these parameters based on the measurements provided. The study is limited to the non sorbing tracer (Iodine), we consider constant fracture aperture and algebraic relation between porosity and diffusion coefficient (as inferred from available measurements). So the inverse problem can be strictly expressed in terms of matrix diffusion coefficient estimation.

We work here in the framework of stochastic modeling : simulations are produced with a gaussian simulator existing in our Cast3M code. Selection of the best fits against the experimental breakthrough curves are retained and probabilistic treatment of the selected parameters are provided. This is a classical inverse procedure based on a Monte-Carlo approach with trial and error procedure. The criterion is a uniformly weighted average of the relative absolute differences between simulation and experimental breakthrough curves considering the times for which experimental concentration is provided. This is the same measure as the one considered previously (see equation 4.1). We show below the results in terms of identification of the parameter profiles in the matrix as well as the consequences in terms of breakthrough curves for a unit concentration input as well as the derivative of these concentration breakthrough curves. This is here done for the quick experimental velocity conditions. In the following section, the results for PA time conditions will be presented.

In fact, we introduce here some additional features leading to additional parameters subject to calibration (like here mean and variance of the Gaussian process, its correlation length and the shape of the profile superimposed on the diffusion coefficient, porosity, K_d fields). The influence of a longitudinal heterogeneity can be observed on the breakthrough curves but in an averaged way : the heterogeneous retention effects are averaged over the travel distance, leading to the final curve.

More precisely, we choose a mean diffusion coefficient representative of the more diffusive matrix zones (gouge, fracture coating, mylonite and cataclasite). The variance and correlation length of the process was chosen after a preliminary series of simulations. The variance of the process is chosen large enough to provide contrasted realizations. The choice of the correlation length bears more consequences on the final results. The choice of this coefficient represents the main frequency of the signal we search for :

- For a very small correlation length ($30cm$ were considered), the variability in the breakthrough curves is very limited. This is not surprising since the plume 'sees' a large number of realizations (over the 5.03 meters between wells, 16 correlation lengths). The same is true for distances roughly smaller than $1m$.
- For distances smaller than $2.5m$, the heterogeneity roughly reduces to comparatively constant fields for each single realization.
- For correlation lengths between $1m$ and $2.5m$, the variability of the signal allows for identification of potential characteristic features.

No statistics is available for the diffusion coefficient. We chose a correlation length by $1.6m$ (3 correlation lengths over the $5m$ inter distance). This is the best situation to study the potential influence of a heterogeneous field. Furthermore, for sake of computational costs the penetration depth into the matrix was limited to $1.5cm$ which is a sufficient depth according to former studies.

The porosity as well as K_d values vary according to the diffusion coefficient field. We use the data provided for porosity of the different zones in [*Winberg et al. 02*] in relation with the diffusion coefficients : the relation between porosity and diffusion coefficient is an interpolation between the available data. The same is done for the relation between K_d and diffusion coefficient for Strontium (values of K_d provided in [*Winberg et al. 02*]). For Cobalt or other tracers detailed measurement of K_d in the different immobile zones is not provided. In these cases we consider the provided value as characteristic for all zones. The variability in K_d is nevertheless limited.

To comment on this heterogeneity, one should stress that we introduce here a variability structure based on the diffusion coefficient. This implies corresponding variability in terms of porosity and K_d as mentioned before. What is here at stake is nevertheless the coupling term between the matrix and the fracture. We can see from [*Maloszewski et Zuber 85*] that the expression for the matrix diffusion source term for 1D matrix diffusion is

$$\frac{\omega D_p}{e}\frac{\partial C_{matr}}{\partial z})_{z=e} \tag{4.7}$$

where ω stands for porosity, D_p for diffusion coefficient, e for fracture aperture, $\partial C_{matr}/\partial z$ for the concentration gradient in the matrix. So, considering a variability in the diffusion

coefficient corresponds to considering heterogeneity of the exchange term. This approach is also similar to other approaches where heterogeneity of the fracture aperture is considered.

Results

As shown on figure 4.10-c, the simulation domain corresponds to a flow tube with adjacent heterogeneous immobile zone. We model half of the system, meaning that the heterogeneity on the other mouth of the fracture is the mirror of the one shown here. We should stress here that diffusion in the matrix is not 1D as for other approaches but close to 2D : access to low diffusion zones can be obtained laterally, through higher diffusion zones.

The inverse procedure was conducted for the non sorbing tracer (Iodine). 1000 realizations of the process were done, transport was simulated, comparison with the experimental breakthrough curve was done and the realizations ordered by distance to the experimental curve. From these 1000 realizations, the best 10% were kept (so 100 realizations).

We present here the results of this Monte Carlo approach first in terms of inverse procedure : what can be learned about the diffusion coefficient profile ? The results are presented on figures 4.11 where the first figure provides the 100 realizations and the mean and standard deviation associated. The solutions present clear features for the shape of the mean as well as the standard deviation.

- The variance is larger on the side of the pumping well (left side, pumping well at 0) as on the injection side (right side, injection at $5m$). For the left side, the standard deviation is close to the standard deviation of the simulated process ($1.510^{-10}m^2/s$) : incorporation of the information contained in the breakthrough curve was not very efficient in reducing the level of uncertainties in the diffusion coefficient close to the pumping well. In contrary, tracer experiment allows for better identification of the zones far away from the pumping well (conditional standard deviation around $0.510^{-10}m^2/s$). This standard deviation profile can be generally explained by the velocity profile for radial flow. The velocity varies indeed inversely proportional to the distance to the well. The velocity is very large close to the well as compared with the injection location. As a consequence, in the vicinity of the well, a small perturbation in matrix diffusion coefficient should not have large consequences on the shape of the breakthrough curve For locations close to the injection well (far away from pumping well where velocity is reduced), the contact time of the plume with the matrix zones is large. So, the plume should better 'see' the matrix close to the injection well than close to the pumping well : these zones should be more precisely determined in the present inverse problem. We should nevertheless point out that these features would probably be different for lower Peclets (when the influence of the advection term is limited as compared with matrix diffusion). In that case, the variability in the velocity profile would potentially play a minor role.
- The mean diffusion coefficient profile weakly increases from right to left (toward the pumping well location). Its values are around the mean value of the initial process for the right side ($3.10^{-10}m^2/s$) whereas it is roughly a 30% higher close to the pumping well. We can't propose here a general theoretical explanation to this result consisting in a variable mean profile. A constant profile would in fact be more

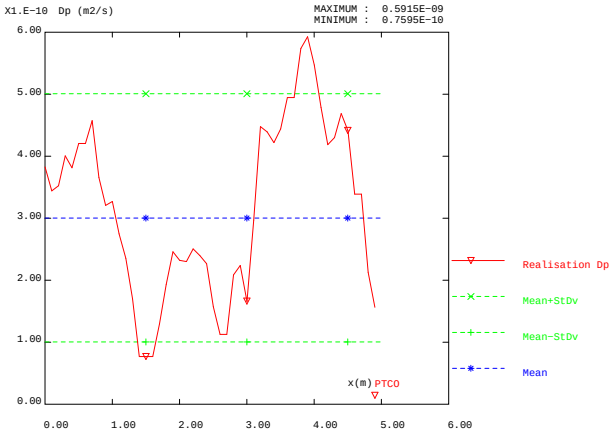

(a) Realization of the process in diffusion coefficient (m^2/s), along the flow tube (injection to pumping well); mean and standard deviation of the process. The correlation length is $1.66m$ for a domain of roughly $5m$

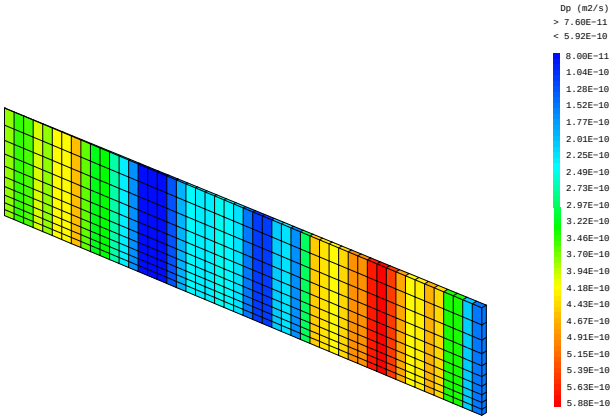

(b) Realization of the process for the matrix zone over the first $1.5cm$ considered for the calibration phase (constant orthogonal profile)

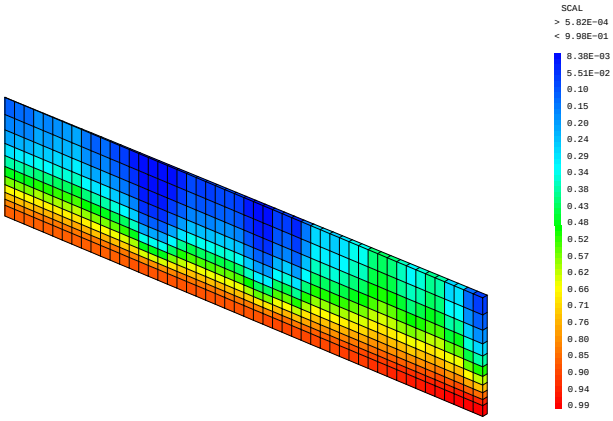

(c) Example of a concentration profile in the heterogeneous system (after 20h)

Figure 4.10: Situation considered for one realization: diffusion coefficient profile simulated, diffusion coefficient field in the matrix for the first 1.5cm zone, concentration field after 20h

intuitive since the output signal provides a sort of average of all matrix diffusion behaviors along the fracture path. The importance of distant locations is, as seen previously, higher than for locations in the vicinity of the production well but it does not seem possible to specify one configuration. This result was nevertheless obtained for a limited number of realizations and might not have a statistical sense. It would be interesting to carry on the simulations over a larger amount of realizations. It was not done here due to time constraints.

In our opinion, the most interesting result here corresponds to the variance profile as well as the level of variance reduction. As mentioned above, diffusion coefficients in the vicinity of the well are poorly constrained whereas further zones are better constrained. It should nevertheless be stressed that the variance reduction is globally interesting by remains limited. One should compare the initial (unconditional) level of standard deviation ($1.510^10m^2/s$) with the standard deviation a posteriori (conditional). The variance reduction is around 60% for the best locations (the further locations are certainly under the influence of boundary conditions) but decreases toward the output well. So the conclusion is that such a tracer test provides information on the system (diffusion coefficients here) but is not sufficient to strongly constrain the diffusion coefficient field.

One should as well mention that, in equation 4.7, the exchange term with the matrix is represented by the product of diffusion coefficient and porosity divided by the fracture aperture. This means in fact that the present study, considering variable diffusion coefficient as well as porosity could be as well interpreted in terms of fracture aperture variability.

Another interesting point concerns the variability in the breakthrough curves associated with the selected fields. We show below the breakthrough curves corresponding to the 100 best realizations. This is provided on figures 4.11 showing the 100 breakthrough curves (for imposed constant unit concentration at the input location) as well as the corresponding statistical treatment and 4.13 providing similar results for the temporal derivative of the breakthrough curves. Some comments follow :

- The reduction of the spreading of the results due to calibration against the experimental breakthrough curve is important : approximately 3 times reduced as compared with the 1000 original non conditional simulations (not illustrated here).
- The variability of the arrival time peaks is reduced as well as the shapes of the curves.
- We observe two populations among the breakthrough curves : some realizations corresponding to relatively high peak levels and a larger group corresponding to lower peak levels. This smaller population corresponds to a comparatively low average diffusion coefficient. In fact several types of solutions can be observed in relation with the quality of the visualized fit : some reproduce well the beginning of the experimental curve, others better the peak, others the tail of the curve. The other categories all merge in the same kind group of breakthrough curves.

So it appears that even if the constraining power of the tracer test is limited, the selection tends to be fairly efficient in reducing the spread of the breakthrough curves. This is

indeed not surprising since these curves are indirectly the performance measure. The performance measures correspond more precisely to their convolution with the input signal injected. Another remark is that the breakthrough curves tend to gather around two major behaviors. These two groups appear as direct consequence of the actual shape of the breakthrough curve measured since they fit different parts of the curve without succeeding in matching the whole curve.

Extension of the approach to the other tracer tests provided (Strontium and Cobalt) could prove interesting but was not attempted due to time constraints. It should nevertheless be stressed that another degree of freedom is introduced for each test : the K_d. These values are largely uncertain so that the integration of the information contained in these complementary tracer tests might not be large in terms of diffusion coefficient field characterization.

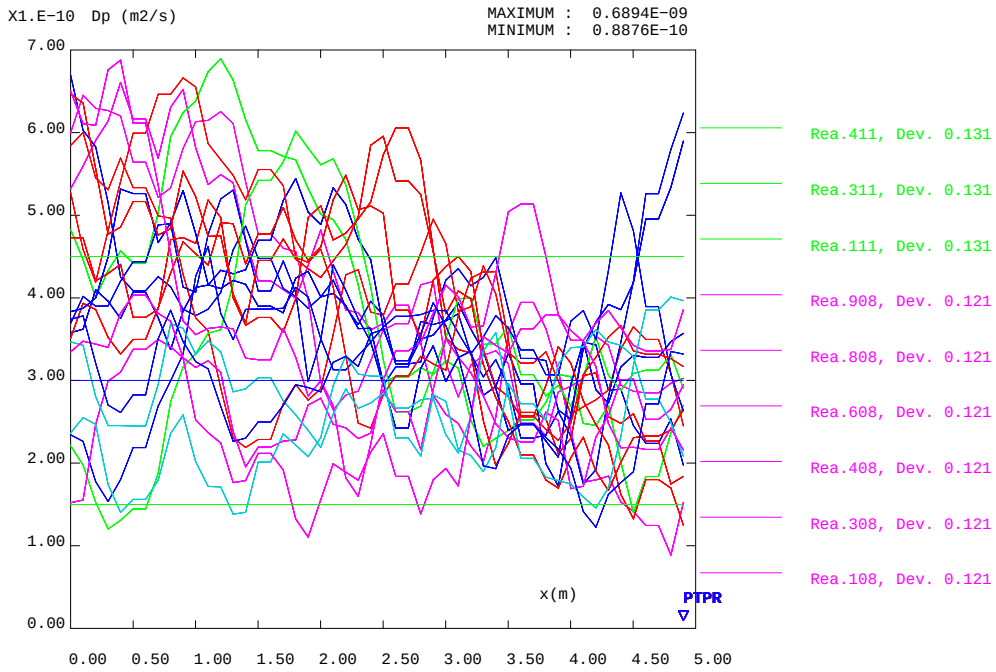

(a) 100 best realizations, mean (blue horizontal line at $3.10^{-10} m^2/s$) and standard deviations (green horizontal lines around) of the initial process in the background

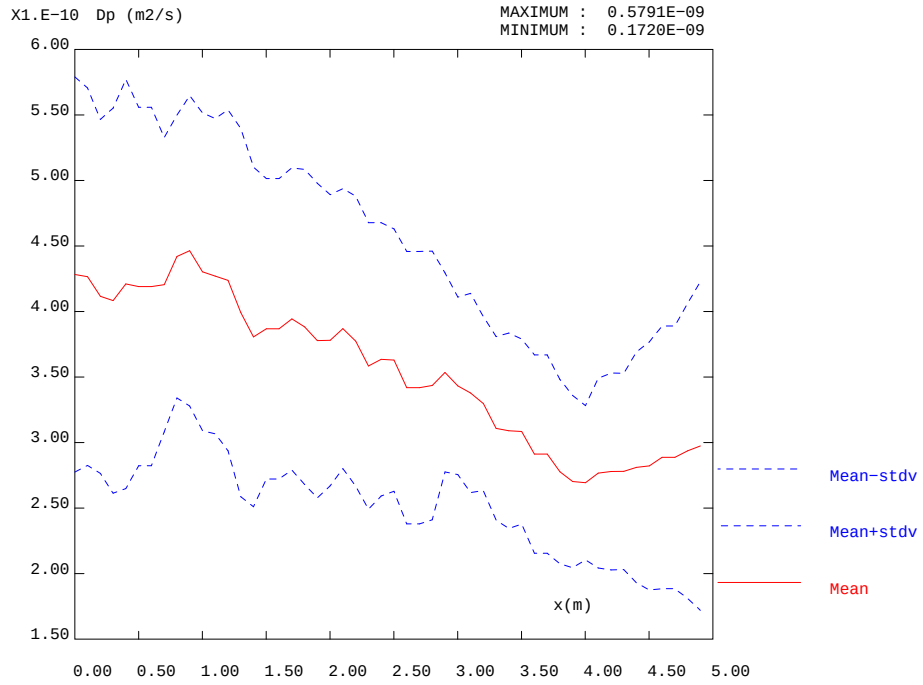

(b) Mean and standard deviation

Figure 4.11: 100 best diffusion coefficient realizations and the mean and variance associated. Pumping location is situated at 0, injection at the other end ($5m$)

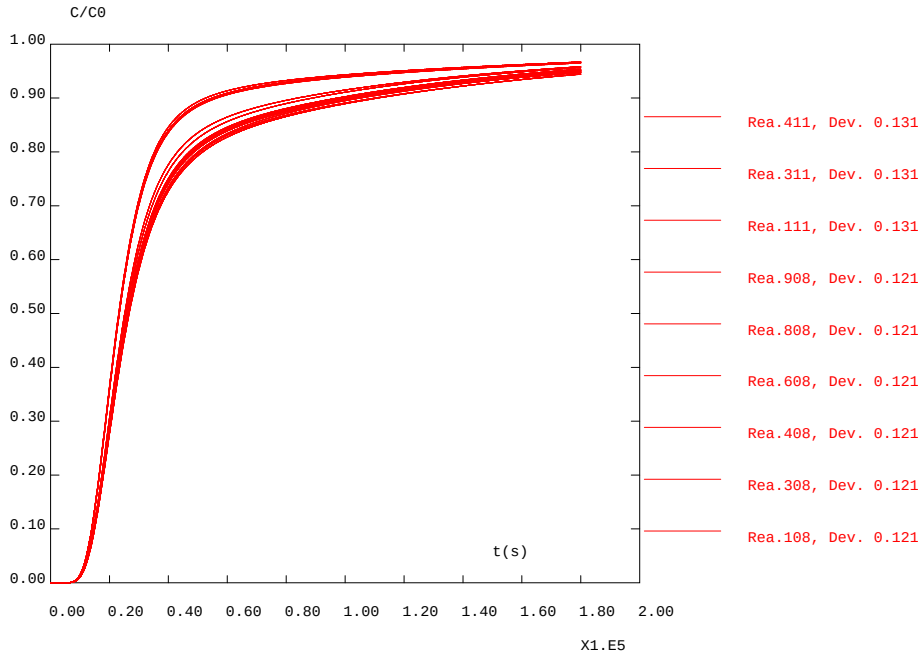

(a) Breakthrough curves : 100 best realizations

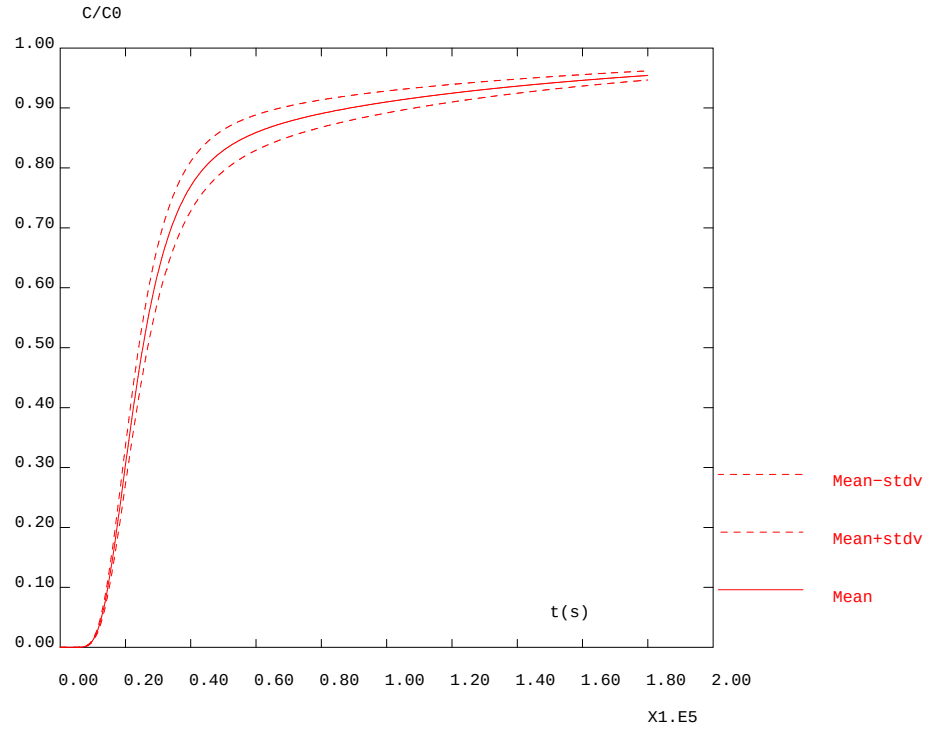

(b) Breakthrough curves : Mean and standard deviation

Figure 4.12: Breakthrough curves for the 100 best diffusion coefficient realizations and the mean and variance associated

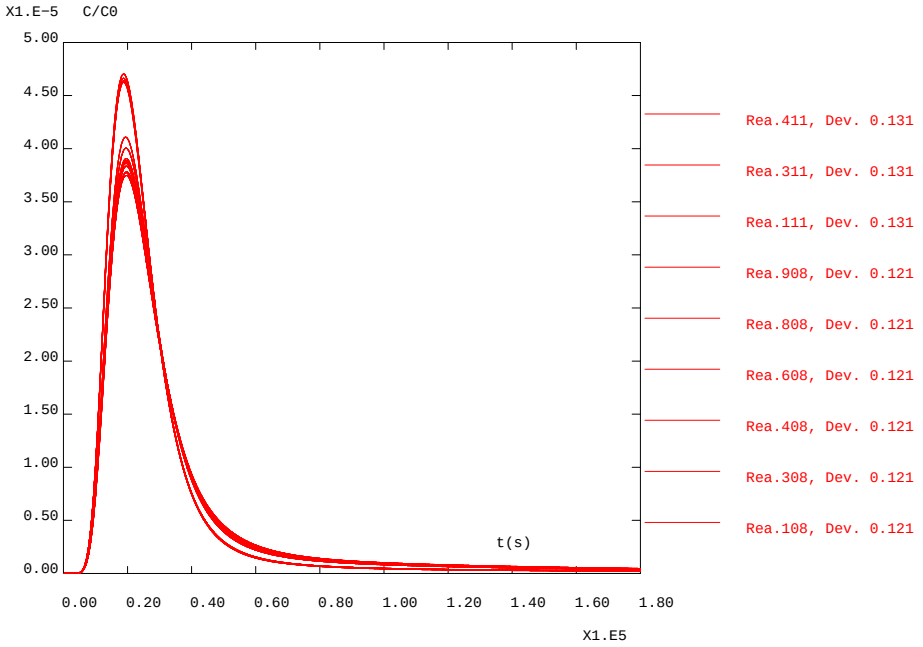

(a) dC/dt : 100 best realizations

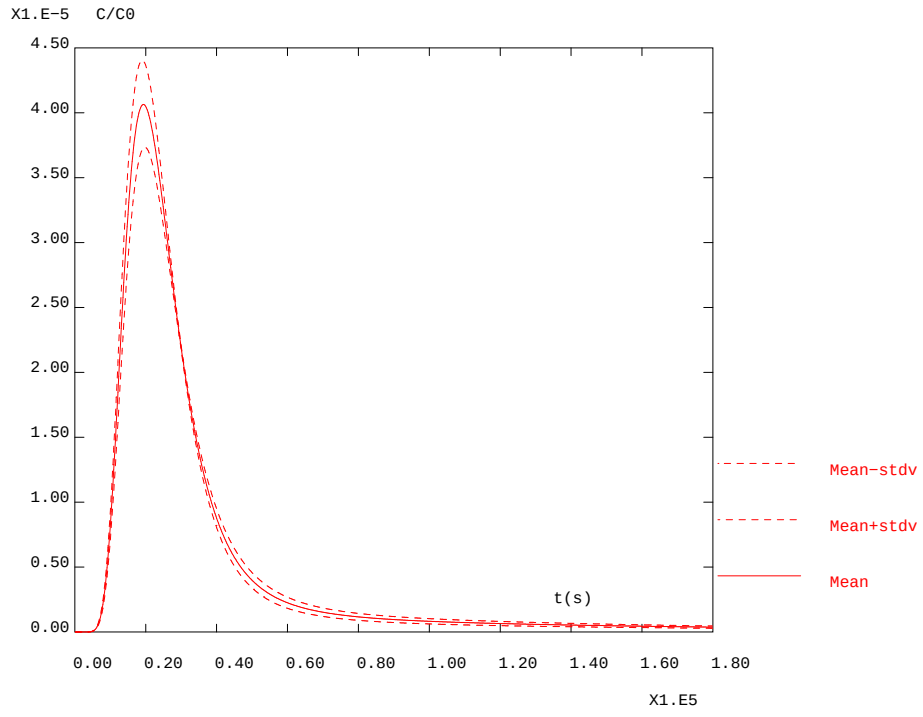

(b) dC/dt : Mean and standard deviation

Figure 4.13: dC/dt for the 100 best diffusion coefficient realizations and the mean and variance associated

Chapter 5

Predictions (Task6B1)

The second phase of the work is related to the same feature and flow type but for 1000 lower velocity. We study in the following the situation encountered for this slower regime and for the 3 models considered previously.

In the following, these models remain limited to a single flow line. One should nevertheless expect the plume to diffuse or disperse within the fracture plane and diffuse into the matrix zones. This phenomenon should be stronger for this slower flow case. Simple considerations involving the Green function of the diffusion problem show that a dispersed plume transfers the same mass to the matrix zones as the same mass in any other configuration. In addition to this a fraction of mass moving from one flow line to a neighbor one (transverse direction) will in fact be collected at the well within the same advective travel time. So, since we consider breakthrough curves at the well, transverse dispersion has no influence on the result (see [*Chen et al. 99*]). As a consequence, by limiting our system to a single flow line, we are indeed equivalently dealing with a system with constant properties in the plane, ie homogeneized properties. This is the assumption made in the following work.

5.1 First model

5.1.1 Results

We consider here the first model we worked with (see section 4.1) : a fracture adjacent to a unique immobile zone. This model was calibrated against the experimental breakthrough curves available. The model used here for prediction includes an additional immobile zone where we consider properties related with the so called altered zone ([*Winberg et al. 02*]). The properties of the altered and non altered zones are very close.

As a conclusion, two zones are considered, the first acting as a buffer zone instantaneously (as compared with flow kinetic) filled up with tracer. The second provides dual porosity characteristics.

The results for the five tracers considered are provided on figure 5.1. The order of arrival is related with the sorbing properties of each tracer : first Iodine, then Strontium, Cobalt, Technecium, Americium.

5.1.2 Sensitivity analysis

We study here the sensitivity to the parameters of both zones on these results. The sensitivity to the first zone corresponds to the total porosity available. We consider several zone sizes : $2.5mm$, $5mm$, $1cm$, $2cm$, $3cm$. The effect corresponds to delay in the arrival times as expected (increasing the total transport porosity is equivalent to introducing a retardation coefficient). The actual depth obtained by calibration was $1cm$. One may report to figures 5.2.

The sensitivity to the depth of the second immobile zone is more reduced as can be seen on figure 5.3. We consider here different depths : $5cm$, $10cm$, $20cm$, $30cm$. The second zone plays a dual porosity role. The maxima are comparable for all cases. The main effect corresponds to longer tailing effects.

5.1.3 Discussion

This prediction exercise based on the first type of model considered shows that precise estimation of the total porosity of the first zone is of major importance. Since these zones play a retardation role translating the whole breakthrough curve.

Estimation of the total porosity is nevertheless difficult. It could originate from calibration of tracer tests obtained in the quick flow regime. But (1) only a parameter group involving diffusion coefficient, porosity and fracture aperture can be estimated based on such a test (see equation 4.2); (2) the depth of the zone is not necessarily explored by the plume to allow for clear identification. So we suggest relying on independent measurements for this parameter.

The second zone (porosity, diffusion coefficient, depth) does not affect the transport process. One should here rely upon independent measurements as well. Its role in changing the shape of the breakthrough curves is nevertheless of minor importance since it dominantly changes the tailing of the curve but not the maximum peak.

This result, obtained with the proposed data set should not be generalized to all flow regimes, matrix properties and matrix depth. We chose here a low diffusion zone as expected $1cm$ in the depth of the matrix (according to the information provided in [*Winberg et al. 02*]).

Since more information was made available to the participants of the task we prefer using it in the following under Model 2. The difference in the predictions illustrates the impact of dependent information on the quality of the predictions.

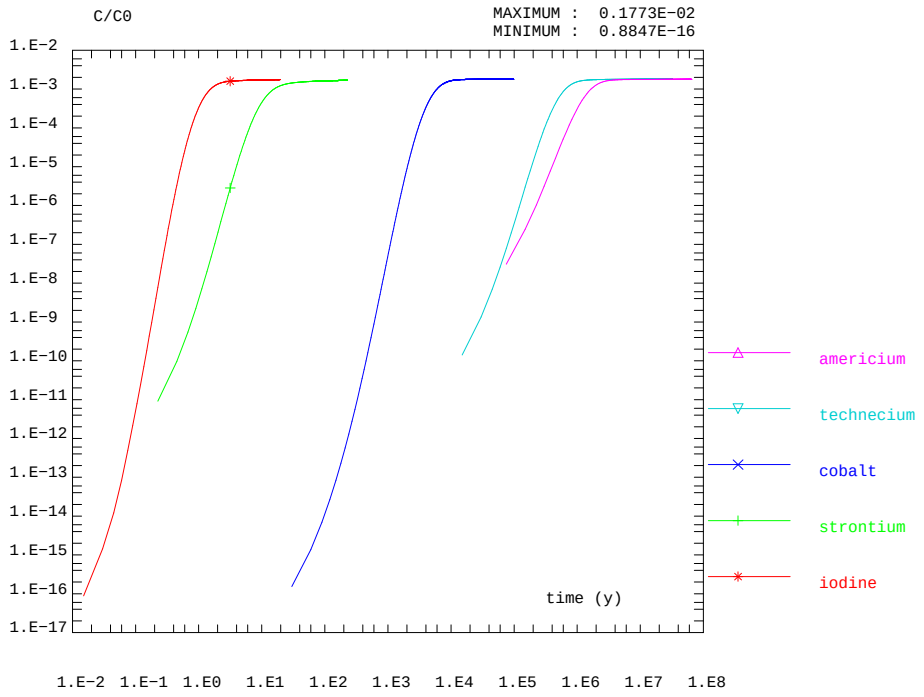

(a) Breakthrough curve for constant unity concentration input

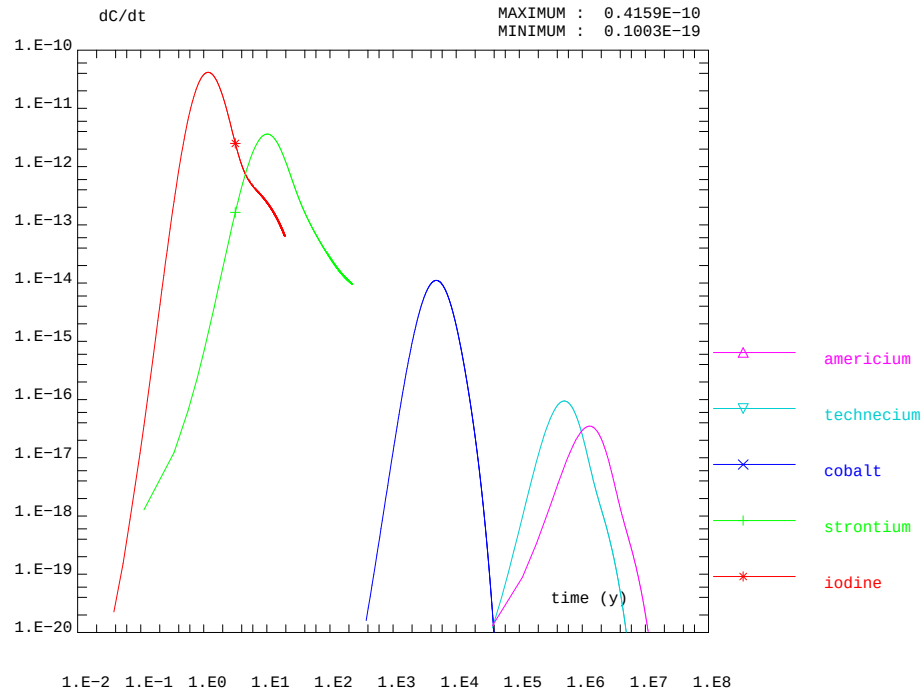

(b) dC/dt

Figure 5.1: First model (two diffusion zones, the first obtained by calibration, the second relative to altered diorite parameter values). Prediction for the five tracers in terms of breakthrough curve (constant concentration) and its temporal derivative

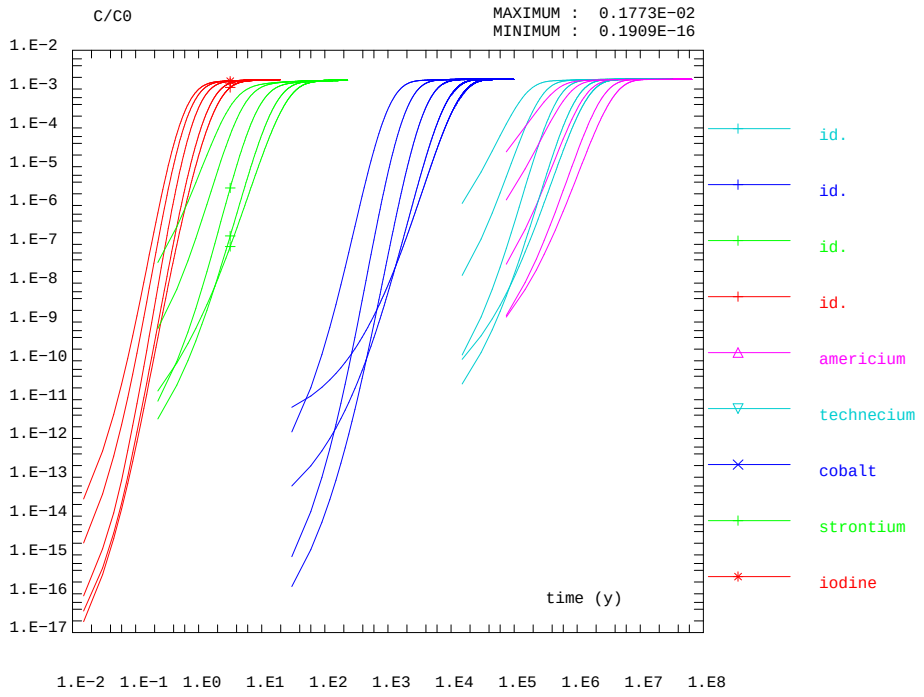

(a) Breakthrough curve for constant unity concentration input

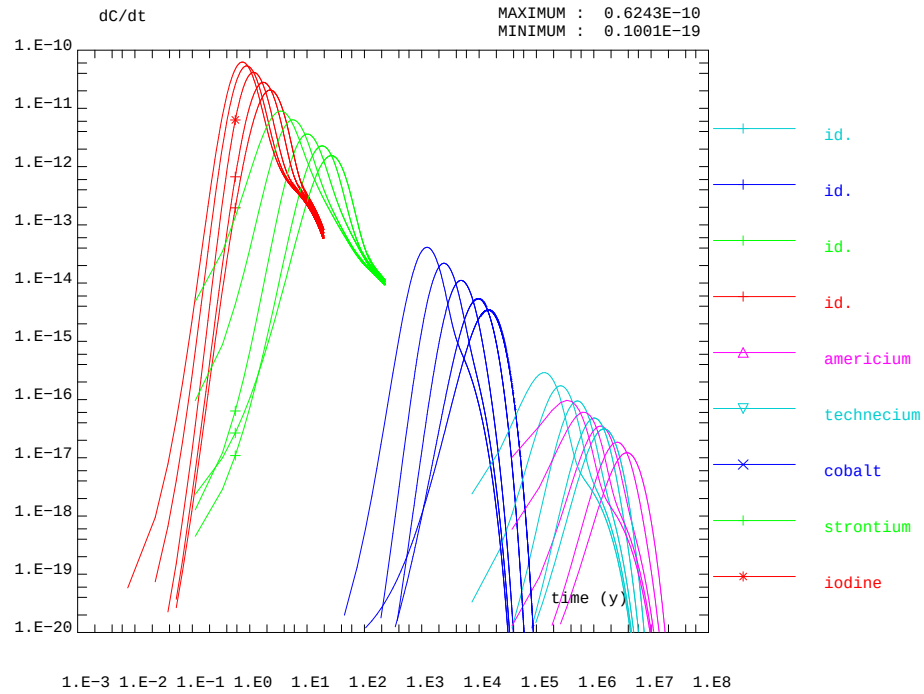

(b) dC/dt

Figure 5.2: Model 1 : Sensitivity to the depth of the first immobile zone (the one calibrated previously) : $2.5mm$, $5mm$, $1cm$, $2cm$, $3cm$

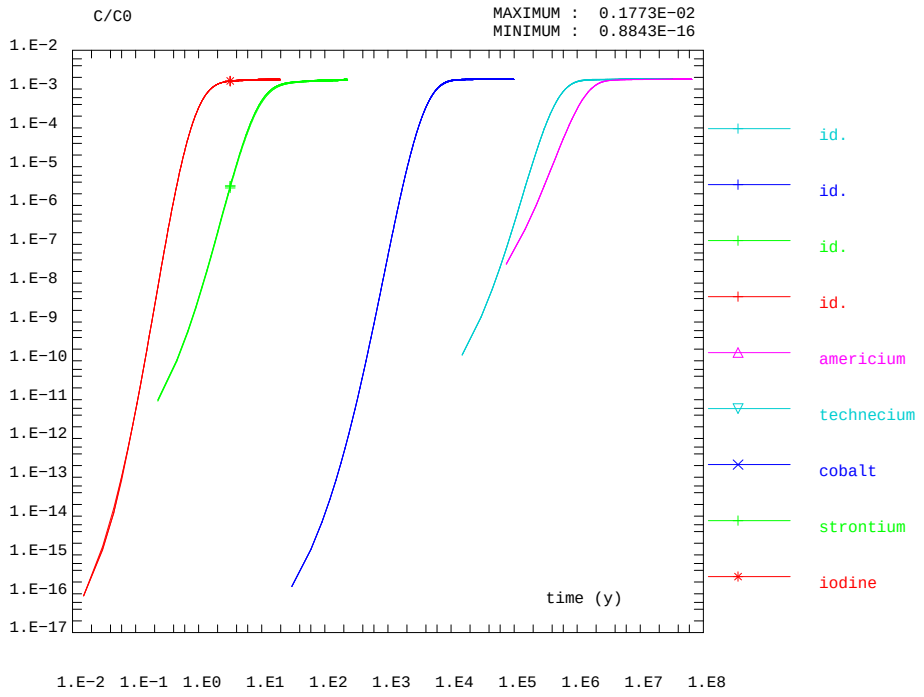

(a) Breakthrough curve for constant unity concentration input

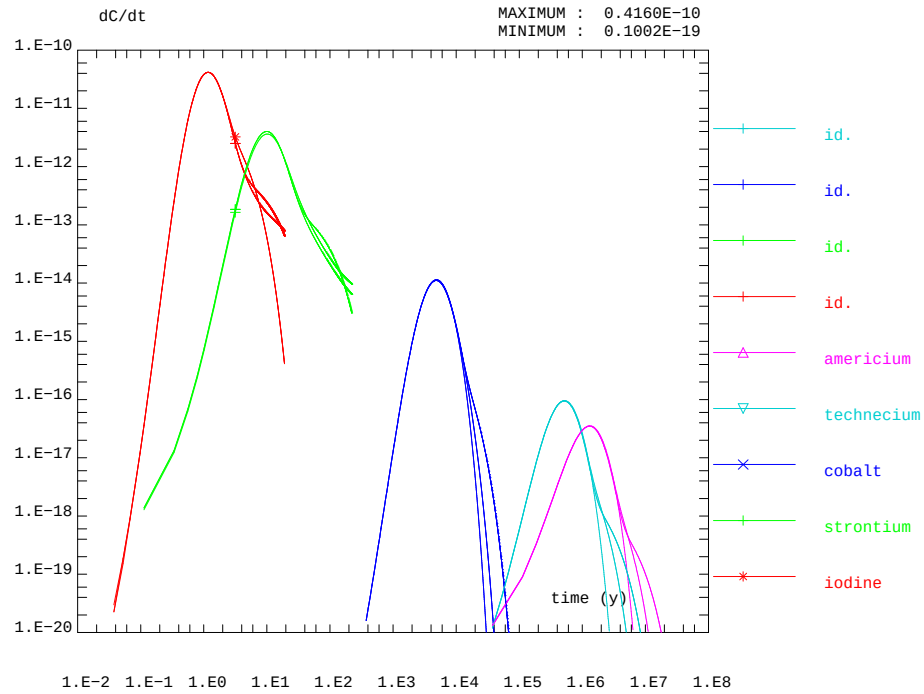

(b) dC/dt

Figure 5.3: Model 1 : Sensitivity to the depth of the second immobile zone (the one introduced presently) : $5cm$, $10cm$, $20cm$, $30cm$

5.2 Second model, deterministic heterogeneity

5.2.1 Results

We introduce more detailed features in this next model. This model was considered in our work when the information about the different fracture types was provided ([*Winberg et al. 02*]). In the sense used previously this type of information can be qualified of independent measurements. The richer information contained allows for more detailed considerations. We see in the following that these measurements are very informative and allow for a more precise description of the transport phenomena. This model was previously calibrated against the experimental curves provided. Similarly to the former case, we add a further $20cm$ zone consisting of properties for altered diorite as provided in [*Winberg et al. 02*]. The results of the prediction for low velocity regime are provided on figure 5.4. The parameter set is summed up below :

Task6B1	Fracture	Gouge	Fr. Coating	Mylonite	Altered Rock	Non Alt. R.
Extent	$2mm$	$5mm$	$0.5mm$	$2cm$	$20cm$	$20cm$
Porosity	1	15%	5%	1%	0.6%	0.3%
Diffusion coefficient (m^2/s)	10^{-9}	3.10^{-10}	2.10^{-10}	10^{-10}	8.10^{-10}	5.10^{-10}
Strontium $K_a(m)$, $K_d(m^3/kg)$	5.10^{-4}	7.110^{-4}	2.310^{-4}	6.710^{-5}	6.10^{-5}	6.10^{-5}
Strontium R_a or R_d	1.5	11.8	12.8	180	26.8	53.8
Cobalt $K_a(m)$,$K_d(m^3/kg)$	8.10^{-3}	8.10^{-4}	8.10^{-4}	8.10^{-4}	8.10^{-4}	8.10^{-4}
Cobalt R_a or R_d	9	13.2	42	215	358	718
Technecium $K_a(m)$, $K_d(m^3/kg)$	0.2	0.2	0.2	0.2	0.2	0.2
Technecium R_a or R_d	201	3061	10261	53461	89460	1.810^5
Americium $K_a(m)$, $K_d(m^3/kg)$	0.5	0.5	0.5	0.5	0.5	0.5
Americium R_a or R_d	501	7651	25651	1.310^5	2.210^5	4.510^5
Dispersivity (longit.)	$50cm$					
Dispersivity (transv.)	$50cm$					

Table 5.1: Parameter set for the task6B1 predictions (fracture and the 3 most diffusive zones : gouge, fracture coating, mylonite and cataclasite). The parameters are the ones provided in [*Winberg et al. 02*] and [*Selroos et Elert 01*] except for the gouge material where the original data set considered a porosity by 20% and a diffusion coefficient by $5.10^{-10}m^2/s$

Breakthrough curves for Cobalt differ from the ones obtained in section . This is due to the fact that we considered here the sorption properties provided in the documentation. We formerly considered the calibrated data set for the first modeled zone.

The curves are all moved to the shorter time arrivals as compared with results from Model 1. This is due to the fact that the quick diffusion zones around the fracture provide less total porosity. In addition, the Mylonite zone acting as a single porosity zone for the non sorbing or weakly sorbing tracers is not completely filled up for more strongly sorbing

tracers. For the latter, this zone acts as a dual porosity zone leading to tailing effects, not to a retardation effect.

Arrival times and values for peak maximum are provided in chapter 7 for a unit mass Dirac and continuous ($1 Mbq/y$) injection in the format required.

5.2.2 Sensitivity analysis

We consider here the sensitivity of the results to the incorporation of surface sorption or not. In our base case data set, we consider surface sorption on the fracture walls. The corresponding retention coefficients range from 1.5 for Strontium to nearly 500 for Americium (see Tab. 5.2.1). [*Winberg et al. 02*] suggests considering diffusion and bulk sorption into fracture coating zone as the actual surface sorption phenomenon for PA time scale. In our study, both surface sorption and diffusion and bulk sorption in explicitely modeled fracture coating zone are considered. We show here the influence of considering surface sorption in addition to transfers into fracture coating zone by providing predictions in both cases, including it or not. Results provided on figure 5.5 show for a Dirac input that all tracers except Cobalt are weakly sensitive to both options. This is due to the fact that sorption is limited for Strontium and the mass associated with sorption is small as compared with bulk sorption in the different matrix zones for more sorbing tracers (Technecium and Americium). The situation is similar for the Task6B2 conditions. In the following we consider both surface sorption and diffusion and sorption in the fracture coating zone as provided in Tab. 5.2.1.

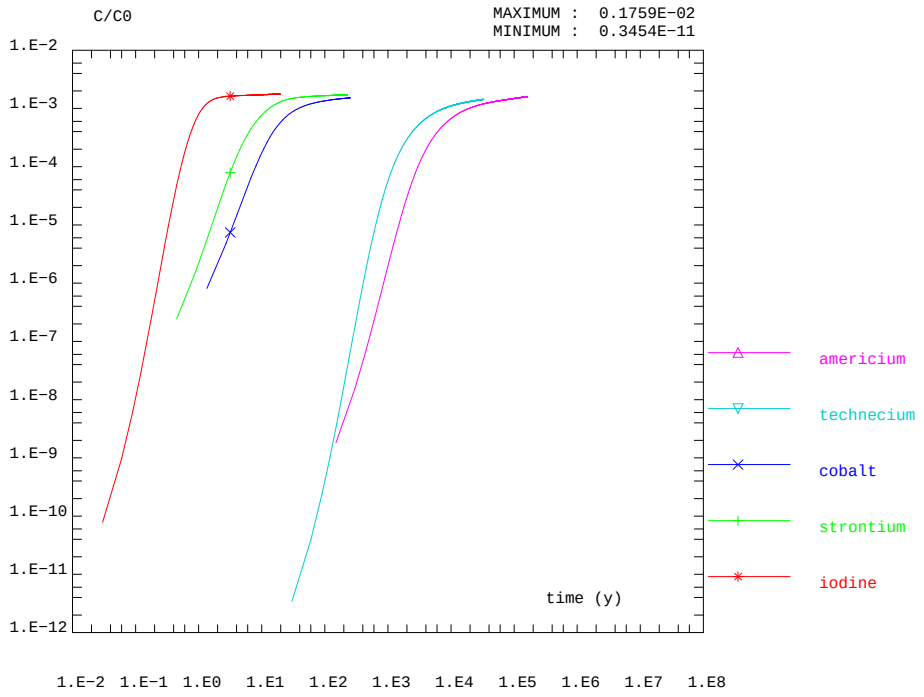

(a) Breakthrough curve for constant unity concentration input

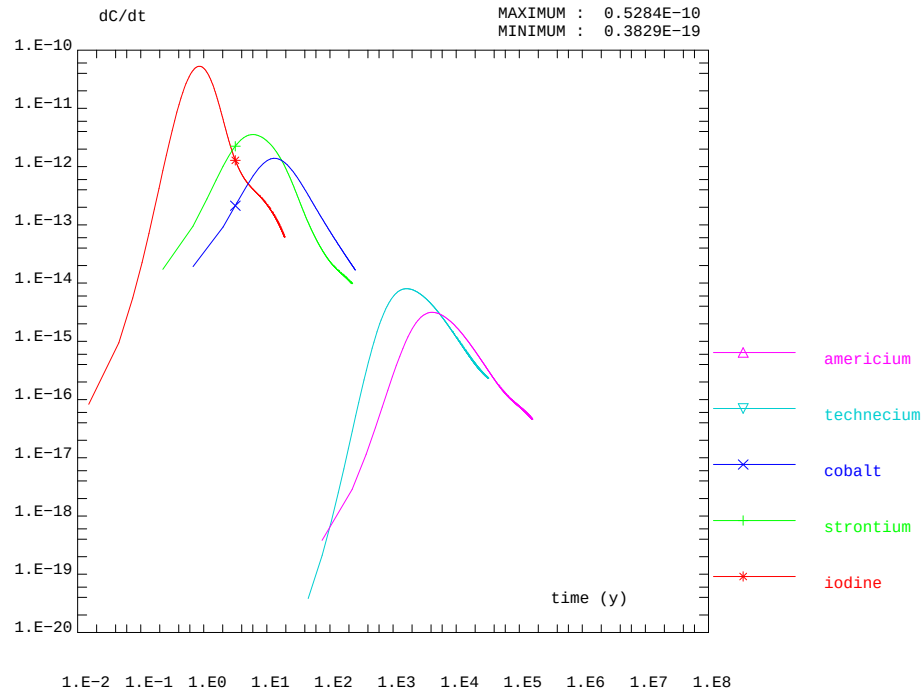

(b) dC/dt

Figure 5.4: Second model, involving gouge, fracture coating, Mylonite (cataclasite) and additional altered diorite zone. Prediction for the five tracers in terms of breakthrough curve (constant concentration) and its temporal derivative

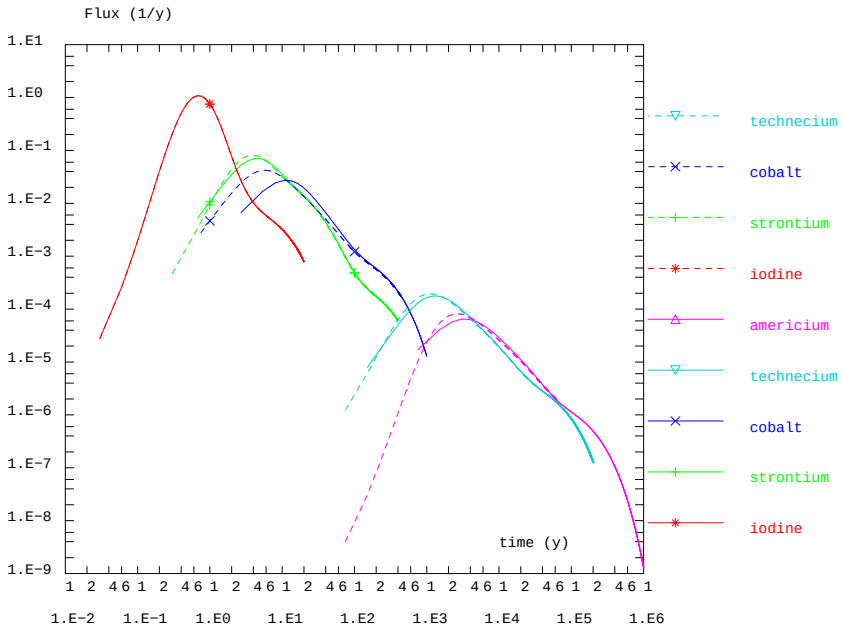

(a) Total flux at the outlet for Dirac input

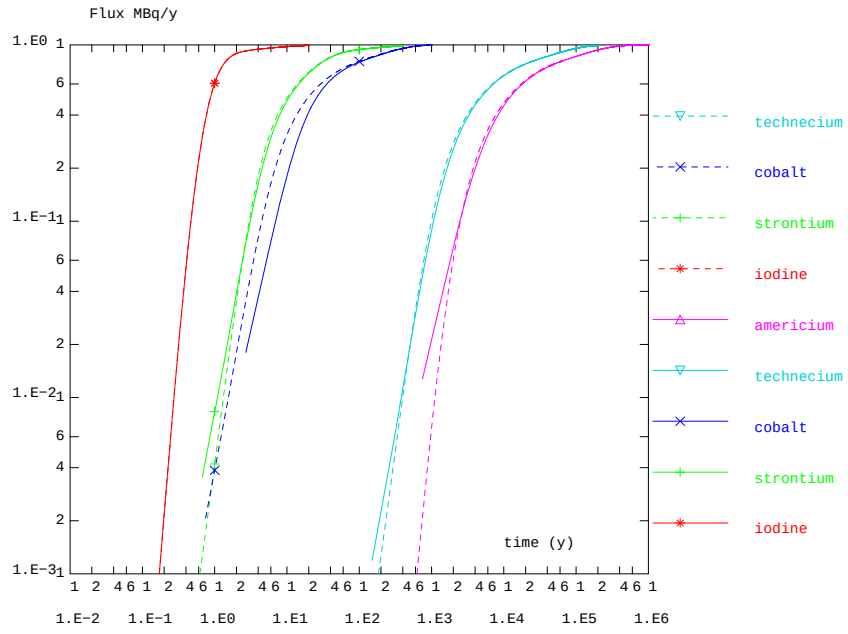

(b) Continuous injection

Figure 5.5: Sensitivity to the incorporation of surface sorption in addition to diffusion and sorption in fracture coating zone.

5.3 Third model, stochastic heterogeneity

In this section we deal with a longitudinal heterogeneity as in section 4.3.2. This approach requires extensive computing resources and was limited here to one tracer : Iodine. Our intention with this study is to assess the importance of heterogeneity along the fracture within a stochastic framework. We consider as previously a heterogeneous diffusion coefficient field following a gaussian law. As mentioned before, this approach is equivalent to considering a heterogeneity in the fracture aperture for the transport problem. Porosity is heterogeneous and deduced from the diffusion coefficient field according to the data provided for the different zones (gouge, fracture coating, cataclasite, altered and non altered diorite).

We conducted in section 4.3.2 a Monte Carlo study involving 1000 simulations of the statistics chosen. The transport problem was solved and simulated breakthrough curves compared with experimental ones. The realizations were then ordered according to the distance to the experimental curve (objective function corresponding to the mean relative error over the measurement times provided, see equation 4.1).

5.3.1 Results

We previously provided the spreading of the breakthrough curves and their temporal derivatives. The same is done here for the longer time scale (1000 times slower). The calibration was conducted on a system involving $1cm$ of immobile zone. We add here further depth to account for more in depth diffusion into the matrix zones. This is done by expanding the diffusion coefficient field in the depth of the zones and super imposing a mean diffusion profile. This profile is constant over the first centimeter and decreases linearly over 20 further centimeters. This allows the realizations to reach values characteristic of non altered zones at $20cm$ depth. So we don't consider a two zone approach but rather a variation profile as sketched out on figure 4.7-b.

The results are provided on figure 5.6 where the breakthrough curves associated with the PA scale time are provided with their derivatives. We consider indeed a constant imposed concentration at the inlet. Results show that the dispersion is rather large. These results depend of course in part on the type of profile chosen but for the retardation effect, mostly from the diffusion coefficient profile in the vicinity of the fracture. So we consider that it largely depends upon what is in fact a calibrated data set. So it seems legitimate to infer that the spreading in the breakthrough curves (related with fact that several solutions can be considered) is amplified when moving from short time tests to PA time scale.
Another remark concerns the fact that two groups of solutions come out on figures 5.6. As mentioned before, the best fits (as measured by mean quadratic error as compared with the experimental curve) are obtained in several manners providing (i) optimal fit for the beginning of the curve or (ii) better local fitting for the peak part of the curve and the

tailing effect. Optimally, both features should be captured. In practice, minimal errors (around 15%) are obtained in both ways without completely satisfying at the same time the overall distance to the curve.

5.3.2 Conclusions

In conclusion, we conducted here a study on the influence of heterogeneity on calibration of the experimental curves as well as its impact in the prediction phase. Contrary to the second model introduced, largely relying upon information available on the positions as well as parameter values associated with each immobile zone within Type 1 feature (gouge, fracture coating, Mylonite cataclasite, altered and non altered zones), we consider here further refinements of the heterogeneity : longitudinal heterogeneity. The structure introduced does not rely upon available information but is rather confirmed by the calibration procedure against the experimental curves. Results show that considering such a level of possible heterogeneity has a certain impact on the behavior of the system. Unfortunately, conditioning the fields to the breakthrough curves, though visible in terms of variance reduction, remains very limited in the vicinity of the pumping well. A breakthrough curve indeed carries the averaged information of the retention heterogeneity met and mostly focus on the zone far from the pumping well due to the velocity profile in radial flow conditions.

In short, heterogeneity in matrix zones is an important issue for a PA procedure but the structure of it can hardly be assessed from tracer test measurements. We suggest relying as much as possible upon independent measurements of the different immobile zones and their spatial statistical structure. This does not include only statistics for the fracture aperture as commonly done but as well similar statistics on the matrix zones parameter values. In fact, these zones play a more dominant role at PA scale as compared with fracture aperture heterogeneity since they correspond to a large total porosity fraction, responsible for strong retardation effects. As a consequence, we suggest measuring the matrix diffusion coefficient on a plane orthogonal to a fracture for a geologically analogous zone at Äspö.

Another interesting conclusion is that we observed that the spread in the breakthrough curves corresponding to the selected realizations increases when moving from short time scales to PA scale time scale : dispersion of the results is amplified. Or said differently, uncertainties are amplified.

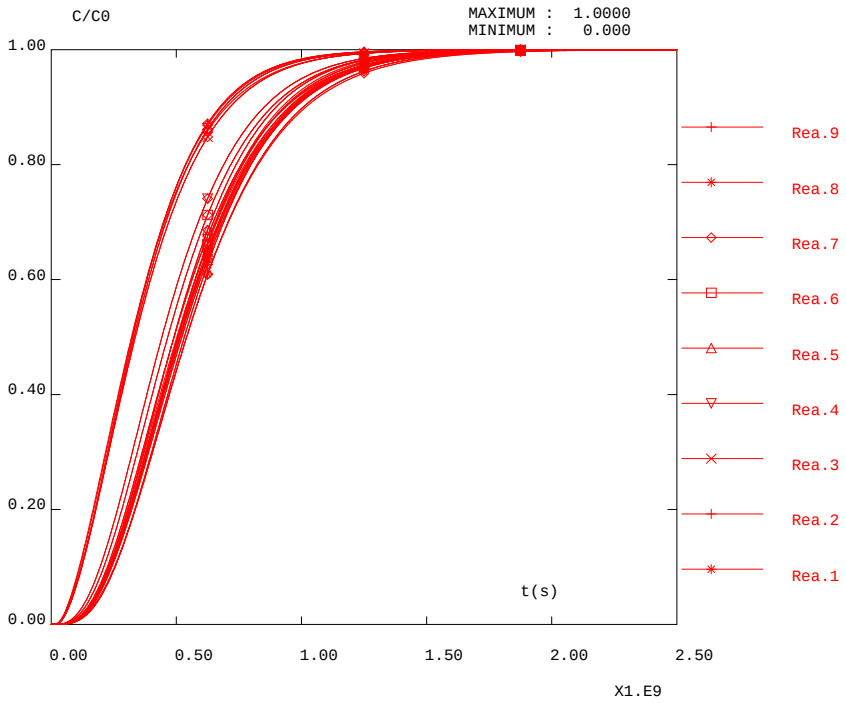

(a) Breakthrough curves

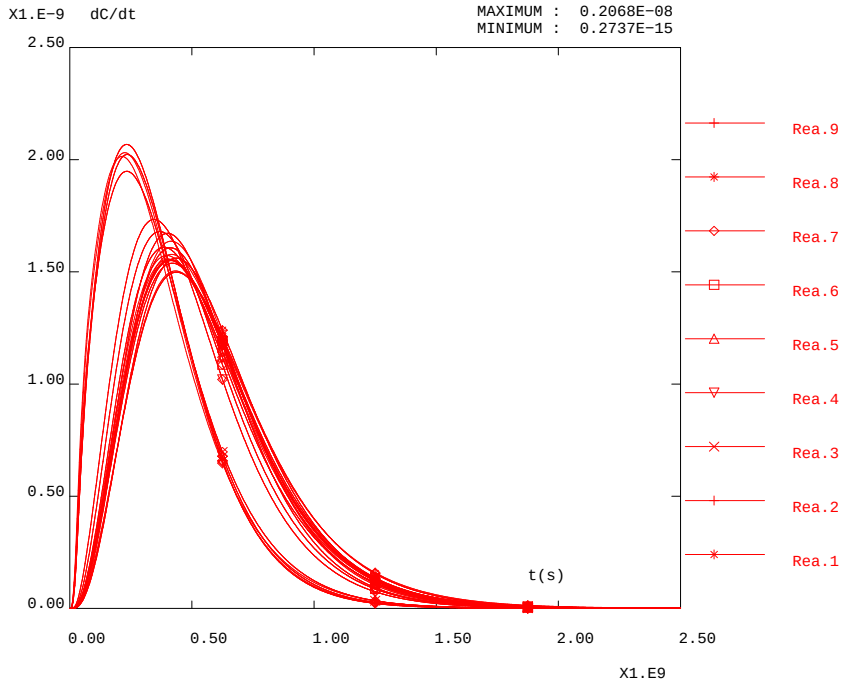

(b) Derivatives associated

Figure 5.6: Third model : dispersion of the results for the best realizations selected (Iodine only).

Chapter 6

Predictions (Task6B2)

6.1 Presentation for the second model case

The task specifications are provided in [*Elert et Selroos 01*].

We consider in the following the same feature as previously but the conditions are here natural uniform flow conditions. The numerical approach is similar to the one exposed for radial flow conditions (see chapter 3) except that we apply constant velocity in the fracture. The fracture domain modeled is $15m$ times $15m$. We include in addition the matrix zones. The source term consists of a $2m$ long unit located $10m$ from the outlet (fracture plane limit).

The quantitative conditions are proposed in [*Elert et Selroos 01*] : head gradient by 0.1% and transmissivity in the domain 8.10^{-9} to $4.10^{-7}m^2/s$. We consider in the following as base case transmissivity by $4.10^{-8}m^2/s$, corresponding to the geometrical mean of the transmissivities measured at the five boreholes within feature A. Furthermore, we considering a flow aperture (fracture opening) by $2.10^{-3}m$ as previously. These conditions lead to a advective travel time to the border (distant by 10 m from the injection) approximately by 5.10^8s. This means that we have in this subtask the longest travel time and the slowest velocity. The retention effects should be here stronger than in the Task6B1 case.

We propose here a deterministic prediction roughly corresponding to the situation by model 2 :

- The matrix zones geometry and parameters considered previously are kept. These originate from [*Winberg et al. 02*] and were considered already for **Model 2** : open fracture, gouge material, fracture coating, mylonite, altered zone, unaltered zone.
- **No further heterogeneity is introduced**. For instance fracture aperture heterogeneity was not considered here for the following reasons, mostly related to the weak level of relevant information available :
  We showed previously (see section 5.3 related to model 3), that the important features to be considered for long time scales enclose the most diffusive zones (gouge, fracture coating and Mylonite/Cataclasite) in addition to the open fracture.

In fact, the total transport porosity has to be increased to take these zones into account. So, for long term transfers, addressing heterogeneity at all requires indeed addressing heterogeneity of this total equivalent zone. The information for gouge, fracture coating and Mylonite/Cataclasite are not provided in the documents. Some information is provided for fracture aperture variability (or equivalently transmissivity variability) in [*Elert et Selroos 01*]. The level of information remains limited and mostly relies upon the transmissivity measurements from the 5 boreholes and some aperture analysis conducted at other locations at Äspö. We conclude that the level of heterogeneity is weak, the correlation structure uncertain and the amount of information within the fracture plane almost limited to the vicinity of the 5 boreholes.
Due to the low level of quantitative information available about the heterogeneity structure (for fracture and matrix zones), we prefer modeling here these different units in the most simple way : as deterministic constant aperture and depth units. We address the uncertainties in terms of parameter values by sensitivity analysis.

- No match for the head fields was attempted in relation with the former discussion.

6.2 Procedure to move from SC models to PA scale

As previously, we focus here our concern on retention effects due to sorption and matrix diffusion in a heterogeneous matrix system. The idea in building a PA scale model is to simplify the flow conditions and retain the main retention effects (ie the main matrix zones contributions).

The next step consist in identifying the roles played by the different matrix zones in the transport mechanisms. As studied previously, the general rule is that the high porosity and diffusivity zones close to the fracture plane tend to contribute to the advective part of the transfer since these thin zones are almost instantaneously filled up by the plume located in the fracture. These zones contribute to the total advective porosity and contribute to retardation effects (single porosity behavior). Further zones act as transitory retention zones, more representative of dual porosity behavior (reduced maximum and tailing effect for the breakthrough curves). A rationale behind the building of the PA model should then be in (1) selecting the matrix zones contributing to single porosity behavior and identifying the resulting total porosity and (2) select the matrix zones contributing to dual porosity behavior and possibly homogenize this behavior in 3 coefficients : porosity of the zone, diffusion coefficient and depth of the unit. This would lead to a simple PA model consisting of :

- A 1D uniform flow zone (transmissivity and flow aperture associated; larger transport total porosity equivalent to a retention term).
- A dispersion coefficient homogenizing at the proper scale the effects of heterogeneity in the fracture velocity field.

- An orthogonal no flow zone corresponding to matrix diffusion effects : equivalent parameters are selected as well as penetration depth.

This is a classical model which can further be simplified considering 1D orthogonal diffusion in the matrix zones. For this model, analytical solutions were provided in the literature (see [*Tang et al. 81*]).

Nevertheless, the role played by the different zones depends upon the flow velocity as well as the type of tracer used (sorbing or not sorbing). The access to the different zones clearly depends on the contact time with the matrix zones (inversely to flow velocity) as well as the matrix zones depth and apparent diffusivity (diffusion coefficient divided by retention coefficient). As a conclusion, such a model is only valid for a precise range of flow velocities as well tracer parameters.

In the following we prefer modeling more details of the matrix system as explained below. We first show the role played by the different zones modeled for different tracers : Iodine and Technecium. We consider the 7 matrix zone model presented previously as model 2 (see figure 4.7-a).

One may refer to figures 6.1 to see the evolution of the masses in the whole system as well as a more detailed view of the evolution of masses in the different matrix zones. We consider here a Dirac pulse injection. The total normalized mass declines in the system due to mass exiting the system. The mass in the fracture decreases rapidly as a consequence of the advection mechanism. Mass is nevertheless is stored for a while in the matrix zones (increase and decrease of mass in the matrix zones). The impact of matrix diffusion in the retention process is here important. The more detailed view of the evolution of masses in the matrix zones shows two kinds of kinetic : the first is very similar to the rapid decrease of mass observed in the fracture. This concerns the gouge, fracture coating as well as mylonite. These zones are filled up and emptied almost instantaneously as compared with the fracture flow velocity. Mass is dominantly in the gouge as compared with these other units due to its total porosity. The altered and non altered zones act as transitory retention zones typical of matrix diffusion. The altered zone plays here the major role due to its position as well as diffusion properties. All these zones play a role and should in one way or another be introduced into the system. This is for instance the case for the non altered rock. The unaltered rock depth was chosen here $20cm$ (same as for the altered zone). Refer to table below for the parameter database considered.

For a more sorbing tracer, the situation is similar except that matrix diffusion becomes strongly dominant over fracture transport as can be seen from figures 6.2. The characteristic time for the transport is far slower than the fracture advective time. The role played by the second diffusion zone (non altered rock) as compared with the first diffusion zone (altered rock) is here dominant for the long time tailing effects whereas this zones plays more of a corrective role for a non sorbing tracer. The figures correspond to Cobalt. The situation for Strontium, Technecium and Americium is similar.

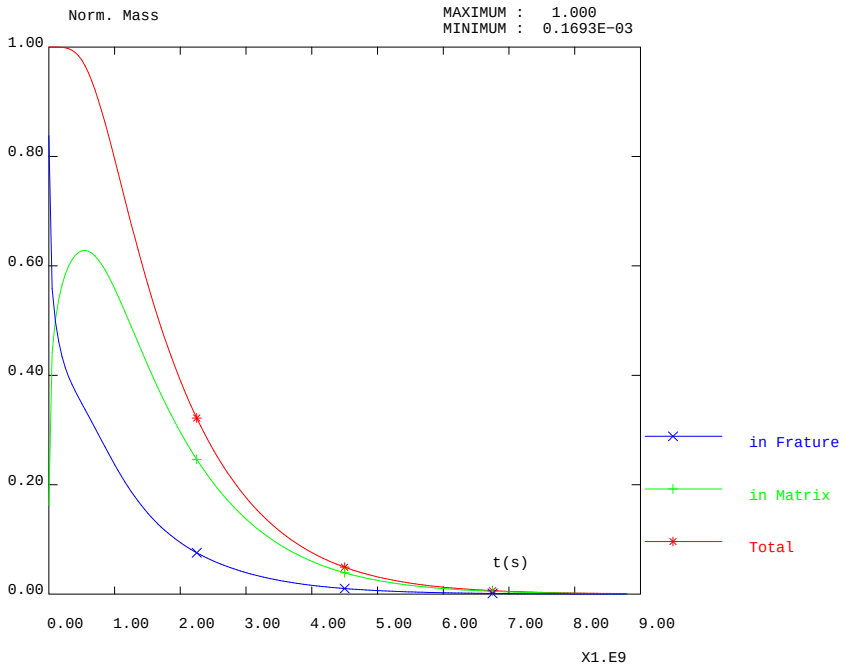

(a) Masses in the system

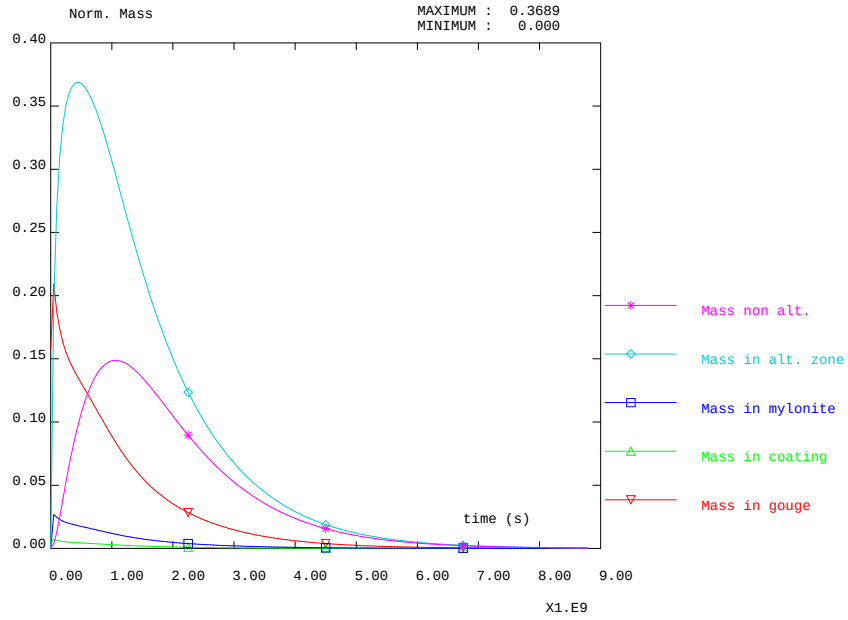

(b) Masses in the matrix zones

Figure 6.1: Iodine for second model geometry (see figure 4.7 : tracer masses in the different units of the system. (a) Total, in fracture and matrix zones. (2) Within the matrix zones : gouge, fracture coating, altered diorite, unaltered rock.

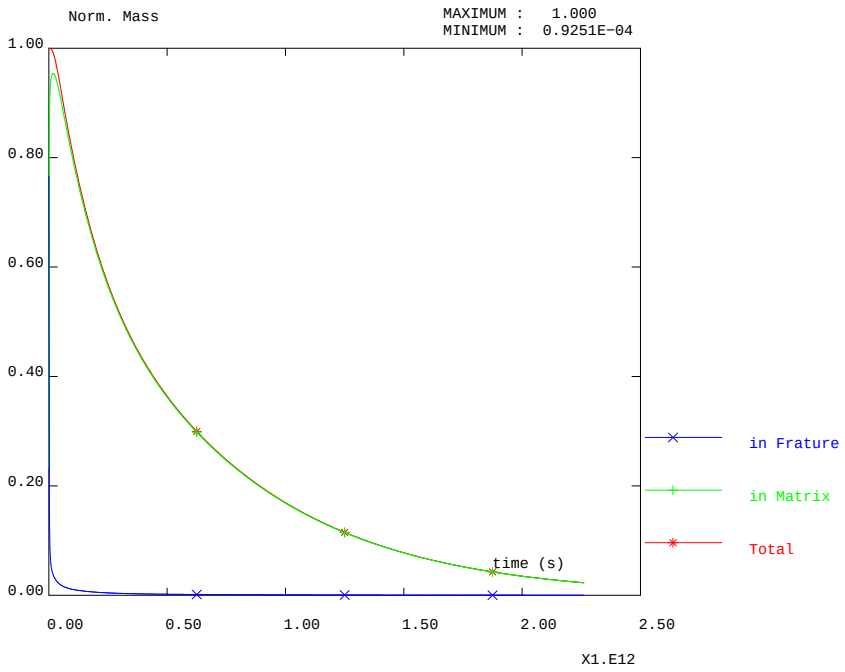

(a) Masses in the system

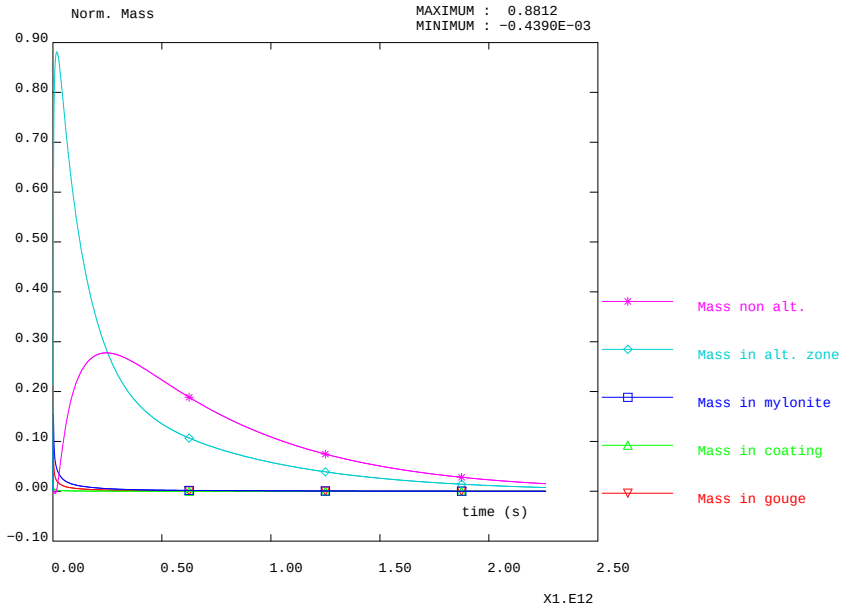

(b) Masses in the matrix zones

Figure 6.2: Cobalt for second model geometry (see figure 4.7 : tracer masses in the different units of the system. (a) Total, in fracture and matrix zones. (2) Within the matrix zones : gouge, fracture coating, altered diorite, unaltered rock.

Task6B2	Fracture	Gouge	Fr. Coating	Mylonite	Altered Rock	Non Alt. R.
Extent	$2mm$	$5mm$	$0.5mm$	$2cm$	$20cm$	$20cm$
Porosity	1	15%	5%	1%	0.6%	0.3%
Diffusion coefficient m^2/s	10^{-9}	3.10^{-10}	2.10^{-10}	10^{-10}	8.10^{-10}	5.10^{-10}
Strontium $K_a(m)$ or $K_d(m^3/kg)$	5.10^{-4}	7.110^{-4}	2.310^{-4}	6.710^{-5}	6.10^{-5}	6.10^{-5}
Strontium R_a or R_d	1.5	11.8	12.8	180	26.8	53.8
Cobalt $K_a(m)$, $K_d(m^3/kg)$	8.10^{-3}	8.10^{-4}	8.10^{-4}	8.10^{-4}	8.10^{-4}	8.10^{-4}
Cobalt R_a or R_d	9	13.2	42	215	358	718
Technecium $K_a(m)$, $K_d(m^3/kg)$	0.2	0.2	0.2	0.2	0.2	0.2
Technecium R_a or R_d	201	3061	10261	53461	89460	1.810^5
Americium $K_a(m)$, $K_d(m^3/kg)$	0.5	0.5	0.5	0.5	0.5	0.5
Americium R_a or R_d	501	7651	25651	1.310^5	2.210^5	4.510^5
Dispersivity (longit.)	$50cm$					
Dispersivity (transv.)	$50cm$					

Table 6.1: Parameter set for the task6B2 predictions (fracture and the 3 most diffusive zones : gouge, fracture coating, mylonite and cataclasite). The parameters are the ones provided in [*Winberg et al. 02*] and [*Selroos et Elert 01*] except for the gouge material where the original data set considered a porosity by 20% and a diffusion coefficient by $5.10^{-10}m^2/s$

6.3 Results for a Dirac input

Results are provided on figures 6.3. The same order in the arrival times of the different tracers is observed as for previous Task6B1. The characteristic time of the transport is here nevertheless longer since flow is here slower. Here, all units of the system play a role in the transport whereas for more sorbing tracers, in conditions of Task6B1, unaltered rock units played a minor role.

Arrival times and values for peak maximum are provided in chapter 7 for a unit mass Dirac and continuous ($1Mbq/y$) injection in the format required.

6.4 Sensitivity analysis

Sensitivity of the system to different parameters was studied previously in the frame of Task6B1. Results showed that the system is strongly sensitive to the total porosity associated to the most diffusive matrix units in the vicinity of the fracture. Differences in porosity lead to delay in the arrival times of the breakthrough curves. The other matrix units play a less important role in delaying the peak of the breakthrough curves but reduces the level of the peak and increase tailing effect of the mass.

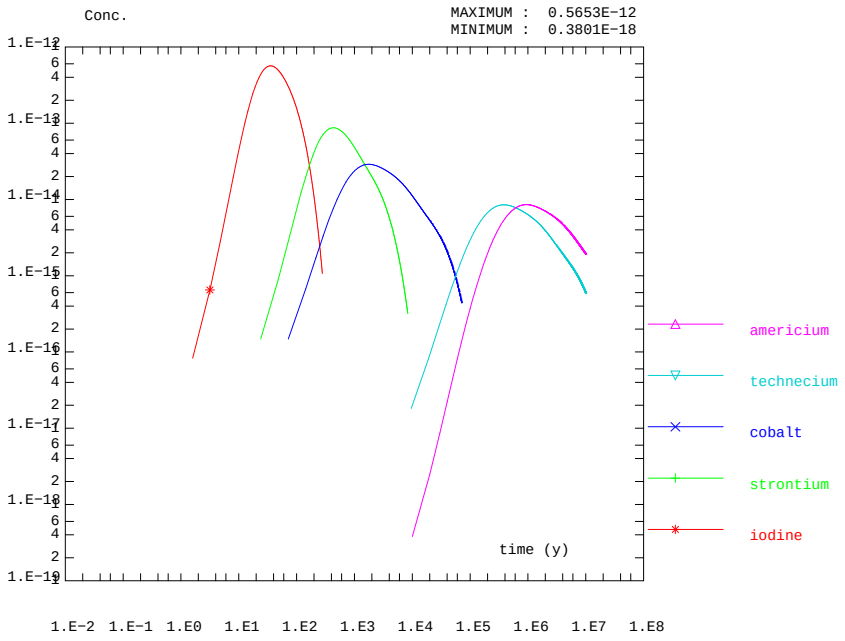

(a) Total flux at the outlet for Dirac input

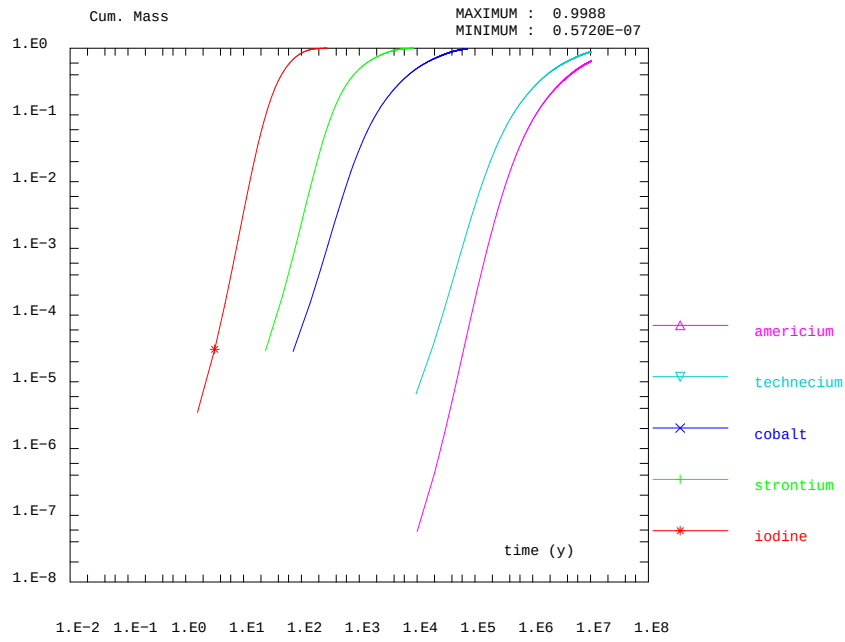

(b) Cumulative mass

Figure 6.3: Model2, (see figure 4.7) : Output for a Dirac input

Sensitivity analysis to flow velocity

We conduct here a sensitivity analysis on another degree of freedom : the velocity of the flow in the fracture (or equivalently the overall head gradient). We consider in the following the previous velocity (or head gradient) as well as two other values around : the same divided and multiplied by a factor of 5. This study is not equivalent to changing the transmissivity values since the fracture aperture should be changed correlatively, for instance one could consider a classical cubic law for the transmissivity.

Results are provided on figures 6.4. For each tracer, the later arrival correspond to the lower velocity value. The output fluxes are sensitive to the velocity although matrix diffusion effects play an important role in these systems. The delay in the peak times for the different cases roughly corresponds to the velocity ratios. An apparently surprising point relies in the fact that tailing effects appear in some cases less important for lower transmissivity values. This is due to the fact that the matrix diffusion is limited in the altered and non altered zones (extension limited to $20cm$ for both units in our case). The maximal retention capacity is here obtained.

As a conclusion, special care should be put into the estimation of the flow velocity and total porosity of the most diffusive zones in the vicinity of the fracture. These parameters are important for the arrival time of the maximum release rate. More in depth matrix zones are mostly responsible for tailing effects having a minor impact on the peak arrival time and amplitude as shown below.

Sensitivity analysis to matrix depth

In the former section, the impact of deeper matrix zones on breakthrough curves appeared limited as compared with the role played by other matrix zones closer to the fracture. Nevertheless, the matrix zones provide the larger storage volume for the plume : porosities are rather low (0.3% for unaltered rock) but large volumes of rock are available for retention. The question rather concerns the accessibility of these storage zones. The main parameter to be considered is the exchange time of the plume with the matrix zones. The mechanism considered here for transport into the matrix zones is indeed diffusion (corrected by linear sorption effects for sorbing tracers). One may report to figure 6.5 where we show the total fluxes corresponding to different non altered zone depths. We have :

- the base case considered previously, non altered zone by $20cm$ in full line,
- the same case without non altered zone (depth $0cm$), in long dots,
- the same case with longer non altered zone by $1m$, in short dots.

As can be seen on log-log scale, the curves poorly differ from each other, showing that, for the flow velocity considered, matrix diffusion does not play a dominant role. Here for instance, even in the case of the $1m$ deep zone, the non altered zone controls less than 20% of the total initially mass present in the system.

This could nevertheless be different for slower velocity regimes for which the penetration depth would increase. So the above conclusion should not be extrapolated to other

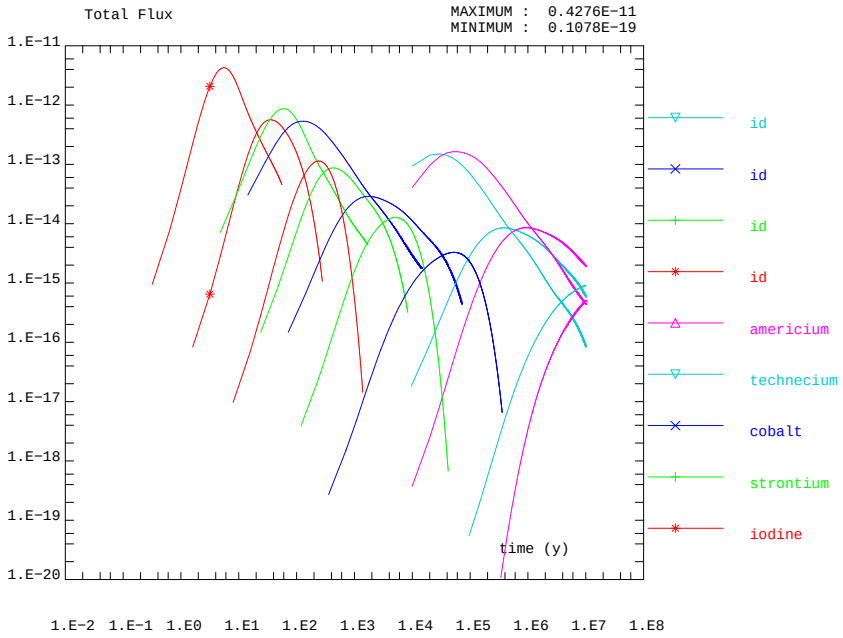

(a) Total flux at the outlet for Dirac input

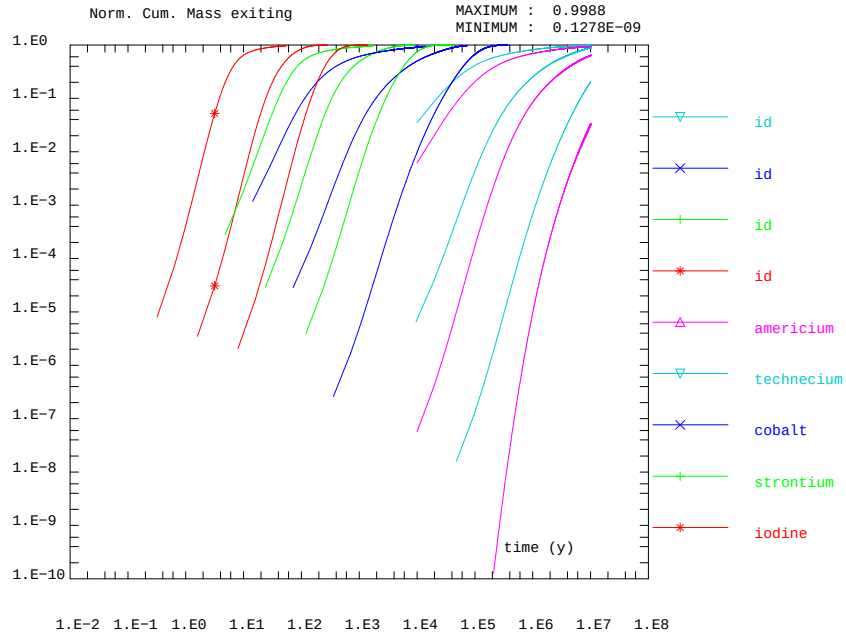

(b) Cumulative mass

Figure 6.4: Sensitivity to the transmissivity value : $T_1 = 8.10^{-9} m^2/s$, $T_2 = 4.10^{-8} m^2/s$ and $T_3 = 2.10^{-7} m^2/s$.

systems involving sufficient immobile zone volume and slower flow field. Such a slower flow field can be obtained as the consequence of a lower head gradient or as well for fractures showing smaller aperture (smaller transmissivity).

As a consequence, the present results can be considered as pessimistic as to matrix diffusion importance. The picture provided in the recent [*Winberg et al. 02*] report shows that fault zones at Äspö can differ from the present representation due to the presence of minor subparallel fractures (type 2). These provide slow velocity channels that are important pathways toward the matrix zones. These in some sense irrigate the matrix zones and would potentially lead to overall increased matrix retention effects as is the case for a single high velocity channel as modeled here.

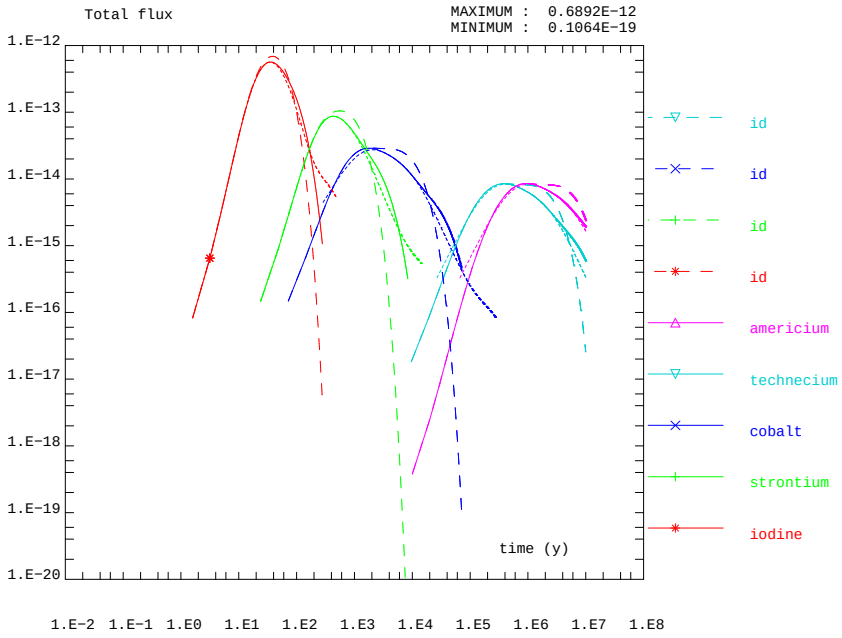

Figure 6.5: Sensitivity to non altered zone depth : $0cm$ (long dots), $20cm$ (continuous line), $1m$ (short dots)

Chapter 7

Performance measures

Performance measures correspond to different boundary conditions :

- Dirac input : we consider here the release of a unit mass at the initial simulation time. The mass is located in the mesh corresponding to the input well (Task 6A and B1) and along the source term (Task 6B2).
- Constant input : we consider a constant unit input expressed in unit per year introduced in the system (1 MBq/year).

We show for these boundary conditions :

- Breakthrough curves (for both Dirac and constant injection conditions). These correspond to the total mass leaving the system (in the pumping well for Task 6A and B1, or in the outer fracture for Task 6B2).
- Maximum release rate for Dirac input.
- Breakthrough time recovery (5, 50 and 95 percents of the injected mass)

The graphs are provided as required in the specifications : in log-log scale in a frame 20cm * 12cm.

Each tracer is associated a color on the figures as follows :

- Red for Iodine
- Green for Strontium
- Blue for Cobalt
- Cyan for Technecium
- Magenta for Americium

Task6AB	Fracture	Gouge	Fr. Coating	Mylonite	Altered Rock	Non Alt. R.
Extent	$2mm$	$5mm$	$0.5mm$	$2cm$	$20cm$	$20cm$
Porosity	1	15%	5%	1%	0.6%	0.3%
Diffusion coefficient (m^2/s)	10^{-9}	3.10^{-10}	2.10^{-10}	10^{-10}	8.10^{-10}	5.10^{-10}
Strontium $K_a(m)$, $K_d(m^3/kg)$	5.10^{-4}	7.110^{-4}	2.310^{-4}	6.710^{-5}	6.10^{-5}	6.10^{-5}
Strontium R_a or R_d	1.5	11.8	12.8	180	26.8	53.8
Cobalt $K_a(m)$, $K_d(m^3/kg)$	8.10^{-3}	8.10^{-4}	8.10^{-4}	8.10^{-4}	8.10^{-4}	8.10^{-4}
Cobalt R_a or R_d	9	13.2	42	215	358	718
Technecium $K_a(m)$, $K_d(m^3/kg)$	0.2	0.2	0.2	0.2	0.2	0.2
Technecium R_a or R_d	201	3061	10261	53461	89460	1.810^5
Americium $K_a(m)$, $K_d(m^3/kg)$	0.5	0.5	0.5	0.5	0.5	0.5
Americium R_a or R_d	501	7651	25651	1.310^5	2.210^5	4.510^5

Table 7.1: Parameter set for task6A and task6B1&2 (fracture and the matrix zones : gouge, fracture coating, mylonite and cataclasite, altered rock, non altered diorite). The parameters are the ones provided in [*Winberg et al. 02*] and [*Selroos et Elert 01*] except for the gouge material where the original data set considered a porosity by 20% and a diffusion coefficient by $5.10^{-10}m^2/s$

The parameter data set is the same for all regimes considered (Task 6B 1 and 2). More details are to be found on the following table.

One may remark that this data set considers surface sorption in addition to taking fracture coating zone into account. Including this feature or not in fact leads to minor differences in the results as can be seen in section (see section 5. This is due to the limited mass that can be sorbed on the fracture walls as compared with the masses stored in the rest of the system.

7.1 Task6A

Tracer	$t_{5\%}(y)$	$t_{50\%}(y)$	$t_{95\%}(y)$	Max. Rel. Time (y)	Max. rel. rate (MBq/y)
Iodine	$2.54\,10^{-4}$	$6.14\,10^{-4}$	$2.08\,10^{-3}$	$5.09\,10^{-4}$	1516.4
Strontium	$3.93\,10^{-4}$	$1.29\,10^{-3}$	$1.94\,10^{-2}$	$8.99\,10^{-4}$	572.52
Cobalt	$2.36\,10^{-3}$	$6.40\,10^{-3}$	$2.73\,10^{-2}$	$4.72\,10^{-3}$	127.67
Technecium	$4.52\,10^{-2}$	0.256	5.015	0.150	2.66
Americium	0.112	0.638	12.50	0.375	1.065

Table 7.2: **Task6A** : Times corresponding to 5%, 50% and 95% of the total mass; maximum of released flux and corresponding time

7.2 Task6B1

Tracer	$t_{5\%}(y)$	$t_{50\%}(y)$	$t_{95\%}(y)$	Max. Rel. Time (y)	Max. rel. rate (MBq/y)
Iodine	0.40	0.88	4.54	0.69	1.08
Strontium	2.36	10.45	123.10	4.72	$7.05\,10^{-2}$
Cobalt	4.04	25.61	378.71	10.78	$2.73\,10^{-2}$
Technecium	828.31	4744.0	92696.	1355.4	$1.77\,10^{-4}$
Americium	1876.9	11637.	$2.32\,10^{5}$	3003.0	$6.4\,10^{-5}$

Table 7.3: **Task6B1** : Times corresponding to 5%, 50% and 95% of the total mass; maximum of released flux and corresponding time

7.3 Task6B2

Tracer	$t_{5\%}(y)$	$t_{50\%}(y)$	$t_{95\%}(y)$	Max. Rel. Time (y)	Max. rel. rate (MBq/y)
Iodine	19.91	53.36	142.58	35.05	$1.49\,10^{-2}$
Strontium	250.90	1039.5	4576.0	430.12	$7.23\,10^{-4}$
Cobalt	1254.5	10000.	56525.	1792.2	$7.76\,10^{-5}$
Technecium	$2.72\,10^{5}$	$2.48\,10^{6}$	$1.41\,10^{7}$	$4.16\,10^{5}$	$3.12\,10^{-7}$
Americium	$7.5\,10^{5}$	$6.18\,10^{6}$	$3.53\,10^{7}$	10^{6}	$1.25\,10^{-7}$

Table 7.4: **Task6B2** : Times corresponding to 5%, 50% and 95% of the total mass; maximum of released flux and corresponding time

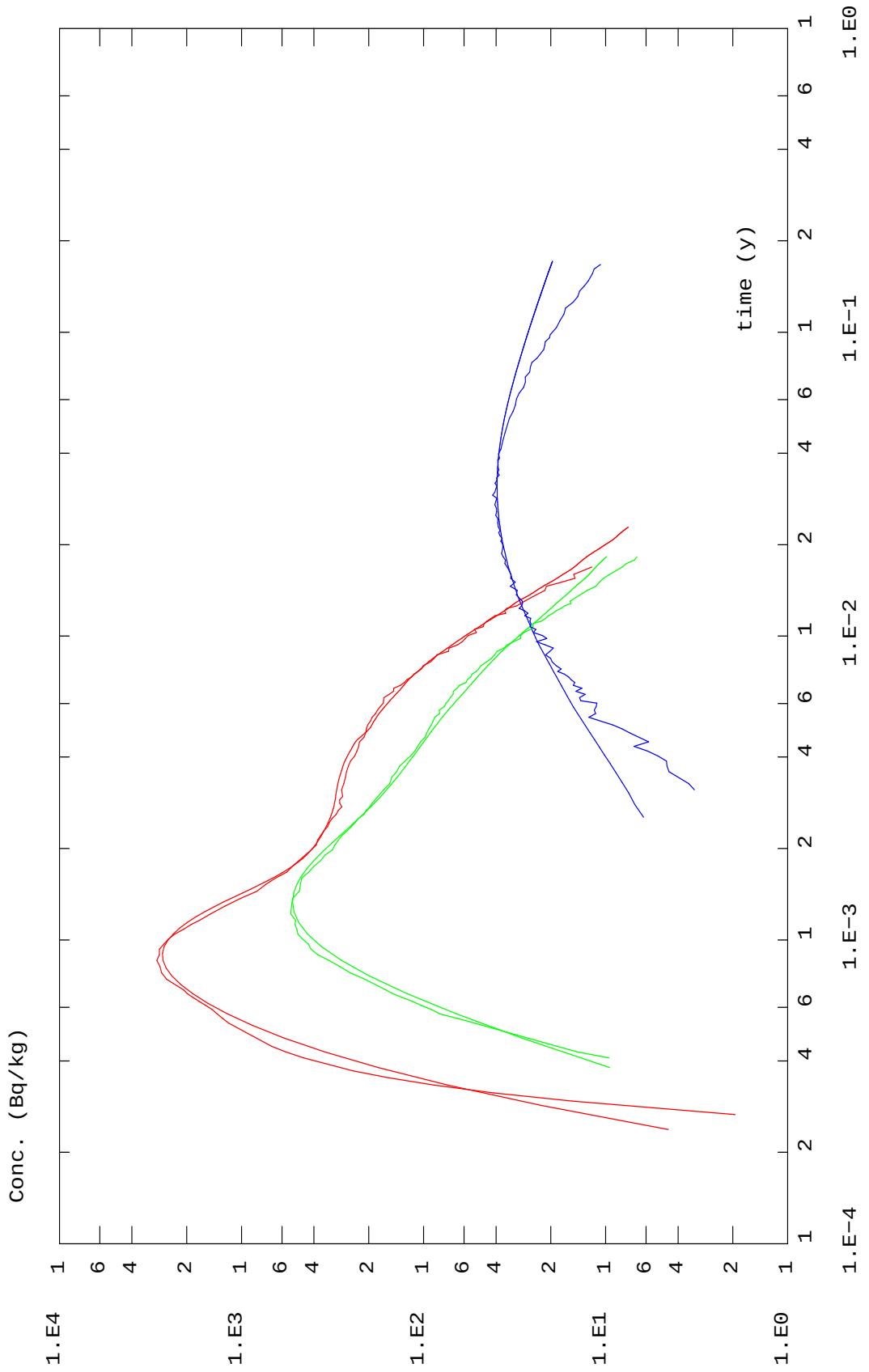

Figure 7.1: **Task6A** : fits for Iodine, Strontium, Cobalt

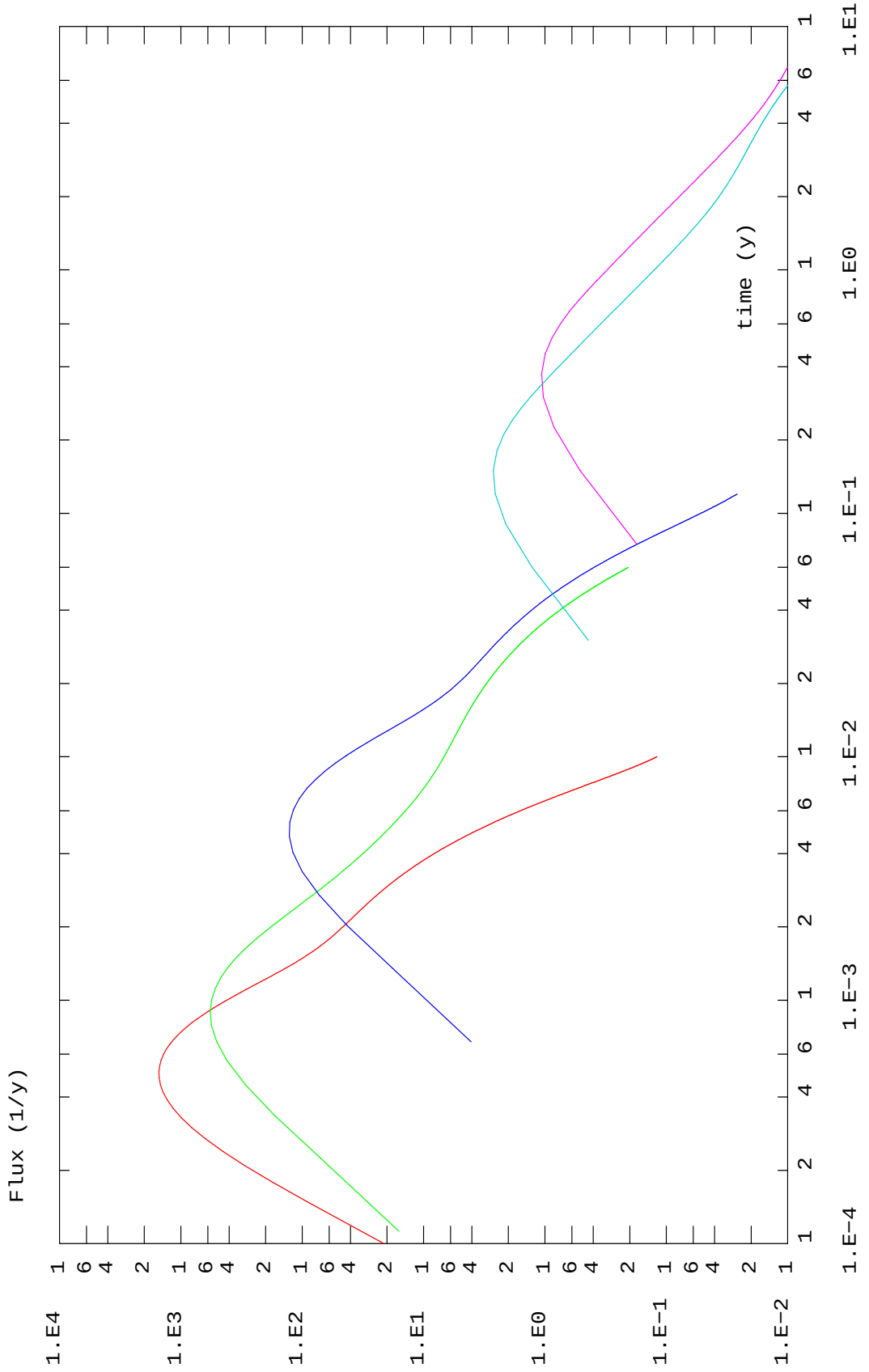

Figure 7.2: **Task6A** : Breakthrough for mass Dirac pulse (Iodine, Strontium, Cobalt, Technecium and Americium) 83

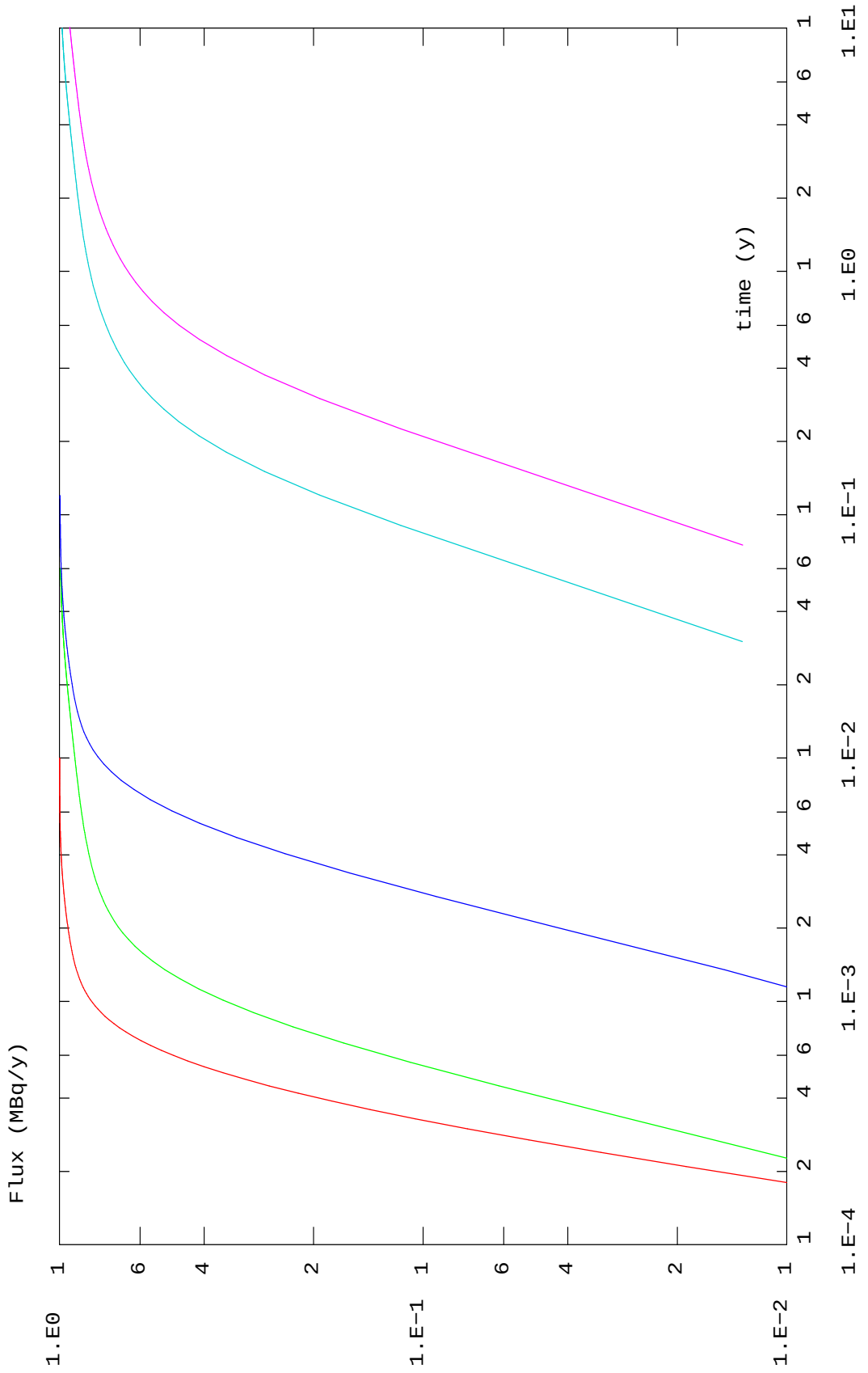

Figure 7.3: **Task6A** : Breakthrough for continuous injection (Iodine, Strontium, Cobalt, Technecium and Americium) 84

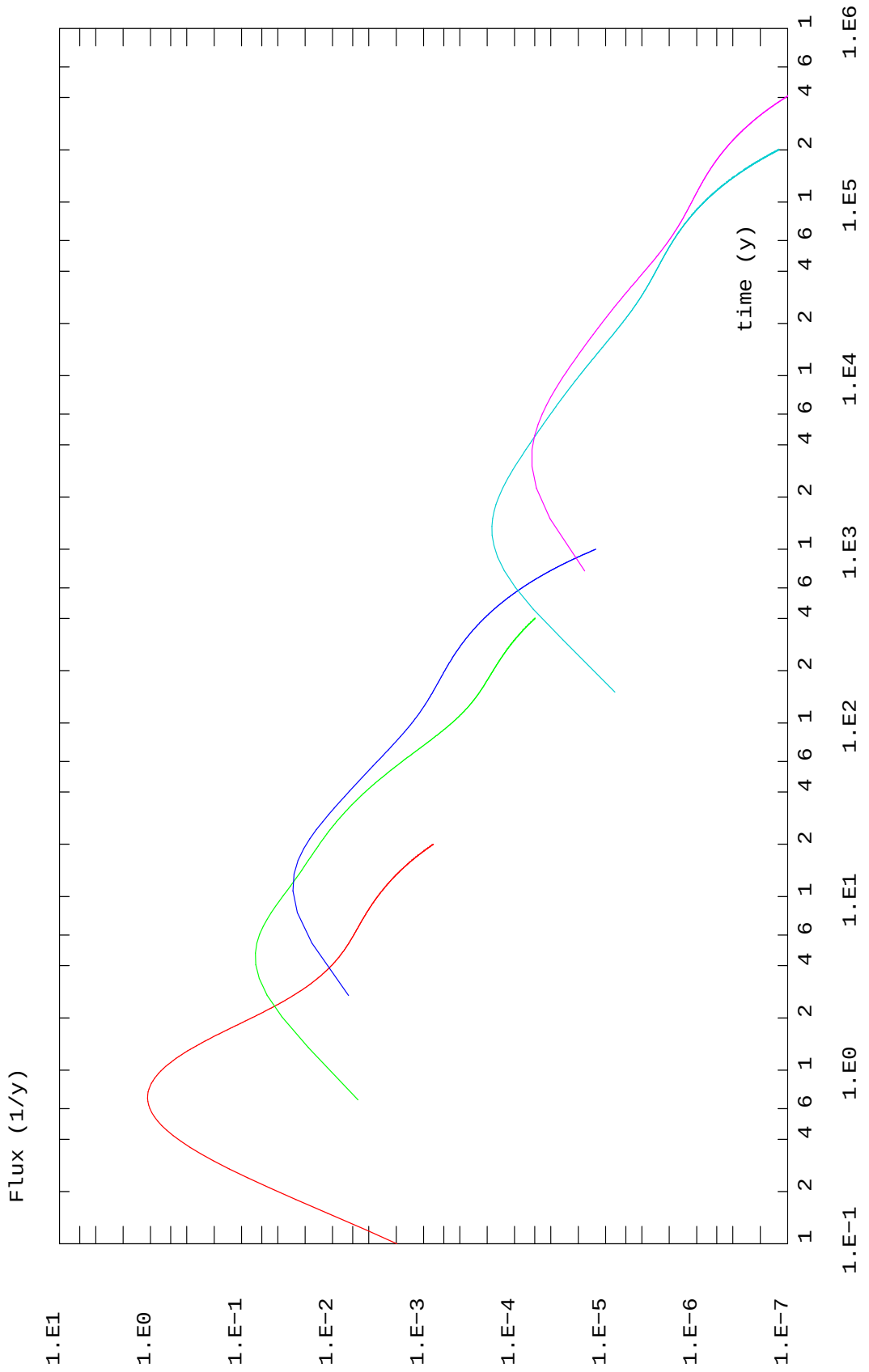

Figure 7.4: **Task6B1** : Breakthrough for mass Dirac pulse (Iodine, Strontium, Cobalt, Technecium and Americium) 85

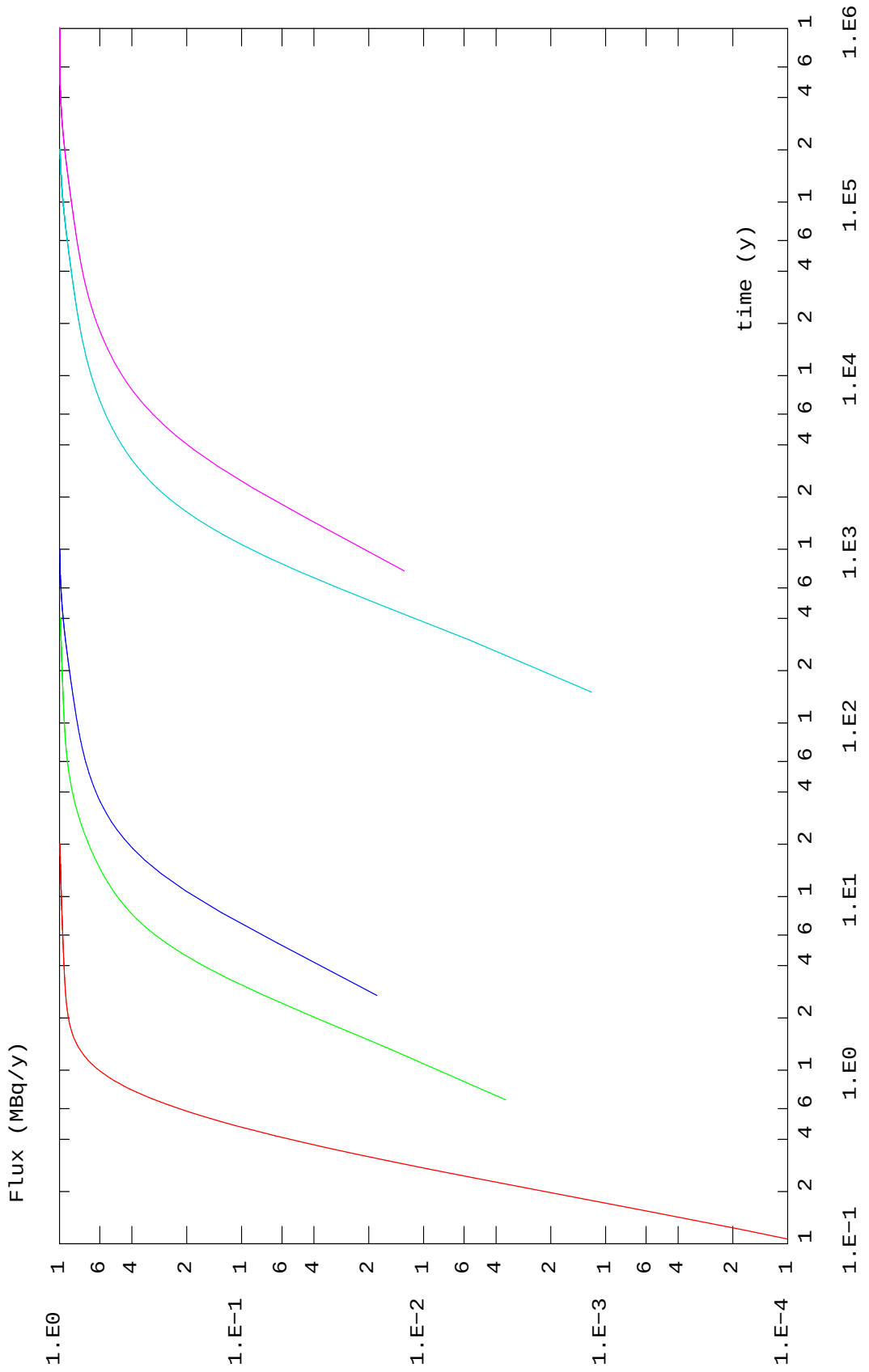

Figure 7.5: **Task6B1** : Breakthrough for continuous injection (Iodine, Strontium, Cobalt, Technecium and Americium) 86

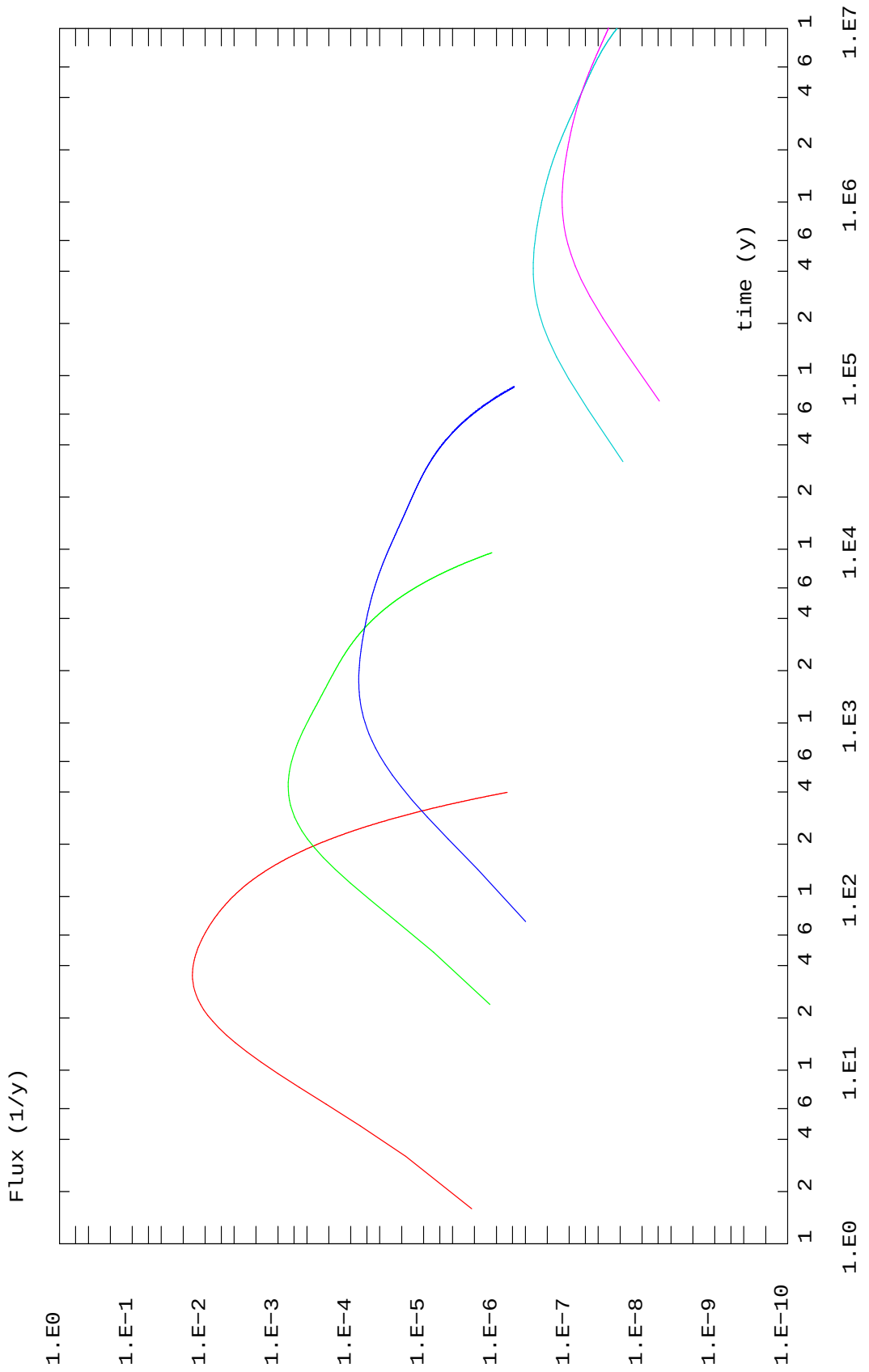

Figure 7.6: **Task6B2** : Breakthrough for mass Dirac pulse (Iodine, Strontium, Cobalt, Technecium and Americium) 87

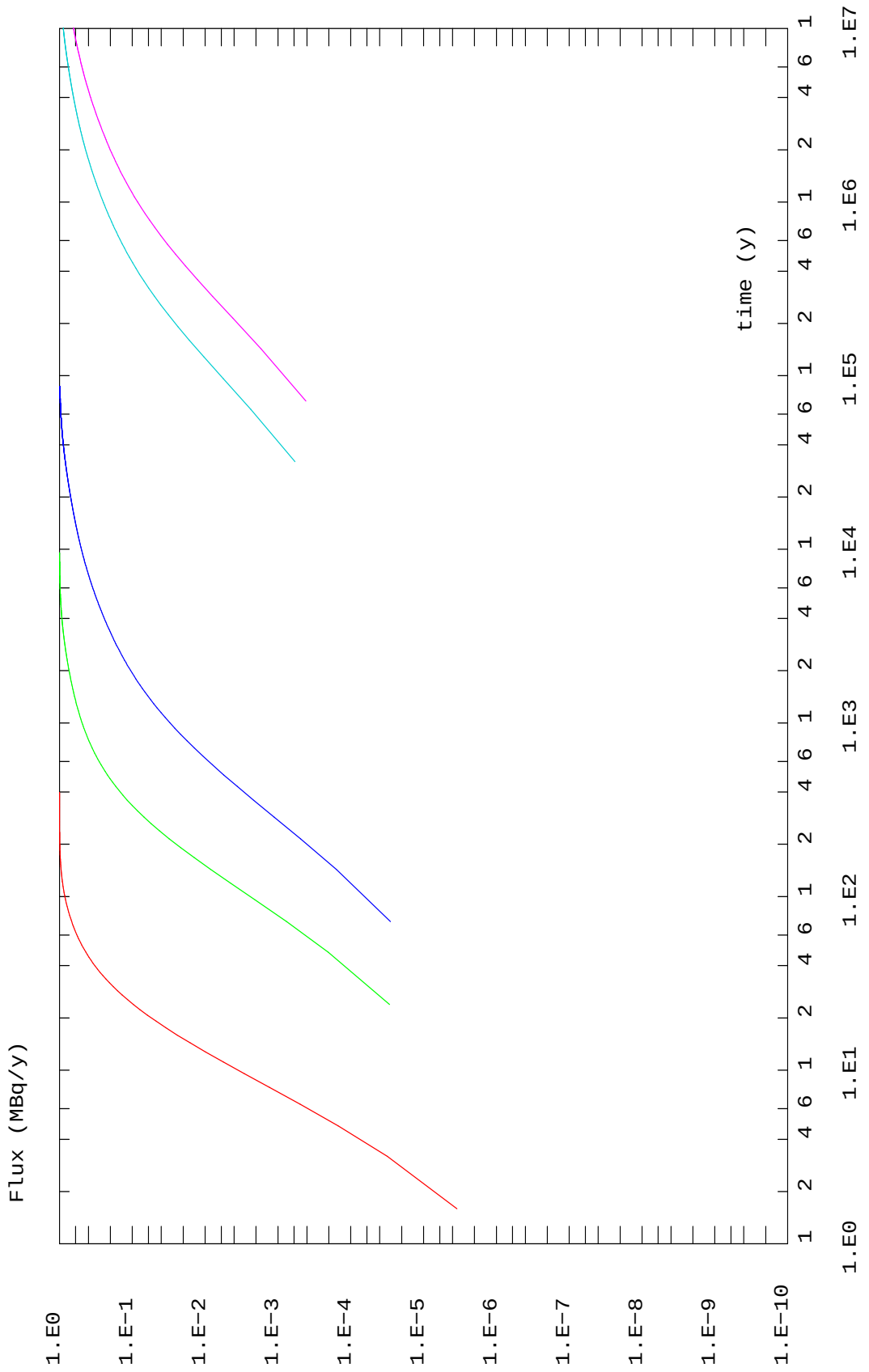

Figure 7.7: **Task6B2** : Breakthrough for continuous injection (Iodine, Strontium, Cobalt, Technecium and Americium) 88

Chapter 8

Discussion

We studied the role played by different immobile matrix zones in the transport and retention of a plume. We conclude here in terms of importance of the different immobile zones for both regimes, the way a PA model can be build and how to constrain the parameter values associated with the selected units.

We identified two groups of immobile zones : roughly the most diffusive and porous zones in the vicinity of the fracture (Gouge, fracture coating, partly Mylonite) and deeper matrix zones providing the large storage capacities but corresponding to the less porous and diffusive material (altered Diorite, non altered rock).

The first type of zones is explored by short term experiments. Access to the deeper zones requires very slow regimes only accounted for at the PA scale. These deeper zones provide the largest storage volume (accessible by diffusion) and at the limit of a very slow transfer in the fracture they would control the transfer. For the flow velocity considered here at PA scale (TaskB1 and 2) and the system characteristics, these zones don't play a dominant role. The dominant role is played by the first more diffusive zones in the vicinity of the fracture. They contribute differently to the transport mechanisms for the short timescale and the PA time scale considered : for short time tests, they act as dual porosity zones providing a transitory retention of the plume; for long times, they only act as a buffer, quasi instantaneously filled up by the tracer mass (as compared with a flow characteristic time). They contribute to a transport total porosity that can be as well modeled with a retardation factor. For the PA scale, precise knowledge of the depth as well as porosity of these zones is required. Some distinctions could be introduced depending on the type of tracer considered (if sorbing or not) but the previous conclusions remain fair for all tracers as considered here.

So we suggest the following as a procedure to build PA models. These suggestions rely upon the present stage in relation with a single fracture case (and the regimes considered) and will have to be improved for the block scale situation corresponding to more complex flow features. First, focus should be put upon obtaining the clearest vision possible of the flow properties. Then, the role played by the different immobile zones should be identified. Due to the complexity of the system, we proceeded here by numerical simulation to assess the role of each zone for each flow regime. It appeared for the flow regimes considered as well as the geometrical features and transport parameter provided that the immobile

zones fell in two categories :

- The immobile zones close to the fracture providing larger diffusivities and lower depth : gouge material, fracture coating, mylonite.
- The immobile zones more in the depth of the matrix blocs like altered rock or non altered rock.

The first type of zone only is relevant for experimental tracer tests but plays a buffer role for the PA time scale considered and can be replaced by a retention factor. The second type of zone acts as a dual porosity zone for PA time scale.
Based on this analysis a simple PA model can be proposed and used for PA purposes. It includes a single flow channel with orthogonal diffusion in an equivalent matrix zone (second zone) whereas the presence of the other matrix zones (first zone) can be accounted for by a retardation factor. Analytical solutions for such a model exist in the literature (see [*Tang et al. 81*] or [*Maloszewski et Zuber 85*] for instance). It should be nevertheless be stressed that for general cases, the domain of validity has to be identified depending in particular on the flow regime considered as developed below.

The last point to be mentioned is the way to come to the information about the geometrical features of the zones as well as their parameter values. The first type of immobile zones close to the fracture are accessed by tracer tests. Unfortunately, integration of the information contained in the breakthrough curves measured does not strongly constrain the system, leaving the space for large uncertainties. This is true for the favorable case where a relation can be brought between matrix diffusion coefficient, porosity and retention coefficient leaving the matrix diffusion coefficient field as the only parameter to be estimated. But for the general case, the data requirements for the PA time scale simulations are not met. Indeed, the tracer tests provide information about these zones as a dual porosity system : one may identify a parameter group function of porosity, diffusion coefficient, fracture aperture and retardation factor. For PA time scale, these zones don't act as a transitory retention zone but for the time scale considered act as an extension of the fracture, contribute to the retardation factor. The parameter required is here the total porosity (involving retention factor for sorbing tracers). This parameter can't be deduced from tracer tests. So, for prediction, one should rely upon independent measurements. This is true for these high porosity zones as well as for the deeper zones which are not accessed at all by tracer tests.
Detailed characterization of the system could be done on a geological analogous at another location of the system. Characterization of the heterogeneity of the matrix zones should be done including the spatial statistical structure of the more porous zones in the vicinity of the fracture. The variability of this more diffusive zone is for PA time scale the major information to be obtained, the variability of the fracture aperture playing a minor role due to its limited total volume.

The present approach was devoted to analysis of the impact of heterogeneous immobile zones on the transfer patterns. This approach was limited to a single channel case (it was indeed implicitly the case for Task6B2 since no heterogeneity was considered in the fracture plane). Perspectives for the present approach should include consideration of several flow channels or more generally fractures zones consisting of various number of fractures of as

contemplated in the Task6D task specifications : different types of fracture zones, type 1 and type 2. This increase in complexity as well as realism will be considered in the future including the study of the impact of a fracture network leading to dispersion of the plume and involving mixing at the intersections.

Bibliography

[1] Äspö Hard Rock Laboratory - 10 years of research. SKB. 1996.

[2] *Radionuclide retention in geologic media.* Workshop proceedings, Oskarsham, Sweden, 7-9 may 2001. Nuclear Energy Agency, OECD 2002.

[*Carrera et al. 98*] J. Carrera, X. Sanchez Vila, I. Benet, A. Medina, G. Galarza, J. Guimera. *On matrix diffusion : formulations, solution methods and qualitative effects.* Hydrogeology Journal (1998) 6:178-190

[*Chen et al. 99*] J.-S. Chen, C.-S. Chen, H.-S. Gau, C.-W. Liu. *A two well method to evaluate transverse dispersivity for tracer tests in radially converent flow field.* Journal of Hydrogeology 223 (1999) 175-197

[*Chen et al. 96*] J.-S. Chen, C.-W. Liu, C.-S. Chen, H.-D. Yeh. *A laplace transform solution for tracer tests in a radially convergent flow field with upstream dispersion.* Journal of Hydrogeology 223 (1999) 175-197

[*Elert et Selroos 01*] M. Elert, J. O. Selroos. *TASK 6B2 modeling task specifications.* sp Task Force, Version 1.0, 7 december 2001

[*Grenier et Benet 02*] C. Grenier, L.-V. Benet. *Grounwater flow and solute transport modelling with support of chemestry data - Task 5.* International Progress Report, SKB. IPR-02-39. September 2000

[*Grenier et al. 99*] C. Grenier, A. Genty, E. Mouche, E. Tevissen. *Modeling matrix diffusion in fractured media : from single fracture scale to block scale.* Proceedings du congrs Dynamics of fluids in fractured rocks. Concepts and recent advances. February 10-12, 1999. Rapport Lawrence Berkeley National Laboratories LBNL-42718

[*Grenier et al. 98*] C. Grenier, E. Mouche, E. Tevissen. *Influence of variable fracture aperture on transport of non sorbing solutes in a fracture : a numerical investigation.* Joural of contaminant hydrology., 35, (1998), 305-313

[*Haggerty et al. 00*] R. Haggerty, S. McKenna, L. Meigs. *On late time behavior of tracer test breakthrough curves.* Water resources research, Vol. 36, No 12, PP 3467-3479, 2000

[*Maloszewski et Zuber 85*] P. Maloszewski, A. Zuber. *On the theory of tracer experiments in fissured rocks with a porous matrix.* Journal of Hydrology, 79 (1985) 333-358.

[*Maloszewski et Zuber 90*] P. Maloszewski, A. Zuber. *Mathematical modeling of tracer behavior in short term experiments in fissured rocks.* Water resources research, Vol. 26, No. 7, pp. 1517-1528, 1990

[*Maloszewski et Zuber 93*] P. Maloszewski, A. Zuber. *Tracer experiments in fractured rocks : matrix diffusion and the validity of models.* Water resources research, Vol. 29, No. 8, pp. 2723-2735, 1993

[*Maugis et al. 02*] P. Maugis, E. Mouche, L. Dewiere. *Analysis of displacement variances in stochastic non uniform flows by means of a first order analytical model and comparison with Monte Carlo simulations.* Transport in Porous Media, Vol. 47, 1-27, 2002.

[*Moench 89*] A. Moench. *Convergent radial dispersion : a laplace transform solution for aquifer tracer testing.* Water resources research, Vol. 25, No 3, PP 439-447, 1989

[*Moench 95*] A. Moench. *Convergent radial dispersion in a double porosity aquifer with fracture skin : analytical solution and application to a field experiment in fractured chalk.* Water resources research, Vol. 31, No 8, PP 1823-1835, 1995

[*Neretnieks 80*] I. Neretnieks. *Diffusion in the rock matrix : an important factor in radionuclide retardation ?.* Journal of geophysical research, Vol. 85, No B8, PP4379-4397, 1980

[*Mouche et Treille 98*] E. Mouche, E. Treille. *Scoping calculations on sorbing tracer test STT1.* CEA internal report. DMT/SEMT/TTMF/RT/98-036

[*Mouche et al. 96*] E. Mouche, E. Treille, L. Dewiere. *Predictive modeling of radial converging tests. TRUE project, first stage.* CEA internal report. DMT/96/386

[*Ostensen 98*] R. Ostensen. *Tracer tests and contaminent transport rates in dual porosity formations with application to the WIPP.* Journal of Hydrology, 204 (1998) 197-216

[*Selroos et Elert 01*] J. O. Selroos, M. Elert. *TASK 6A and B modeling task specifications.* Äspö Task Force, Version 1.0, 3 april 2001

[*Selroos et al. 02*] J.-O. Selroos, D. Walker, A. Stm, B. Gylling, S. Follin. *Comparison of alternative modelling approaches for groundwater flow in fractured rock..* Journal of Hydrology 257 (2002) 174-188

[*Tang et al. 81*] D. H. Tang, E. O. Frind, E. A. Sudicky, *Contaminant transport in fractured porous media : analytical solution for a single fracture.* Water Resources Research, Vol. 17, No. 3, Pages 555-564, June 1981

[*Wang et Crampon 95*] H. Q. Wang, N. Crampon. *Method for interpreting tracer experiments in radial flow using modified analytical solutions.* Journal of Hydrology, 165 (1995) 11-31

[*Winberg et al. 02*] A. Winberg, B. Dershowitz, J. Hermanson, J. Byegard, E.-L. Tullborg, P. Andersson, M. Mazurek. *TASK 6C - Construction of a block scale semi synthetic hydrostructural model and attribution of hydraulic and transport properties.* sp Task Force, Draft, june 10, 2002

[*Winberg et al. 98*] A. Winberg, P. Andersson, J. Hermanson, J. Byegard. *Updated structural model of the TRUE-1 block and detailed description of Feature A.* Final Draft 1998-12-23

[*Zuber et Motyka 94*] A. Zuber, J. Motyka. *Matrix porosity as the most important parameter of fissured rocks for solute transport at large scales.* Journal of Hydrology, 158 (1994) 19-46

Appendix A

Task6 Questionnaire

Questionnaire_Task6.xls

Questionnaire ver 1.0	**Alternatives**	**ANDRA / CEA**	
C. Grenier			
Revised			
Question			
1. Geometry			
1.1 Single fracture vs Fracture Network			
1-1) Are you modeling the Feature A as a single fracture or fracture network?	- single fracture, 2D plane, flow tube modelled for T6A		
1.2 Microscale Geometry			
1.2.1) Are you modeling advective pore space as:	-a single flow porosity		
1.2.2)Are you modeling in-plane heterogeneity of aperture?	- No		
1.2.3)If yes, what kind of heterogeneity are you assuming?	- Deterministic and stochastical matrix diffusion heterogeneity is modelled but not fracture aperture heterogeneity		
1.2.4)Are you modeling anisotropy, and if so what parameters are treated as anisotropy	- No		
1.2.5)Are you modeling correlation, and if so which parameters are correlated	- No for models 1 and 2 - Yes for model 3 and limited to matrix diffusion and matrix porosities		
1.3 Diffusive Pore Space			
1.3.1)Are you modeling the effect of stagnant pool/dead-end pores within the fracture plane?	- Yes, in model 3 - No, not in models 1 and 2		
1.3.2)Are you modeling gouge and/or breccia materials?	- Implicitely in model 1 - Explicitly in models 2 and 3		
1.3.3)Are you modeling effect of fracture coating minerals which potentially limit the diffusion?	Implicitely in model 3, not in models 1 and 2		
1.4 Rock Matrix			
1.4.1)Which porosities in matrix are you modeling?	For model 2, all provided in task6d specifications. The same is implicitely true for model3		

Figure A.1: Questionnaire

Questionnaire_Task6.xls

Questionnaire ver 1.0	**Alternatives**	**ANDRA / CEA**	
1.4.2)How thick will each porosity be?	fracture coating 0,5mm- Fault gouge 5mm- mylonite 20mm, - altered rock 200mm, - intact block		
2 Processes			
2.1)Please make a simple sketch showing the geometry and processes you are considering (see Figure 1 below as an example)	refer to 3 sketches showing the 3 geometries considered : from simple homogeneeous matrix zones to complex heterogeneous matrix zones, deterministic and stochastic approaches		
2.2)Which processes are you modeling?	- Advection, - Dispersion, - Surface sorption, - Matrix diffusion, - Hydrodynamic dispersion, - Matrix bulk sorption		
2.3)How do you evaluate the relative importance between different retention processes?	contained in exchange terms with apparent diffusivities vs. matrix zones total porosity offered		
2.4)The advective velocity in the STT-1b is much higher than at the PA scale. Will you consider changes in mass-transfer processes or dispersion due to change in velocity? (□**No**, □)	Yes. Dispersivity is constant so that dispersion coefficient is dispersivity*velocity field (radial here). Contact time of the plume with the matrix zones is higher leading to increased transfers and retention in the matrix. Nevertheless only linear sorption phenomena are considered here (Kd).		
2.5)How is dispersion treated in your analysis ?	- constant dispersivity tensor (radial flow field) : Dispersion = dispersivity*Velocity(radius) - multirate diffusion, ie heterogeneous diffusion coefficient field leads to spreading of the plume		
3 Parameters			
3.1 Porosities/Diffusivities			
3.1.1)Provide the porosity values for each pore space?	model 2 : - gouge 20% - fracture coating 5% - mylonite 1% - altered rock 0,6% - intact rock 0,3%		
3.1.2)Provide the effective water diffusivity De for each pore space? (m2/s for model 2, for model 3 gaussian variable within stochastic modeling	- gouge, 1,D-10 - fracture coating, 1,D-11 - mylonite, 1,D-12 - altered rim, 4,8E-13 - intact rock, 1,5E-13		
3.2 Advection and Dispersion			
3.2.1) What is the mean advective velocity t50 for Task 6A and Task 6B in your modeling?	- t50 6A (hours) - t50 6B (hours)		
3.2.2)What are the effective (apparent) longitudinal and transverse dispersion observed in your model for 6A and 6B . Fracture dispersivities provided here, radial flow patterns	- longitudinal 6A: 0,25 (m) - longitudinal 6B: 0,25 (m) - transverse 6A: 0,05 (m) - transverse 6B: 0,05 (m)		
3.3 Matrix and Surface Sorption Kd and Ka			
3.3.1)Do you change Kd values for each pore space? (□**Yes**, □No) See Table 1.	- Yes		

Figure A.2: Questionnaire

Questionnaire_Task6.xls

Questionnaire ver 1.0	Alternatives	ANDRA / CEA	
3.3.2)How do you relate surface sorption Ka to matrix sorption Kd:			
How are Kd and Ka values derived from measurements for each porosity:	Provided in Task Force documentation, mainly T6A and T6D reports		
3.3.3)Describe any treatment of correlations of immobile zone properties, sorption properties such as Kd, and advective properties such as transmissivity:	limited to model3. Gaussian Dp fields are generated, mean=, standard deviation= , correlation length=. Porosity as well as Kd are deduced by linear interpolation through the database involving the different matrix zones parametersets provided.		
3.4 Flow Wetted Surface			
3.4.1)Is flow wetted surface a direct input into your model or is it back calculated from geometric and transport parameters ?.	- direct, considering provided range and arrival time for Iodine		
3.4.2)If flow wetted surface area is a direct input, provide the range of values specified. Otherwise, calculate the flow wetted surface as reactive surface area per unit volume of all immobile zones. Specify as a range or distribution if possible:	Fracture opening is 2 mm, flow tube by 5,03 meter is modelled, one opening enclosing the input well		
3.4.3) Is F-ratio or □-parameter a direct input into your model or is it back calculated from geometric and transport parameters ?.			
3.4.4) If F-ratio or □-parameter are direct inputs, provide the range of values specified. Otherwise, calculate the □-parameter according to the definition of Cvetkovic (2001). Specify as a range or distribution if possible:.			
3.4.5) Describe any treatment of heterogeneity of immobile zones and surface minerals:	For model 3, stochastic modeling (longitudinal and transverse), for models 1 and 2 deterministic treatment and only transverse heterogeneity for model 2. See figures below		
4. Numerical Model			
4.1 Flow Model			
4.1.1)What flow code do you use:	- Mixed Hybrid Finite Element: CAST3M		
4.1.2)What is the flow model dimensionality	For Task 6A and B1, 1D radial flow tube. No flow in the matrix zones		
4.1.3)What is the level of discretization of the model (	- Largest element size: 0,1 (m) - Smallest element size: 1,E-3 (m) - Number of elements.		
4.1.4)What is the CPU time for a single flow solution:	scale of few seconds, permanent calculation		
4.1.5)What is the accuracy of the flow solution:	excellent as compared with Moench solutions		
4.1.6)How does the numerical model deal with out-of plane flow and boundary conditions:	- no out of plane flow - flow tube with constant flow rate		
4.2 Transport Model			
4.2.1)What transport code do you use:	- Mixed Hybrid Finite Element: CAST3M		

Figure A.3: Questionnaire

Questionnaire_Task6.xls

Questionnaire ver 1.0	**Alternatives**	**ANDRA / CEA**	
4.2.2)What is the transport model dimensionality	- 3-D		
4.2.3)What is the level of discretization of the model	- Largest element size: 0,1 (m) - Smallest element size: 1,D-3 (m) - Number of elements.		
4.2.4)What is the CPU time for the transport solution: .	level of minutes to few hours		
4.2.5)What is the accuracy of the transport solution:	globally estimated below 15% for breakthrough curves		
4.2.6)How does the numerical model deal with multiple transport pathways:	- none		
4.3 Integration			
4.3.1)How are flow and transport linked:	- through velocity field		
4.3.2)How is uncertainty addressed: .	- sensitivity (2*5 cases for model 1), - Monte Carlo (1000-100 runs)		
Basis for number of cases or runs:	10 to 20 for the deterministic model2, 1000 for Monte Carlo model3 case		
5 Conceptual Issues			
5.1)What were the most significant technical issues in achieving Task 6A:	multiple calibration, identify role played by different diffusion zones		
5.2) What were the most significant technical issues in achieving Task 6B:	Sensitivity analysis, role played by different matrix diffusion zones		
5.3) What were the primary differences in transport processes observed between Task 6A and 6B:	(1) deeper matrix zones are at stake for retention, (2) others in the vicinity of the fracture contribute to retardation coefficient. Type of measurements provided by calibration vs. required for prediction		
5.4) If sensitivity studies were carried out, what were most important sensitive assumptions for Task 6A and Task 6B:	Total porosity of the first matrix zones met by the plume in the matrix block		
5.5) Does your modeling and analysis support the use of the conventional advection-dispersion-diffusion (ADD) approach, or do you feel that an alternative formulation is necessary to explain and extrapolate from observed breakthrough: support the use of the conventional advection-dispersion-diffusion (ADD) approach .	Yes. But further modeling steps including several similar channels were contemplated but not done due to time constraints		

Figure A.4: Questionnaire

Table 1a Sorption and diffusivity data for tracers in fracture for model2 and Task 6a and 6b.

Tracer	Surface sorption coefficient			
	Ka (m)			
	Task 6a	Task 6b		
I	0	id		
Sr	5,00E-04	id		
Co	8,00E-03	id		
Tc	0,2	id		
Am	0,2	id		

Table 1b Sorption and diffusivity data for tracers in gouge for model2 and Task 6a and 6b.

Tracer	Matrix sorption coefficient		Effective matrix diffusivity	
	Kd (m3/kg)		De (m2/s)	
	Task 6a	Task 6b	Task 6a	Task 6b
I	0	0	1,00E-10	1,00E-10
Sr	7,10E-04	id	id	id
Co	8,00E-04	id	id	id
Tc	0,2	id	id	id
Am	0,5	id	id	id

Table 1c Sorption and diffusivity data for tracers in fracture coating for model2 and Task6a & 6b.

Tracer	Matrix sorption coefficient		Effective matrix diffusivity	
	Kd (m3/kg)		De (m2/s)	
	Task 6a	Task 6b	Task 6a	Task 6b
I	0	id	1,00E-11	1,00E-11
Sr	2,30E-04	id	id	id
Co	8,00E-04	id	id	id
Tc	0,2	id	id	id
Am	0,5	id	id	id

Table 1d Sorption and diffusivity data for tracers in mylonite for model2 and Task 6a and 6b.

Tracer	Matrix sorption coefficient		Effective matrix diffusivity	
	Kd (m3/kg)		De (m2/s)	
	Task 6a	Task 6b	Task 6a	Task 6b
I	0	id	1,00E-12	1,00E-12
Sr	6,70E-04	id	id	id
Co	8,00E-04	id	id	id
Tc	0,2	id	id	id
Am	0,5	id	id	id

Table 1e Sorption and diffusivity data for tracers in altered rock for model2 and Task 6a and 6b.

Tracer	Matrix sorption coefficient		Effective matrix diffusivity	
	Kd (m3/kg)		De (m2/s)	
	Task 6a	Task 6b	Task 6a	Task 6b
I	0	id	5,00E-13	5,00E-13
Sr	6,00E-05	id	id	id

Figure A.5: Questionnaire

Co	8,00E-04	id	id	id
Tc	0,2	id	id	id
Am	0,5	id	id	id

Table 1f Sorption and diffusivity data for tracers in non altered rock for model2 and Task6a & 6b.

Tracer	**Matrix sorption coefficient**		**Effective matrix diffusivity**	
	Kd (m3/kg)		**De (m2/s)**	
	Task 6a	**Task 6b**	**Task 6a**	**Task 6b**
I	0	id	1,50E-13	1,50E-13
Sr	6,00E-05	id	id	id
Co	8,00E-04	id	id	id
Tc	0,2	id	id	id
Am	0,5	id	id	id

Model 1

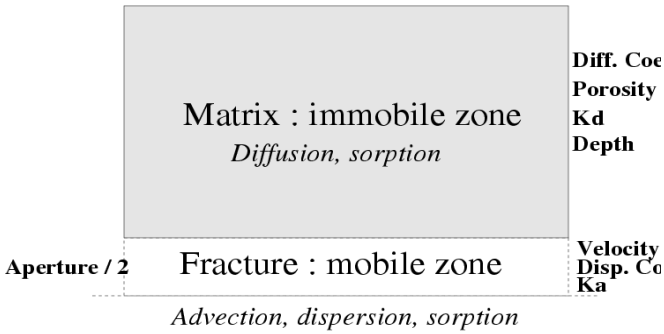

Model 1 : Basic case considered and maximal level of simplification expected for PA model

Model 2

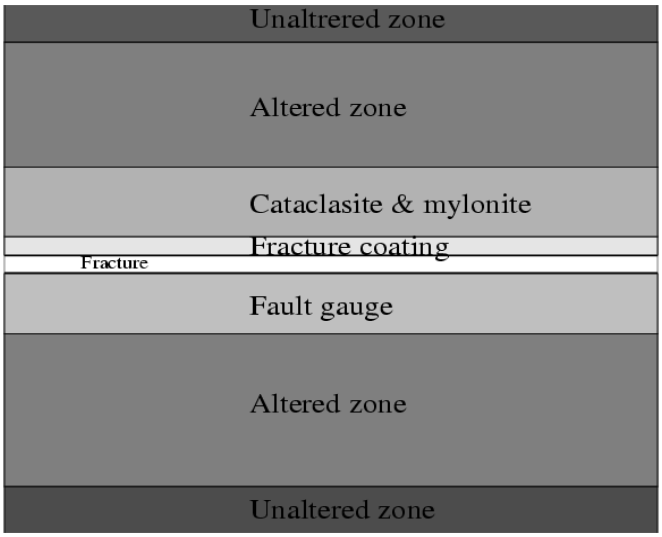

Model2 : Base case model for performance measures. Show pertinent simplifications for PA scale

Figure A.6: Questionnaire

Model 3

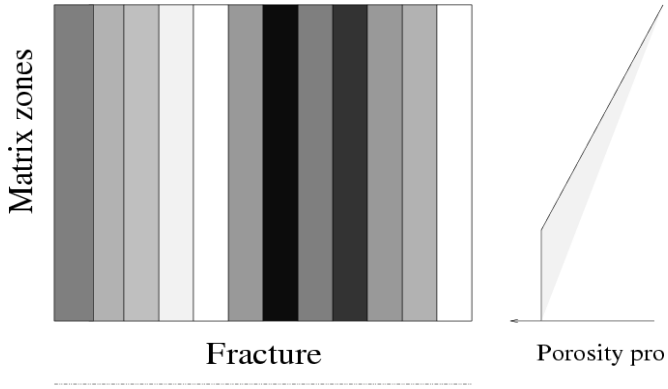

Model3 : Model to address (i) the inverse problem (ii) the consequences on PA scale predictions.

Figure A.7: Questionnaire